

**Angiopoietin receptor Tie2 is required for vein specification and  
maintenance via regulating COUP-TFII**

Man Chu<sup>1#</sup>, Taotao Li<sup>1#</sup>, Bin Shen<sup>1,2</sup>, Xudong Cao<sup>1</sup>, Haoyu Zhong<sup>1</sup>, Luqing Zhang<sup>1,2</sup>,  
Fei Zhou<sup>1,2</sup>, Wenjuan Ma<sup>1</sup>, Haijuan Jiang<sup>1</sup>, Pancheng Xie<sup>1</sup>, Zhengzheng Liu<sup>1</sup>,  
Ningzheng Dong<sup>1</sup>, Ying Xu<sup>1</sup>, Yun Zhao<sup>1</sup>, Guoqiang Xu<sup>1</sup>, Peirong Lu<sup>1</sup>, Jincal Luo<sup>3</sup>,  
Qingyu Wu<sup>1</sup>, Kari Alitalo<sup>4</sup>, Gou Young Koh<sup>5</sup>, Ralf H. Adams<sup>6</sup>, Yulong He<sup>1\*</sup>

<sup>1</sup>Cyrus Tang Hematology Center, Collaborative Innovation Center of Hematology,  
Cam-Su Genomic Resources Center, Jiangsu Key Laboratory of Preventive and  
Translational Medicine for Geriatric Diseases, College of Pharmaceutical Sciences,  
Jiangsu Institute of Hematology, the First Affiliated Hospital, Soochow University, 199  
Ren-Ai Road, Suzhou 215123, China

<sup>2</sup>MOE Key Laboratory for Model Animal and Disease Study, Model Animal Research  
Institute, Nanjing University, 12 Xue Fu Road, Nanjing 210061, China

<sup>3</sup>Laboratory of Vascular Biology, Institute of Molecular Medicine, Peking University,  
Beijing 100871, China

<sup>4</sup>Wihuri Research Institute and Translational Cancer Biology Center of Excellence,  
Biomedicum Helsinki University of Helsinki, 00014 Helsinki, Finland.

<sup>5</sup>Center for Vascular Research, Institute of Basic Science and Korea Advanced  
Institute of Science and Technology (KAIST), Daejeon, 305-701, Korea.

<sup>6</sup>Max-Planck-Institute for Molecular Biomedicine, Department of Tissue  
Morphogenesis, University of Münster, Faculty of Medicine, D-48149 Münster,  
Germany

Short title: Tie2 in vein specification and maintenance

# These authors contributed equally to this work

Key words: Tie2, COUPT-FII, vein specification, venous malformation, vascular tufts

\* Correspondence should be addressed to Dr. Yulong He,  
Phone: +86-512-65884937; Fax: +86-512-65880929; E-mail: heyulong@suda.edu.cn

41    **Abstract**

42    Mechanisms underlying the vein development remain largely unknown. Tie2 signaling  
43    mediates endothelial cell (EC) survival and vascular maturation and its activating  
44    mutations are linked to venous malformations. Here we show that vein formation are  
45    disrupted in mouse skin and mesentery when Tie2 signals are diminished by targeted  
46    deletion of *Tek* either ubiquitously or specifically in embryonic ECs. Postnatal Tie2  
47    attenuation resulted in the degeneration of newly formed veins followed by the  
48    formation of haemangioma-like vascular tufts in retina and venous tortuosity.  
49    Mechanistically, Tie2 insufficiency compromised venous EC identity, as indicated by a  
50    significant decrease of COUP-TFII protein level, a key regulator in venogenesis.  
51    Consistently, angiopoietin-1 stimulation increased COUP-TFII in cultured ECs, while  
52    Tie2 knockdown or blockade of Tie2 downstream PI3K/Akt pathway reduced  
53    COUP-TFII which could be reverted by the proteasome inhibition. Together, our  
54    results imply that Tie2 is essential for venous specification and maintenance via Akt  
55    mediated stabilization of COUP-TFII.

56

## 57    **Introduction**

58    The mechanisms underlying arteriovenous specification have been under intensive  
59    investigation during the past years, and this has led to the identification of several  
60    signaling pathways involved in the coordination of this process. The  
61    VEGF-A/VEGFR-2 pathway mediates activation of RAF1 and ERK1/2 kinases to  
62    induce the expression of genes required for arterial development<sup>1, 2</sup>, including  
63    Delta-like 4 (Dll4) that activates NOTCH signaling<sup>3-5</sup>. Wnt/ $\beta$ -catenin, SOX17 and  
64    FOXC1/2 were also reported to participate in arterial development via activation of the  
65    NOTCH pathway<sup>6-8</sup>. In contrast, knowledge on venogenesis is still limited. COUP-TFII,  
66    a transcription factor expressed in venous but not arterial endothelial cells (ECs), has  
67    been shown to regulate venous identity via the inhibition of NOTCH mediated signals<sup>9</sup>.  
68    Vice versa, NOTCH activation has been shown to down-regulate COUP-TFII  
69    expression<sup>10</sup>. Furthermore, Akt activation was shown to inhibit Raf1-ERK1/2 signaling  
70    in ECs to favor venous specification<sup>11</sup>. To date, however, the specific factors upstream  
71    of the Akt pathway that define venous EC identity remain unclear.

72

73    Tie2 is a receptor tyrosine kinase that mediates angiopoietin signaling for EC survival,  
74    vascular remodeling and integrity<sup>12</sup>. Tie2 deficiency led to embryonic lethality resulting  
75    from the defective vascular remodeling and heart development<sup>13, 14</sup>, and combined  
76    deletion of Tie2 ligands Ang1 and Ang2 in mice was also shown to disrupt Schlemm's  
77    canal formation leading to ocular hypertension and glaucoma<sup>15</sup>. Patients with venous  
78    malformations were shown to have Tie2 missense point mutations<sup>16</sup>, leading to

79 ligand-independent Tie2 activation<sup>17</sup>. However, the underlying mechanism of Tie2  
80 function in the blood vessels has not been fully elucidated. In this study, we show that  
81 Tie2 deficiency or insufficiency induced by gene targeting leads to defective vein  
82 formation and maintenance during embryogenesis and postnatal development.  
83 Findings from this study suggest that Tie2 is essential for the specification of venous  
84 EC identity via the Akt mediated regulation of COUP-TFII protein stability.

85

## 86 **Results**

### 87 **Disruption of vein development after Tie2 deletion during embryogenesis**

88 To characterize Tie2 function in vascular development, a conditional knockout mouse  
89 model targeting the *Tek* gene<sup>18</sup> was employed in this study. Ubiquitous deletion of *Tek*  
90 led to embryonic lethality by E10.5 (Figure 1-figure supplement 1A-C), as previously  
91 reported<sup>14</sup>. As shown in Figure 1A, B and Figure 1-figure supplement 1D, E, no veins  
92 (arrows) were detected in the head or somite regions of the *Tek* null embryos at E9.5,  
93 unlike in the littermate control embryos. Interestingly, Tie2 expression in the E9.5  
94 embryos was higher in veins than in arteries (arrowhead, Figure 1B). The lack of veins  
95 in the intersomitic regions of *Tek* deleted mice was also evident by Dll4 and PECAM-1  
96 double staining (Figure 1-figure supplement 1E).

97

98 To investigate the role of Tie2 later during embryogenesis, we employed the  
99 *Ubc-Cre<sup>ERT2</sup>* and *Cdh5-Cre<sup>ERT2</sup>* deleter mouse lines<sup>19</sup>, to generate the doubly  
100 transgenic mice (*Tek<sup>Flox/-</sup>/Ubc-Cre<sup>ERT2</sup>*, named *Tek<sup>-f/i</sup>UCKO*; or *Tek<sup>Flox/-</sup>/Cdh5-Cre<sup>ERT2</sup>*,



101 named  $Tek^{-fIECKO}$ ).  $Tek^{Flox/+}/Ubc-Cre^{ERT2}$  or  $Tek^{Flox/+}/Cdh5-Cre^{ERT2}$  littermate mice were  
 102 used as controls. Tie2 deletion efficiency was examined by immunostaining with skin  
 103 and also by real-time RT-PCR with lung of *Tek* mutant mice ( $Tek^{-fIECKO}$ :  $0.33 \pm 0.07$ ,  
 104  $n=3$ ;  $Tek^{+/fIECKO}$ :  $1.0 \pm 0.26$ ,  $n=3$ ;  $Tek^{-fIUCKO}$ :  $0.25 \pm 0.02$ ,  $n=4$ ;  $Tek^{+/fIUCKO}$ :  $1.0 \pm 0.11$ ,  $n=4$ ).  
 105 Analysis of veins in skin at E15.5 showed that venogenesis was disrupted in both  
 106 types of mutant embryos, in which *Tek* deletion was induced by intraperitoneal  
 107 injections of tamoxifen into pregnant mice at E10.5-12.5 (Figure 1C-E and Figure  
 108 1-figure supplement 2A). In addition, defective vein formation was also observed in  
 109 the skin of E17.5  $Tek^{-fIUCKO}$  embryos when *Tek* deletion was induced at E12.5-14.5  
 110 (Figure 1F). Lack of bleeding or edema with the later targeting suggests a  
 111 stage-dependent function of Tie2 during the establishment of vascular integrity.  
 112 Interestingly, veins were detected in mesentery, but unlike in littermate controls, they  
 113 did not align properly with the arteries (Figure 1-figure supplement 2B). Furthermore,  
 114 lymphatic vessels originate mainly from veins during embryonic development in  
 115 mammals. It is therefore interesting to find out whether lymphatic development is  
 116 altered in Tie2 knockout mice when the vein formation is defective. We found that  
 117 lymphatic vessels were present in the skin of  $Tek^{-fIECKO}$  mutant mice, but became  
 118 dilated (Figure 1-figure supplement 3). This may be secondary to tissue edema  
 119 resulting from the impairment of blood vasculature. However, it is also possible that  
 120 Tie2 may have a role at earlier stages of lymphatic development.

121

## 122 **Retardation of retinal vascularization after Tie2 attenuation**

123 To study the role of Tie2 in postnatal vascular formation, the *Tek*<sup>Flox/-</sup>/*Ubc-Cre*<sup>ERT2</sup>  
 124 neonatal mice were treated with tamoxifen via intragastric injection during postnatal  
 125 days (P1-4) and analyzed at P7 (Figure 2A). The efficiency of *Tek* deletion was  
 126 examined by Western blot analysis, immunostaining and real-time RT-PCR. Little Tie2  
 127 protein was detected in the lung and retina of *Tek*<sup>-f/UCKO</sup> mice (Figure 2B, C). The level  
 128 of Tie2 mRNA in the same tissues of *Tek*<sup>-f/UCKO</sup> mice was approximately 13-18 % of the  
 129 control mice as shown in Table 1. Consistent with the results from Western blot  
 130 analysis, the deletion efficiency of Tie2 as analyzed by real-time RT-PCR in lungs of  
 131 *Tek*<sup>-f/ECKO</sup> mice was lower than that of *Tek*<sup>-f/UCKO</sup> mutants (*Tek*<sup>-f/ECKO</sup>: 0.40 ± 0.10, n=4;  
 132 *Tek*<sup>+f/ECKO</sup>: 1.0 ± 0.21, n=4). The partial Tie2 deletion was also indicated by the mosaic  
 133 GFP expression when the mTmG allele was crossed into the *Tek* mutant mice to  
 134 generate the compound genetic mouse model (*Tek*<sup>-f/ECKO</sup>;*mTmG*; Figure 2-figure  
 135 supplement 1A-B)<sup>20</sup>. Interestingly, the decrease of Tie2 in the *Tek*<sup>-f/UCKO</sup> and *Tek*<sup>-f/ECKO</sup>  
 136 mice resulted in a significant decrease of retinal vascularization, as indicated by a  
 137 lower vascular index (Figure 2C-F). As Tie2 is also expressed by some hematopoietic  
 138 cells, we generated mutant mice with *Tek* deletion in blood cells (*Tek*<sup>Flox/-</sup>;*Vav-iCre*)<sup>21</sup>.  
 139 No obvious defects were observed in the retinal blood vessels of the mutant mice  
 140 (Figure 2-figure supplement 2A, B).

141

## 142 **Increase of venous angiogenesis in retina after postnatal deletion of Tie2**

143 In spite of the decreased vascular index in retina, there was a significant increase of  
 144 vascular density at the front of the venous but not arterial segments of *Tek*<sup>-f/UCKO</sup>

145 mutants compared with controls at P7 (Figure 2G-J). Biochemical analysis revealed a  
146 significantly decreased phosphorylation of the Dok-2 docking protein (pDok2 /  
147 beta-actin, Tek<sup>-f/UCKO</sup>: 0.38 ± 0.25, n=6; Control: 1.0 ± 0.24, n=6; P=0.0014; pDok2 /  
148 tDok2, Tek<sup>-f/UCKO</sup>: 0.52 ± 0.10, n=3; Control: 1.0 ± 0.21, n=3; P=0.024), but an increase  
149 of Erk1/2 phosphorylation (pERK1/2 / tERK1/2, Tek<sup>-f/UCKO</sup>: 1.71 ± 0.70, n=10; Control:  
150 1.0 ± 0.30, n=9; P=0.012) in the lungs of Tek<sup>-f/UCKO</sup> mice compared with controls  
151 (Figure 2K, L). It is worth noting that the total Dok-2 protein level also decreased in the  
152 mutant mice after Tie2 reduction compared with that of the littermate control.

153

#### 154 **Tie2 insufficiency leads to vascular tuft formation along retinal veins**

155 The scheme for *Tek* deletion by intragastric administration of tamoxifen was shown in  
156 Figure 3A. The abnormal angiogenesis along the retinal veins was also seen at P11 in  
157 mice with postnatal *Tek* deletion, and the morphology of veins was severely disrupted  
158 at P15 (Figure 3B and C, arrows). Vein degeneration was accompanied by the  
159 formation of haemangioma-like vascular tufts by P21 (Figure 3D, arrows). The  
160 massive angiogenic vascular growth occurred mainly in the first layer of retinal  
161 vessels of Tek<sup>-f/UCKO</sup> mice (Figure 3E). In contrast to wildtype littermate control mice,  
162 Tek<sup>-f/UCKO</sup> mutant mice at P21 exhibited little blood vessel growth towards the deep  
163 layers of retina (Figure 3E). Vessels in the vascular tufts in the Tek<sup>-f/UCKO</sup> mice had  
164 lumens and were covered with NG2<sup>+</sup> pericytes (Figure 3E). Furthermore, *Tek* deletion  
165 at a later stage (P5-8) resulted in a similar but milder vascular phenotype (Figure 3F,  
166 arrows). For comparison, we also performed the analysis of retinal blood vasculature

167 at different time points with Tek<sup>-fIECKO</sup> mice, but did not observe the formation of  
168 vascular tufts. This may be due to the lower efficiency of *Tek* gene deletion as  
169 discussed above.

170

171 Despite the lethality of *Tek* null embryos, the Tek<sup>-fIUCKO</sup> mice deleted at P1-4 survived  
172 with reduced body weight (Figure 3-figure supplement 1). Unlike in the retina,  
173 postnatal attenuation of Tie2 did not produce an obvious effect on blood vessels in tail  
174 skin at P7 (Figure 3-figure supplement 2A), or ear skin at P21 (Figure 3-figure  
175 supplement 2B). However, veins in ear skin were found to be tortuous in 2.5  
176 month-old adult mutants compared with the control mice (Figure 4A, arrows). The  
177 expression analysis by real-time RT-PCR revealed that *Tek* transcript level remained  
178 low in Tek<sup>-fIUCKO</sup> mice at this stage (Tek<sup>-fIUCKO</sup>: 0.26 ± 0.14, n=5; Control: 1.0 ± 0.28,  
179 n=5). Interestingly, the venous tortuosity was also observed in retinas of Tek<sup>-fIUCKO</sup>  
180 mice at the adult stage (2.5 month-old) while the increased angiogenesis along the  
181 retinal veins regressed (Figure 4B). The findings suggest that Tie2 has an important  
182 role in the postnatal maintenance of veins.

183

#### 184 **Requirement of Tie2 for the maintenance of venous EC identity**

185 Mechanistically, we found that Tie2 attenuation led to the alteration of venous EC  
186 identity as shown by the change of EC marker expression (Figure 5A, and Table 1).  
187 Transcript levels of the venous marker APJ and EphB4 were decreased, whereas  
188 COUP-TFII mRNA level was unaltered in the retinas and lungs of Tek<sup>-fIUCKO</sup> mice

189 compared with littermate controls (P7; Figure 5A). Furthermore, there was a  
 190 significant increase of arterial and angiogenic sprout marker Dll4 transcripts in the  
 191 lungs (Figure 5A)<sup>22</sup>. Consistently, Tie2 reduction induced Dll4 expression in retinal  
 192 veins (P9; Figure 5B, arrows point to veins in dotted regions), which were negative by  
 193 immunostaining for Dll4 in littermate control mice (Figure 5C). There was no  
 194 significant alteration of other arterial markers including NRP1, EphrinB2 and NOTCH1  
 195 (P7; Figure 5A). Furthermore, we also examined the expression level of some venous  
 196 and arterial markers, including EphB4, APJ, Ephrin B2 and Dll4 in *Tek* mutant and  
 197 control mice at the adult stage. Consistently, we found that venous genes were  
 198 significantly decreased in lung of *Tek*<sup>-fUcko</sup> mice compared with controls (EphB4,  
 199 *Tek*<sup>-fUcko</sup>:  $0.52 \pm 0.29$ , n=5; Control:  $1.0 \pm 0.18$ , n=5; APJ, *Tek*<sup>-fUcko</sup>:  $0.22 \pm 0.22$ , n=5;  
 200 Control:  $1.0 \pm 0.25$ , n=5). Interestingly, there was also a trend of reduction in the  
 201 arterial gene expression in *Tek*<sup>-fUcko</sup> mice (Ephrin B2, *Tek*<sup>-fUcko</sup>:  $0.71 \pm 0.32$ , n=5;  
 202 Control:  $1.0 \pm 0.23$ , n=5; Dll4, *Tek*<sup>-fUcko</sup>:  $0.70 \pm 0.36$ , n=5; Control:  $1.0 \pm 0.21$ , n=5),  
 203 suggesting that Tie2 retardation may also affect arteries at later stages.

204

## 205 **Regulation of COUP-TFII protein stability by Tie2/Akt pathway**

206 Tie2 deletion led to a decrease of Akt phosphorylation (Ser473, Figure 6A, B).  
 207 Interestingly, COUP-TFII protein was significantly decreased in lung and liver tissues  
 208 of *Tek* mutant mice (Figure 6A, B and Figure 6-figure supplement 1A, B), although  
 209 COUP-TFII mRNA level was not altered, as shown above. This was further verified in  
 210 cultured HUVECs, where COUP-TFII protein was decreased when Tie2 was reduced

211 by siRNA mediated knockdown (Figure 6C-D). Consistently, COUP-TFII protein was  
212 significantly increased by the COMP-Ang1 stimulation of Tie2/Akt pathway (Figure  
213 6E-F). As the Tie2 downstream Akt activation was significantly suppressed in mice  
214 with Tie2 attenuation, we also analyzed COUP-TFII level when the PI3K/Akt pathway  
215 was blocked. COUP-TFII protein was significantly reduced 6h or 12 h after treatment  
216 with the PI3K inhibitor LY294002 (Figure 6G, H; LY-3h:  $1.11 \pm 0.39$ , n=5; LY-6h:  $0.62 \pm$   
217  $0.12$ , n=5; LY-12h:  $0.39 \pm 0.13$ , n=5; values from five independent experiments  
218 normalized against control at three time points respectively). This was further  
219 confirmed with the Akt inhibitor MK2206, and there was a significant decrease of  
220 COUP-TFII after Akt inhibition at the 12 h time point (Figure 6I, J; MK-3h:  $1.32 \pm 0.47$ ,  
221 n=7; MK-6h:  $0.75 \pm 0.31$ , n=7; MK-12h:  $0.23 \pm 0.18$ , n=7; values from seven  
222 independent experiments normalized against control at three time points respectively).  
223 Furthermore, the decrease of COUP-TFII protein by the Akt inhibition could be  
224 reverted by the treatment with a proteasome inhibitor MG132 (Figure 6K-L). These  
225 findings suggest that the Tie2 signaling pathway controls vein specification via  
226 Akt-mediated regulation of COUP-TFII protein stability (Figure 6M).

227

## 228 Discussion

229 We show here that Tie2 is more expressed in veins than arteries in early embryos and  
230 in retina of neonate mice with the newly formed arteries expressing low level of Tie2.  
231 Interestingly, Tie2 is also downregulated in the sprouting tip endothelial cells as  
232 observed in retinal angiogenesis in this study and also by others<sup>12</sup>. It has been

233 recently reported that vein-derived endothelial tip cells contribute to the emerging  
234 arteries during mouse retinal vascularization and also in zebrafish fin regeneration<sup>23</sup>.  
235 This suggests that the downregulation of Tie2 may be required for the initial  
236 establishment of an arterial EC identity. Consistently, we have demonstrated in this  
237 study that Tie2 absence or insufficiency by gene targeting disrupts venogenesis  
238 during embryogenesis and postnatal development. At the molecular level, we have  
239 found that Tie2 participates in the determination of venous EC identity, which may act  
240 via Akt-mediated regulation of COUP-TFII protein stability. This implies that Tie2/Akt  
241 signaling counterbalances VEGFR2/MAPK pathway in arteriovenous specification  
242 during the vascular development. The findings are consistent with previous literature  
243 on the role of Akt in venous development, and with the recent report that  
244 cardiomyocyte derived Ang1 is required for the subepicardial coronary vein formation<sup>2</sup>.  
245 11, 24-26.

246  
247 As Tie2 is expressed by endothelial cells and non-endothelial cells such as  
248 hematopoietic cells, we employed three Cre deletors in this study to analyze the role  
249 of Tie2 in blood vascular development, including a EC-specific Cre line *Cdh5-Cre*<sup>ERT2</sup>,  
250 a hematopoietic Cre line *Vav-iCre* and a ubiquitous Cre line *Ubc-Cre*<sup>ERT2</sup>. Blood  
251 vessels developed normally in mice with *Tek* deletion in blood cells, while disruption of  
252 vein development was observed in *Tek*<sup>-fIUCKO</sup> as well as in *Tek*<sup>-fIECKO</sup> mutant mice. This  
253 suggests that the disruption of cutaneous vein development during embryogenesis is  
254 likely to be a cell-autonomous effect resulting from the deletion of Tie2 in endothelial

255 cells. In postnatal studies, we found that there was a dramatic increase of blood  
256 vessel growth after the ubiquitous Tie2 attenuation, which led to the formation of  
257 haemangioma-like vascular tufts along the retinal veins in the *Tek* mutant mice.  
258 Although a significant decrease of retinal vascularization was observed in *Tek*<sup>-fIECKO</sup>  
259 mice, we did not observe the vascular tuft formation in the retina of these mutants.  
260 This may result from the lower Tie2 deletion efficiency in *Tek*<sup>-fIECKO</sup> mice when  
261 compared with that of *Tek*<sup>-fUCKO</sup> mice. However, we cannot completely rule out the  
262 possibility that Tie2 deletion in other non-endothelial cells may contribute to the  
263 vascular abnormalities in retinas of *Tek*<sup>-fUCKO</sup> mutant mice. As retinal  
264 neovascularization is one of the frequent causes of vision loss in patients with  
265 proliferative diabetic retinopathy and neovascular age-related macular degeneration<sup>27</sup>,  
266 these data suggests that reduction of Tie2 mediated signals in ECs and / or other Tie2  
267 expressing cells may be implicated in the vascular pathologies.

268

269 COUP-TFII is expressed by several cell types including endothelial cells<sup>28</sup>. In the  
270 vascular system, COUP-TFII has been shown to regulate venous EC identity as well  
271 as lymphatic EC specification<sup>9, 29, 30</sup>. At the transcription level, COUP-TFII is regulated  
272 by several factors / pathways including NOTCH and SOX7/18<sup>10</sup>. In this study, we  
273 have found that COUP-TFII protein but not its mRNA level is significantly reduced in  
274 genetically engineered mouse model targeting *Tek*. Based on the evidence obtained  
275 from the biochemical analysis with cultured endothelial cells, we propose that Akt is a  
276 strong candidate mediating Tie2 signals in this process. As Akt acts downstream of



277 many signaling pathways and that it is also activated in many cell types, it remains to  
278 be investigated how Akt regulates COUP-TFII protein stability in venous ECs. Also,  
279 further *in vivo* mechanistic studies are required for validating and fully elucidating Akt  
280 and others factors / pathways downstream of Tie2 in venous specification. In addition,  
281 we have also found that the requirement of Tie2 for vein development differs between  
282 the skin and mesentery. When Tie2 levels were reduced by gene targeting, veins  
283 were mostly undetectable in the skin, but displayed only abnormal arterial-venous  
284 alignment in the mesentery. It is possible that the cutaneous veins are more sensitive  
285 to the loss of Tie2 mediated signals, or that venogenesis occurs earlier in the  
286 mesentery than in the skin. The abnormal arteriovenous alignment resembled that of  
287 the APJ deficient mice<sup>31</sup>, and a significant reduction of APJ in the *Tek* mutants  
288 suggests that APJ acts downstream of Tie2 in the regulation of venous patterning.

289

290 Interestingly, we have also found that both the total and phosphorylated Dok-2  
291 decreased significantly after Tie2 attenuation in this study. As Dok family members  
292 have been shown to negatively regulate ERK1/2 activation<sup>32</sup>, the decrease of Dok-2  
293 may lead to the increase of retinal angiogenesis as detected in mice with Tie2  
294 reduction by gene targeting. Consistently, enhancement of Tie2 signaling via the  
295 inhibition of VE-PTP has been shown to stabilize blood vessels and suppress retinal  
296 angiogenesis in mouse models of ischemia-induced retinal neovascularization<sup>33</sup>.  
297 Furthermore, in experiments using HEK 293T or endothelial cells overexpressing  
298 Dok2, it was found that Dok2, via directly interacting with Tie2, mediated Tie2 pathway

299 in endothelial cell migration<sup>34, 35</sup>. Decreased Dok-2 activation in *Tek* mutants may also  
300 account for the suppression of horizontal and vertical blood vessel growth during  
301 retinal vascular network formation. So far, *in vivo* evidence about the role of Dok2 in  
302 blood vascular development is still missing. Further studies employing animal models  
303 targeting *Dok2* are important to analyze its biological functions in the vascular system.

304

305 In summary, we show that Tie2 is required for the specification and maintenance of  
306 venous EC identity. Related to the findings of this study, activating mutations of Tie2  
307 have been linked to venous malformations in patients<sup>16</sup>. It is still poorly understood  
308 about the difference between the pathways downstream of activating Tie2 mutants  
309 and the wildtype Tie2. Activation of wildtype Tie2 by its ligand Ang1 or VE-PTP  
310 inhibition, at least for a short period, has been shown to stabilize blood vasculature<sup>33</sup>,  
311 while activating Tie2 mutations lead to venous malformations<sup>16, 17, 36</sup>. Mechanisms  
312 underlying the discrepancy require further investigation. As alteration of Tie2  
313 mediated signals may be implicated in a variety of vascular pathologies associated  
314 with the venous system, further investigation along these lines may help to develop  
315 novel Tie2-targeted therapeutics.

316

## 317 **Materials and methods**

### 318 **Animal models**

319 Conditional mice with *Tek* gene targeted flox sites (*Tek*<sup>Flox</sup>) for gene deletion were  
320 generated by the National Resource Center for Mutant Mice, Nanjing University, as

321 previously described<sup>18</sup>. All animal experiments were performed in accordance with the  
322 institutional guidelines of the Soochow and Nanjing University Animal Center  
323 (MARC-AP#YH2). To generate mice with ubiquitous or cell-specific *Tek* gene deletion,  
324 *Tek*<sup>Flox</sup> mice were crossed with transgenic mice expressing Cre recombinase in ECs  
325 (*Cdh5-Cre*<sup>ERT2</sup>)<sup>19</sup>, hematopoietic cells (*Vav1-iCre*)<sup>21</sup>, or ubiquitously (*Ubc-Cre*<sup>ERT2</sup> or  
326 *Ella-Cre*)<sup>37, 38</sup>. The floxed mice used in this study were maintained in C57BL/6J  
327 (RRID:IMSR\_JAX:000664) with at least five backcrosses. In all the phenotype  
328 analysis, littermates were used as control.

329

### 330 **Induction of gene deletion**

331 Induction of gene deletion was performed by tamoxifen treatment as previously  
332 described<sup>18</sup>. Briefly, pregnant mice were treated with tamoxifen (Sigma-Aldrich) at  
333 E10.5-12.5 or E12.5-14.5 (1-2 mg/per mouse for 3 consecutive days by  
334 intraperitoneal injection), and analyzed later. New-born pups were treated with  
335 tamoxifen by four daily intragastric injections and after P7 by four daily intraperitoneal  
336 injections, and analyzed later.

337

### 338 **Quantitative real-time RT-PCR**

339 Tissues from *Tek* mutant and control mice were collected and homogenized in TRIzol  
340 (Ambion). RNA extraction and reverse transcription were performed by standard  
341 procedures (RevertAid First Strand cDNA Synthesis Kit, Thermo Scientific).  
342 Quantitative real-time RT-PCR was carried out using the SYBR premix Ex Taq kit

(TaKaRa). Briefly, for each reaction, 50 ng of total RNA was transcribed for 2 min at 50 °C with a denaturing step at 95 °C for 30 s followed by 40 cycles of 5 s at 95 °C and 34 s at 60 °C. Fluorescence signal was analyzed by using ABI PRISM 7500. The primers used were as follows: GAPDH: 5'-GGTGAAGGTCGGTGTGAACG-3', 5'-CTCGCTCCTGGAAGATGGTG-3'; Tie2: 5'-GATTTTGGATTGTCCCGAGGTCAAG-3', 5'-CACCAATATCTGGGCAAATGATGG-3'; APJ: 5'-CAGTCTGAATGCGACTACGC-3', 5'-CCATGACAGGCACAGCTAGA-3'; Ephb4: 5'-CTGGATGGAGAACCCCTACA-3', 5'-CCAGGTAGAAGCCAGCTTTG-3'; COUP-TFII: 5'-GCAAGTGGAGAAGCTCAAGG-3', 5'-TTCCAAAGCACACTGGGACT-3'; NRP1: 5'-CCGGAACCCTACCAGAGAAT-3', 5'-AAGGTGCAATCTTCCCACAG-3'; EphrinB2: 5'-TGTTGGGGACTTTTGATGGT-3', 5'-GTCCACTTTGGGGCAAATAA-3'; NOTCH1: 5'-TGTTGTGCTCCTGAAGAACG-3', 5'-TCCATGTGATCCGTGATGTC-3'; DII4: 5'-TGCCTGGGAAGTATCCTCAC-3', 5'-GTGGCAATCACACACTCGTT-3'. The transcripts of venous and arterial markers were normalized against GAPDH, and the relative expression level of every gene in the *Tek* mutants (*Tek*<sup>-f<sup>l</sup>UCKO</sup>) was normalized against that of littermate control mice.

360

### 361 **Western blot analysis**

362 To analyze Tie2 mediated signaling pathway, lung tissues from *Tek* mutant and  
363 control mice were homogenized following standard procedures. Antibodies used  
364 included rabbit polyclonal anti-Tie2 (Santa Cruz sc-324, RRID:AB\_631102), rabbit

365 polyclonal anti-Akt (Cell Signaling Technology #9272, RRID:AB\_329827), rabbit  
366 monoclonal anti-phospho-Akt473 (Cell Signaling Technology, #4060), rabbit  
367 polyclonal anti-phospho-p56Dok-2 (Cell Signaling Technology #3911,  
368 RRID:AB\_2095082), rabbit polyclonal anti-p56Dok-2 (Cell Signaling Technology  
369 #3914, RRID:AB\_2095080), rabbit polyclonal anti-Erk1/2 and phospho-Erk1/2 (Cell  
370 Signaling Technology #9101, RRID:AB\_331646; and 9102, AB\_330744), mouse  
371 monoclonal anti-COUP-TFII (R&D Systems #PP-H7147-00, RRID:AB\_2155627), and  
372 mouse monoclonal to beta-actin antibody (C4, Santa Cruz sc-47778,  
373 RRID:AB\_626632).

374

#### 375 **Cell culture, siRNA transfection and Akt inhibition**

376 HUVECs (human umbilical vein endothelial cell, C0035C, GIBCO) were cultured in  
377 endothelial cell basal medium plus supplements (#M200-500 GIBCO, or #1001  
378 ScienCell Research Laboratories). To knock down Tie2 expression in HUVECs, cells  
379 were transfected with Stealth RNAi™ siRNA duplex oligoribonucleotides targeting  
380 human Tie2 (HSS110623, HSS110624 and HSS110625; Invitrogen) using  
381 Lipofectamine RNAiMax (Invitrogen); Stealth RNAi negative control duplexes  
382 (medium GC) were used as a control. COMP-Ang1 (kind gift from Dr. Gou Young Koh;  
383 0.2-0.4 µg/ml) or Ang1 (923-AN, R&D) was used to stimulate Tie2/Akt pathway. To  
384 inhibit PI3K and downstream Akt signaling, HUVECs were treated with LY294002 (40  
385 µM, S1105, Selleckchem) or MK2206 (10 µM, S1078, Selleckchem) and analyzed at  
386 3 h, 6 h or 12 h after treatment. For the experiment with proteasome inhibition,

HUVECs were treated with MG132 (10  $\mu$ M, s2619, Selleckchem). The cells were washed with ice-cold PBS and lysed in the lysis buffer (1 mM PMSF, 2 mM  $\text{Na}_3\text{VO}_4$ , 1 $\times$  protease and phosphatase inhibitor cocktail without EDTA (Roche Applied Science), 20 mM Tris-HCl pH 8.0, 100 mM NaCl, 10% glycerol, 50 mM NaF, 10 mM  $\beta$ -glycerolphosphate, 5 mM sodium pyrophosphate, 5 mM EDTA, 0.5 mM EGTA and 1% NP-40). The lysates were incubated on ice for 0.5 h with rotation and centrifuged. Protein concentration was determined using the BCA protein assay kit (PIERCE), and equal amounts of protein were used for analysis.

#### **Immunostaining**

For whole-mount immunostaining with embryonic skin, mesentery and retina, tissues were harvested and processed as previously described<sup>18</sup>. The tissues were fixed in 4% paraformaldehyde, blocked with 3% (w/v) milk in PBS-TX (0.3% Triton X-100), and incubated with primary antibodies overnight at 4 °C. The antibodies used were rat anti-mouse PECAM-1 (BD Pharmigen, 553370, RRID:AB\_394816), goat anti-mouse Tie2 (R&D, AF762, RRID:AB\_2203220), goat anti-mouse Dll4 (R&D, AF1389, RRID:AB\_354770), goat anti-mouse EphB4 (R&D, AF446, RRID:AB\_2100105), Cy3-conjugated mouse anti-mouse  $\alpha$ SMA (Sigma, C6198, RRID:AB\_476856). Alexa488, Alexa594 (Invitrogen), Cy5- or Cy3- (Jackson) conjugated secondary antibodies were used for staining. Slides were mounted with Vectashield (VectorLabs), and analyzed with the Olympus FluoView 1000 confocal microscope or Olympus BX51 fluorescent dissection microscope. For staining of frozen sections, retinas were

409 collected and fixed in 4% PFA for 1 h at 4 °C, incubated in 20% sucrose overnight and  
410 then embedded in OCT. Consecutive sections (10 µm in thickness) were incubated  
411 with antibodies against PECAM-1 (BD Pharmingen, 553370, RRID:AB\_394816) and  
412 NG2 (Millipore, AB5320, RRID:AB\_11213678), followed by staining with the  
413 appropriate fluorochrome-conjugated secondary antibodies and mounted as  
414 described above.

415

#### 416 **Analysis of retinal vascularization**

417 Retinal vascularization index was quantified as the ratio of vascularized area to total  
418 retinal area. For the quantification of blood vessel parameters in the retina,  
419 fluorescent images were taken from similar regions in all samples. Blood vessel  
420 density was measured and analyzed by using Image Pro Plus (MediaCybernetics), as  
421 previously described<sup>18</sup>.

422

#### 423 **Statistical analysis**

424 Statistical analysis was performed with the unpaired *t* test. All statistical tests were  
425 two-sided. Data are presented as mean ± S.D.

426

#### 427 **Acknowledgements**

428 We thank Dr. Dietmar Vestweber and Martina Dierkes for the discussion and kind help  
429 with experiments using COMP-Ang1, and staff in the Animal facility of Soochow  
430 University and Model Animal Research Institute of Nanjing University for technical

431 assistance. This work was supported by grants from the National Natural Science  
432 Foundation of China (91539101, 31271530, 31071263), the Ministry of Science and  
433 Technology of China (2012CB947600), and the Priority Academic Program  
434 Development of Jiangsu Higher Education Institutions.

435

436



## 437 Reference

- 438 1. Lanahan A, Zhang X, Fantin A, Zhuang Z, Rivera-Molina F, Speichinger K, Prahst C, Zhang J,  
439 Wang Y, Davis G, Toomre D, Ruhrberg C, Simons M. The neuropilin 1 cytoplasmic domain is  
440 required for vegf-a-dependent arteriogenesis. *Dev Cell*. 2013;25:156-168
- 441 2. Deng Y, Larrivee B, Zhuang ZW, Atri D, Moraes F, Prahst C, Eichmann A, Simons M. Endothelial  
442 raf1/erk activation regulates arterial morphogenesis. *Blood*. 2013;121:3988-3996,  
443 S3981-3989
- 444 3. Lawson ND, Scheer N, Pham VN, Kim CH, Chitnis AB, Campos-Ortega JA, Weinstein BM. Notch  
445 signaling is required for arterial-venous differentiation during embryonic vascular  
446 development. *Development*. 2001;128:3675-3683
- 447 4. Duarte A, Hirashima M, Benedito R, Trindade A, Diniz P, Bekman E, Costa L, Henrique D,  
448 Rossant J. Dosage-sensitive requirement for mouse *dll4* in artery development. *Genes Dev*.  
449 2004;18:2474-2478
- 450 5. Wythe JD, Dang LT, Devine WP, Boudreau E, Artap ST, He D, Schachterle W, Stainier DY,  
451 Oettgen P, Black BL, Bruneau BG, Fish JE. Ets factors regulate vegf-dependent arterial  
452 specification. *Dev Cell*. 2013;26:45-58
- 453 6. Seo S, Fujita H, Nakano A, Kang M, Duarte A, Kume T. The forkhead transcription factors,  
454 *foxc1* and *foxc2*, are required for arterial specification and lymphatic sprouting during  
455 vascular development. *Dev Biol*. 2006;294:458-470
- 456 7. Corada M, Nyqvist D, Orsenigo F, Caprini A, Giampietro C, Taketo MM, Iruela-Arispe ML,  
457 Adams RH, Dejana E. The wnt/beta-catenin pathway modulates vascular remodeling and  
458 specification by upregulating *dll4*/notch signaling. *Dev Cell*. 2010;18:938-949
- 459 8. Corada M, Orsenigo F, Morini MF, Pitulescu ME, Bhat G, Nyqvist D, Breviario F, Conti V, Briot A,  
460 Iruela-Arispe ML, Adams RH, Dejana E. *Sox17* is indispensable for acquisition and  
461 maintenance of arterial identity. *Nature communications*. 2013;4:2609
- 462 9. You LR, Lin FJ, Lee CT, DeMayo FJ, Tsai MJ, Tsai SY. Suppression of notch signalling by the  
463 coup-tfii transcription factor regulates vein identity. *Nature*. 2005;435:98-104
- 464 10. Swift MR, Pham VN, Castranova D, Bell K, Poole RJ, Weinstein BM. *Soxf* factors and notch  
465 regulate *nr2f2* gene expression during venous differentiation in zebrafish. *Dev Biol*.  
466 2014;390:116-125
- 467 11. Ren B, Deng Y, Mukhopadhyay A, Lanahan AA, Zhuang ZW, Moodie KL, Mulligan-Kehoe MJ,  
468 Byzova TV, Peterson RT, Simons M. *Erk1/2-akt1* crosstalk regulates arteriogenesis in mice and  
469 zebrafish. *J Clin Invest*. 2010;120:1217-1228
- 470 12. Augustin HG, Young Koh G, Thurston G, Alitalo K. Control of vascular morphogenesis and  
471 homeostasis through the angiopoietin-tie system. *Nature reviews. Molecular cell biology*.  
472 2009;10:165-177
- 473 13. Dumont DJ, Gradwohl G, Fong GH, Puri MC, Gertsenstein M, Auerbach A, Breitman ML.  
474 Dominant-negative and targeted null mutations in the endothelial receptor tyrosine kinase,  
475 *tek*, reveal a critical role in vasculogenesis of the embryo. *Genes Dev*. 1994;8:1897-1909
- 476 14. Sato TN, Tozawa Y, Deutsch U, Wolburg-Buchholz K, Fujiwara Y, Gendron-Maguire M, Gridley T,  
477 Wolburg H, Risau W, Qin Y. Distinct roles of the receptor tyrosine kinases *tie-1* and *tie-2* in  
478 blood vessel formation. *Nature*. 1995;376:70-74
- 479 15. Thomson BR, Heinen S, Jeansson M, Ghosh AK, Fatima A, Sung HK, Onay T, Chen H,  
480 Yamaguchi S, Economides AN, Flenniken A, Gale NW, Hong YK, Fawzi A, Liu X, Kume T,

- 481 Quaggin SE. A lymphatic defect causes ocular hypertension and glaucoma in mice. *J Clin*  
482 *Invest.* 2014;124:4320-4324
- 483 16. Vikkula M, Boon LM, Carraway KL, 3rd, Calvert JT, Diamonti AJ, Goumnerov B, Pasyk KA,  
484 Marchuk DA, Warman ML, Cantley LC, Mulliken JB, Olsen BR. Vascular dysmorphogenesis  
485 caused by an activating mutation in the receptor tyrosine kinase tie2. *Cell.*  
486 1996;87:1181-1190
- 487 17. Limaye N, Wouters V, Uebelhoer M, Tuominen M, Wirkkala R, Mulliken JB, Eklund L, Boon LM,  
488 Vikkula M. Somatic mutations in angiopoietin receptor gene tek cause solitary and multiple  
489 sporadic venous malformations. *Nat Genet.* 2009;41:118-124
- 490 18. Shen B, Shang Z, Wang B, Zhang L, Zhou F, Li T, Chu M, Jiang H, Wang Y, Qiao T, Zhang J, Sun W,  
491 Kong X, He Y. Genetic dissection of tie pathway in mouse lymphatic maturation and valve  
492 development. *Arterioscler Thromb Vasc Biol.* 2014;34:1221-1230
- 493 19. Wang Y, Nakayama M, Pitulescu ME, Schmidt TS, Bochenek ML, Sakakibara A, Adams S, Davy  
494 A, Deutsch U, Luthi U, Barberis A, Benjamin LE, Makinen T, Nobes CD, Adams RH. Ephrin-b2  
495 controls vegf-induced angiogenesis and lymphangiogenesis. *Nature.* 2010;465:483-486
- 496 20. Muzumdar MD, Tasic B, Miyamichi K, Li L, Luo L. A global double-fluorescent cre reporter  
497 mouse. *Genesis.* 2007;45:593-605
- 498 21. de Boer J, Williams A, Skavdis G, Harker N, Coles M, Tolaini M, Norton T, Williams K, Roderick  
499 K, Potocnik AJ, Kioussis D. Transgenic mice with hematopoietic and lymphoid specific  
500 expression of cre. *European journal of immunology.* 2003;33:314-325
- 501 22. Hellstrom M, Phng LK, Hofmann JJ, Wallgard E, Coultas L, Lindblom P, Alva J, Nilsson AK,  
502 Karlsson L, Gaiano N, Yoon K, Rossant J, Iruela-Arispe ML, Kalen M, Gerhardt H, Betsholtz C.  
503 Dll4 signalling through notch1 regulates formation of tip cells during angiogenesis. *Nature.*  
504 2007;445:776-780
- 505 23. Xu C, Hasan SS, Schmidt I, Rocha SF, Pitulescu ME, Bussmann J, Meyen D, Raz E, Adams RH,  
506 Siekmann AF. Arteries are formed by vein-derived endothelial tip cells. *Nature*  
507 *communications.* 2014;5:5758
- 508 24. Zimmermann S, Moelling K. Phosphorylation and regulation of raf by akt (protein kinase b).  
509 *Science.* 1999;286:1741-1744
- 510 25. Lamont RE, Childs S. Mapping out arteries and veins. *Science's STKE : signal transduction*  
511 *knowledge environment.* 2006;2006:pe39
- 512 26. Arita Y, Nakaoka Y, Matsunaga T, Kidoya H, Yamamizu K, Arima Y, Kataoka-Hashimoto T, Ikeoka  
513 K, Yasui T, Masaki T, Yamamoto K, Higuchi K, Park JS, Shirai M, Nishiyama K, Yamagishi H, Otsu  
514 K, Kurihara H, Minami T, Yamauchi-Takahara K, Koh GY, Mochizuki N, Takakura N, Sakata Y,  
515 Yamashita JK, Komuro I. Myocardium-derived angiopoietin-1 is essential for coronary vein  
516 formation in the developing heart. *Nature communications.* 2014;5:4552
- 517 27. Gariano RF, Gardner TW. Retinal angiogenesis in development and disease. *Nature.*  
518 2005;438:960-966
- 519 28. Wu SP, Yu CT, Tsai SY, Tsai MJ. Choose your destiny: Make a cell fate decision with coup-tfii.  
520 *The Journal of steroid biochemistry and molecular biology.* 2016;157:7-12
- 521 29. Lin FJ, Chen X, Qin J, Hong YK, Tsai MJ, Tsai SY. Direct transcriptional regulation of neuropilin-2  
522 by coup-tfii modulates multiple steps in murine lymphatic vessel development. *J Clin Invest.*  
523 2010;120:1694-1707
- 524 30. Srinivasan RS, Geng X, Yang Y, Wang Y, Mukatira S, Studer M, Porto MP, Lagutin O, Oliver G.

- 525 The nuclear hormone receptor coup-tfii is required for the initiation and early maintenance  
526 of prox1 expression in lymphatic endothelial cells. *Genes Dev.* 2010;24:696-707
- 527 31. Kidoya H, Naito H, Muramatsu F, Yamakawa D, Jia W, Ikawa M, Sonobe T, Tsuchimochi H,  
528 Shirai M, Adams RH, Fukamizu A, Takakura N. Apj regulates parallel alignment of arteries and  
529 veins in the skin. *Dev Cell.* 2015;33:247-259
- 530 32. Honma M, Higuchi O, Shirakata M, Yasuda T, Shibuya H, Iemura S, Natsume T, Yamanashi Y.  
531 Dok-3 sequesters grb2 and inhibits the ras-erk pathway downstream of protein-tyrosine  
532 kinases. *Genes to cells : devoted to molecular & cellular mechanisms.* 2006;11:143-151
- 533 33. Shen J, Frye M, Lee BL, Reinardy JL, McClung JM, Ding K, Kojima M, Xia H, Seidel C, Lima e  
534 Silva R, Dong A, Hackett SF, Wang J, Howard BW, Vestweber D, Kontos CD, Peters KG,  
535 Campochiaro PA. Targeting ve-tpo activates tie2 and stabilizes the ocular vasculature. *J Clin*  
536 *Invest.* 2014;124:4564-4576
- 537 34. Saharinen P, Eklund L, Miettinen J, Wirkkala R, Anisimov A, Winderlich M, Nottebaum A,  
538 Vestweber D, Deutsch U, Koh GY, Olsen BR, Alitalo K. Angiopoietins assemble distinct tie2  
539 signalling complexes in endothelial cell-cell and cell-matrix contacts. *Nat Cell Biol.*  
540 2008;10:527-537
- 541 35. Master Z, Jones N, Tran J, Jones J, Kerbel RS, Dumont DJ. Dok-r plays a pivotal role in  
542 angiopoietin-1-dependent cell migration through recruitment and activation of pak. *The*  
543 *EMBO journal.* 2001;20:5919-5928
- 544 36. Boscolo E, Limaye N, Huang L, Kang KT, Soblet J, Uebelhoer M, Mendola A, Natynki M, Seront  
545 E, Dupont S, Hammer J, Legrand C, Brugnara C, Eklund L, Vikkula M, Bischoff J, Boon LM.  
546 Rapamycin improves tie2-mutated venous malformation in murine model and human  
547 subjects. *J Clin Invest.* 2015;125:3491-3504
- 548 37. Lakso M, Pichel JG, Gorman JR, Sauer B, Okamoto Y, Lee E, Alt FW, Westphal H. Efficient in  
549 vivo manipulation of mouse genomic sequences at the zygote stage. *Proc Natl Acad Sci U S A.*  
550 1996;93:5860-5865
- 551 38. Ruzankina Y, Pinzon-Guzman C, Asare A, Ong T, Pontano L, Cotsarelis G, Zediak VP, Velez M,  
552 Bhandoola A, Brown EJ. Deletion of the developmentally essential gene atr in adult mice  
553 leads to age-related phenotypes and stem cell loss. *Cell Stem Cell.* 2007;1:113-126

## 554 **Figure legends**

### 555 **Figure 1 Tie2 insufficiency during embryogenesis arrests venous development.**

556 **A, B.** Analysis of blood vessels in head (A, E9.5) and somites (B) by whole-mount  
557 immunostaining for PECAM-1 (green) and Tie2 (red). **C.** Tamoxifen intraperitoneal  
558 (i.p.) administration and analysis scheme. **D-F.** Visualization of veins in E15.5 (D, E)  
559 or E17.5 (F) skin of wildtype and *Tek* mutant mice by immunostaining for PECAM-1

(green) and EphB4 or  $\alpha$ SMA (red). Arrows point to veins and arrowheads to arteries.

The experiments with the ubiquitous or EC-specific *Tek* deletion were repeated for at least three times. Scale bar: 200  $\mu$ m in A, D and F (4 mm in F embryos); 100  $\mu$ m in B and E (2 mm in E embryos).

**Figure 2 Attenuation of Tie2 expression retards retinal vascularization. A.**

Tamoxifen intragastric (i.g.) administration and analysis scheme. **B-D.** The deletion efficiency of Tie2 was examined by Western blot analysis (B) and immunostaining (C, D) for PECAM-1 (green) and Tie2 (red) of tissues from *Tek* deleted and littermate control mice at P7. Note that Tie2 expression is downregulated in tip endothelial cells (asterisk in C and D) and also low in newly formed retinal arteries (arrowhead in C and D) when compared with veins (arrow in C and D). **E, F.** Quantification of the vascularization index (ratio of vascularized area to total retina area normalized against the littermate controls) after ubiquitous (E, *Tek*<sup>-f/UCKO</sup>: 61.95  $\pm$  10.79, n=12; Control: 100.0  $\pm$  10.94, n=12; P<0.0001) or EC-specific deletion (F, *Tek*<sup>-f/ECKO</sup>: 80.69  $\pm$  11.13, n=5; Control: 100.0  $\pm$  3.77, n=7; P<0.0015). **G-J.** Visualization of retinal blood vessels (G, H, P7) by immunostaining for PECAM-1 (green) and EphB4 (red). Arrows point to veins (v) and arrowheads to arteries (a). Quantification of blood vessel density in the distal retinal venous (I, X 10<sup>4</sup>  $\mu$ m<sup>2</sup>/grid; *Tek*<sup>-f/UCKO</sup>: 16.91  $\pm$  0.77, n=6; Control: 14.07  $\pm$  1.54, n=8; P=0.0014) and arterial segments (J, X 10<sup>4</sup>  $\mu$ m<sup>2</sup>/grid; *Tek*<sup>-f/UCKO</sup>: 10.45  $\pm$  2.47, n=6; Control: 10.16  $\pm$  0.76, n=8; P=0.7571) in *Tek* mutants compared with control mice. **K, L.** Analysis of Dok-2 and ERK1/2 phosphorylation. Total Dok-2,

584 ERK1/2 and beta-actin were used as loading controls. The bands were quantified and  
585 normalized against the control group (L). Scale bar: 200  $\mu$ m in C, D, G; 100  $\mu$ m in H.

586

587 **Figure 3 Tie2 attenuation leads to vascular tuft formation along retinal veins. A.**

588 Tamoxifen intragastric (i.g.) administration and analysis scheme. **B-D.** Analysis of  
589 blood vessels in the retinas of *Tek* deleted (P1-4) and control mice at P11 (B), P15 (C),  
590 and P21 (D). **E.** Cross-sectional analysis of the three layers of retinal blood vessels in  
591 *Tek* mutant and control mice. **F.** Tie2 deletion was induced at P5-8, and analysis of  
592 retinal blood vessels was performed at P21. Arrows point to haemangioma-like  
593 vascular tufts. The experiments at each time point were repeated for at least three  
594 times. Scale bar: 100  $\mu$ m in B-D and F, 25  $\mu$ m in E.

595

596 **Figure 4 Effect of long-term postnatal attenuation of Tie2 on cutaneous and**

597 **retinal veins. A.** Analysis of blood vessels in the ear skin of *Tek* mutant and control  
598 mice by immunostaining for  $\alpha$ SMA (red) and EphB4 (green). **B.** Visualization of retinal  
599 blood vessels by immunostaining for Tie2 (red) and PECAM-1 (green). Note tortuous  
600 veins in ear skin and retinas in 2.5 month old *Tek*<sup>-flUcko</sup> mice after Tie2 deletion at P1-4.  
601 Arrows point to veins. The histological analysis for both groups was repeated for at  
602 least three times. Scale bar: 200  $\mu$ m in A, B.

603

604 **Figure 5 Requirement of Tie2 for the maintenance of venous EC identity. A.**

605 Quantitative expression analysis of venous markers including EphB4, APJ and

COUP-TFII, and arterial markers including EphrinB2, NRP1, NOTCH1 and Dll4 in lung and retina tissues of *Tek* mutant and control mice (P7). **B, C.** Immunostaining for Dll4 with retinas of *Tek* mutant and control mice (P9). Scale bar: 100  $\mu$ m in B and C.

**Figure 6 Regulation of COUP-TFII protein level by Tie2 pathway. A, B.** Analysis and quantification of Akt (Ser473) phosphorylation (pAkt / tAkt, *Tek*<sup>-fIUCKO</sup>:  $0.76 \pm 0.27$ , n=10; Control:  $1.0 \pm 0.19$ , n=9;  $P < 0.0407$ ) and COUP-TFII protein in lungs of *Tek* mutant and control mice, and total Akt and beta-actin as loading controls (COUP-TFII/beta-actin; *Tek*<sup>-fIUCKO</sup>:  $0.60 \pm 0.35$ , n=12; control:  $1.0 \pm 0.13$ , n=12;  $P < 0.01$ ). **C, D.** Western blotting of COUP-TFII protein in HUVECs after siRNA mediated Tie2 knockdown. COUP-TFII protein level decreased to  $80.55 \pm 17.79$  % of the control when Tie2 expression was reduced to  $24.33 \pm 13.05$  % of control (normalized by beta-actin; values from six independent experiments). **E, F.** Increase of COUP-TFII (COUP-TFII/beta-actin; COMP-Ang1:  $1.66 \pm 0.45$ , n=12; Control:  $1.0 \pm 0.15$ , n=10;  $P < 0.001$ ; values from five independent experiments) by COMP-Ang1 activation of the Tie2/Akt pathway for 12 h with the recombinant protein added every 4 h (CA1-3, 0.2-0.4  $\mu$ g/ml). Note that COMP-Ang1 added every 1 h (CA1-12) or 2 h (CA1-6) did not further increase the level of COUP-TFII, and that treatment with Ang1 or COMP-Ang1 for half an hour did not produce an obvious difference in the COUP-TFII protein level. **G-J.** Analysis of COUP-TFII in HUVECs after treatment with LY294002 or MK2206 to inhibit the PI3K/Akt signaling pathway for 3 h, 6 h or 12 h. **K, L.** Decrease of COUP-TFII by the Akt inhibitor MK2206 was blocked by the

628 proteasome inhibitor MG132 when analyzed 12 h after the treatment  
629 (COUP-TFII/beta-actin; Control:  $1.0 \pm 0.16$ , n=5; MK2206:  $0.42 \pm 0.17$ , n=5; MG132:  
630  $3.20 \pm 0.38$ , n=7; MK2206 + MG132:  $3.01 \pm 0.46$ , n=7;  $P < 0.001$ ; values from three  
631 independent experiments). **M.** Schematic model of Tie2 mediated signaling in vein  
632 specification via the Akt mediated regulation of COUP-TFII. The Tie2/Akt pathway  
633 may counterbalance VEGFR2/MAPK signaling during arteriovenous specification.

634

# 635 **Table 1**

## 636 **Retina transcript levels of venous and arterial markers**

Venous and arterial markers	mRNA expression level (retina)		n (Tek <sup>-floxKO</sup> )	n (Control)	P value
	Tek <sup>-floxKO</sup>	Control (Tek <sup>-floxKO</sup> )			
Tie2	$0.18 \pm 0.09$	$1.0 \pm 0.31$	7	7	<0.0001
APJ	$0.47 \pm 0.20$	$1.0 \pm 0.36$	7	7	0.00488
EphB4	$0.79 \pm 0.12$	$1.0 \pm 0.20$	7	7	0.0404
COUP-TFII	$0.96 \pm 0.11$	$1.00 \pm 0.10$	7	7	0.449
Dll4	$0.94 \pm 0.16$	$1.0 \pm 0.22$	7	7	0.565
EphrinB2	$0.96 \pm 0.10$	$1.0 \pm 0.24$	6	7	0.699
NRP1	$0.94 \pm 0.06$	$1.0 \pm 0.24$	6	7	0.542
NOTCH1	$0.98 \pm 0.23$	$1.0 \pm 0.22$	6	7	0.889

637

## 638 639 **Lung transcript levels of venous and arterial markers**

Venous and arterial markers	mRNA expression level (lung)		n (Tek <sup>-floxKO</sup> )	n (Control)	P value
	Tek <sup>-floxKO</sup>	Control (Tek <sup>-floxKO</sup> )			
Tie2	$0.13 \pm 0.06$	$1.0 \pm 0.29$	11	11	<0.0001
APJ	$0.55 \pm 0.14$	$1.0 \pm 0.24$	11	11	<0.0001
EphB4	$0.69 \pm 0.16$	$1.0 \pm 0.16$	11	11	0.00026
COUP-TFII	$0.98 \pm 0.24$	$1.0 \pm 0.14$	11	11	0.734
Dll4	$1.53 \pm 0.46$	$1.0 \pm 0.19$	11	11	0.00207
EphrinB2	$0.98 \pm 0.33$	$1.0 \pm 0.23$	11	11	0.856
NRP1	$1.05 \pm 0.19$	$1.0 \pm 0.26$	11	11	0.607
NOTCH1	$0.93 \pm 0.34$	$1.0 \pm 0.12$	11	11	0.549

640

## 641 642 **Figure legends for figure supplement**

### 643 **Figure 1—figure supplement 1 Generation and analysis of Tie2 knockout mice. A.**

644 PCR genotyping of Tie2 knockout and wild-type alleles. **B.** Western blot analysis of

645 Tie2 protein in *Tek* null, heterozygous and wildtype littermate mice. **C.** *Tek* null mice  
646 were smaller, showed bleedings and died at E10.5. **D.** Visualization of veins in the  
647 head region at E10.5 by whole-mount immunostaining for EphB4 and PECAM-1. **E.**  
648 Immunostaining for the arterial marker Dll4 and PECAM-1 showed lack of vein  
649 formation in somites of *Tek* null mice at E9.5. Arrows point to veins and arrowheads  
650 point to arteries. Scale bar: 200  $\mu$ m in D, 100  $\mu$ m in E.

651

652 **Figure 1–figure supplement 2 Defective skin vein formation and abnormal**  
653 **arteriovenous alignment in mesenteries of *Tek* mutant mice (*Tek*<sup>-f/UCKO</sup>).** **A.**  
654 Analysis of skin blood vessels by whole-mount immunostaining for PECAM-1 (green)  
655 in *Tek*<sup>-f/UCKO</sup> and control mice (E15.5; Tamoxifen treatment from E10.5-12.5). **B.**  
656 Analysis of mesenteric blood vessels by whole-mount immunostaining for PECAM-1  
657 (green) and  $\alpha$ SMA (red) in *Tek*<sup>-f/UCKO</sup> and control mice (E17.5; Tamoxifen treatment  
658 from E12.5-14.5). In addition to the immunostaining analysis of Tie2 protein, Tie2  
659 deletion efficiency in embryos was also analyzed by real-time RT-PCR. The level of  
660 Tie2 mRNA in the lung was  $0.25 \pm 0.02$  in *Tek*<sup>-f/UCKO</sup> (n=4), as compared with that of the  
661 heterozygous mice (*Tek*<sup>+f/UCKO</sup>:  $1.0 \pm 0.11$ , n=4). Arrowheads point to arteries and  
662 arrows to veins. Scale bar: 200  $\mu$ m in A and B.

663

664 **Figure 1–figure supplement 3- Lymphatic dilation in the skin of mutant mice**  
665 **with Tie2 deletion in vascular endothelial cells.** Analysis of skin lymphatic vessels  
666 in *Tek*<sup>-f/ECKO</sup> mutant and control embryos (E15.5) by immunostaining for LYVE1 (green).



667 Tie2 mutant mice showed subcutaneous edema (asterisk) with the dilation of  
668 lymphatic vessels (arrows; arrowheads point to the normal lymphatic vessels in  
669 control mice). Scale bar: 200  $\mu$ m.

670

671 **Figure 2-figure supplement 1 Analysis of Tie2 deletion in  $Tek^{flox/+};mTmG$  mice.**

672 The triply compound genetic mouse model ( $Tek^{flox/+};mTmG;Cdh5-Cre^{ERT2}$ , A; and  
673 control, B) was generated by three rounds of mating, and tamoxifen intragastric (i.g.)  
674 administration was performed as described in Figure 2A. The partial Tie2 deletion was  
675 indicated by the mosaic GFP expression (arrow) together with the immunostaining for  
676 Tie2 (arrowhead). Scale bar: 25  $\mu$ m.

677

678 **Figure 2-figure supplement 2 Tie2 deletion in hematopoietic cells does not**  
679 **affect retinal blood vessel growth. A, B.** Analysis of retinal blood vessels by  
680 immunostaining for PECAM-1 (green) and Tie2 (red) in  $Tek^{flox/+};Vav-iCre$  (A) and  
681  $Tek^{flox/+};Vav-iCre$  mice (control, B) at P21. Scale bar: 100  $\mu$ m in A, B.

682

683 **Figure 3-figure supplement 1 Growth curves of  $Tek^{flox/+}$  mutant and littermate**

684 **control mice.** Tie2 attenuation (Tamoxifen treatment at P1-4) led to a significant  
685 decrease in body weight gain as measured until three weeks postnatally: control mice:  
686 P7,  $3.68 \pm 0.48$  g (n=24); P9,  $3.97 \pm 0.34$  g (n=6); P11,  $5.73 \pm 1.37$  g (n=16); P21,  
687  $8.40 \pm 1.29$  g (n=8); and  $Tek^{flox/+}$  mutants: P7,  $2.71 \pm 0.51$  g (n=24;  $P<0.0001$ ); P9,  
688  $3.13 \pm 0.57$  g (n=3;  $P=0.0252$ ); P11,  $4.09 \pm 0.81$  g (n=11;  $P=0.0015$ ); P21,  $5.87 \pm 1.30$

689 g (n=6; P=0.0035).

690

691 **Figure 3—figure supplement 2 Analysis of cutaneous blood vessels at P7 and**  
692 **P21, after Tie2 deletion at P1-4. A, B.** Blood vessels were visualized by  
693 immunostaining for PECAM-1 (green) and  $\alpha$ SMA (red), and the efficiency of gene  
694 deletion was analyzed by Tie2 staining (red). No obvious defects were observed in tail  
695 skin (P7, A) or ear skin (P21, B) of  $\text{Tek}^{-f/\text{UCKO}}$  mice compared with the littermate  
696 controls. Scale bar: 100  $\mu\text{m}$  in A; 200  $\mu\text{m}$  in B.

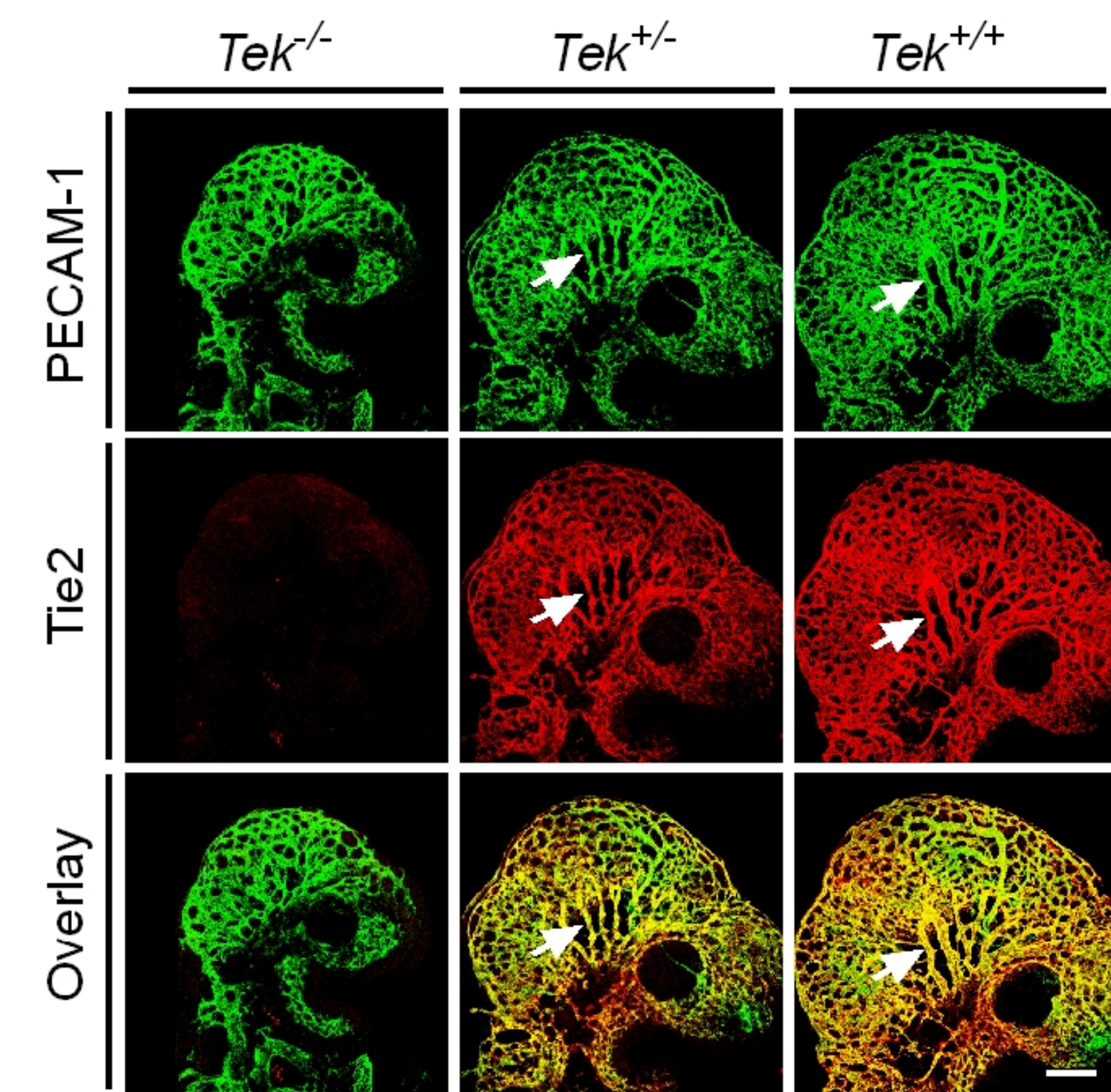
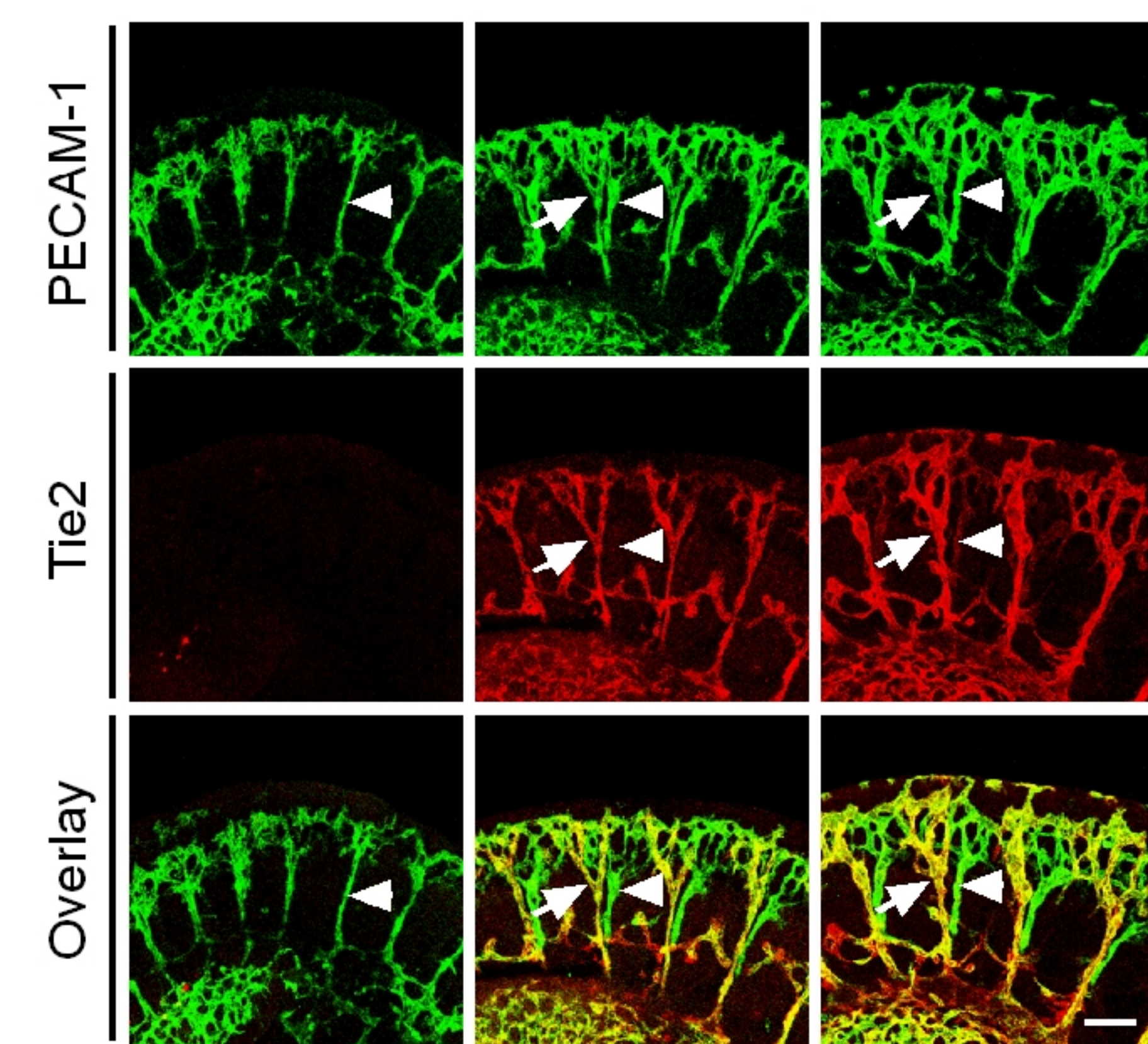
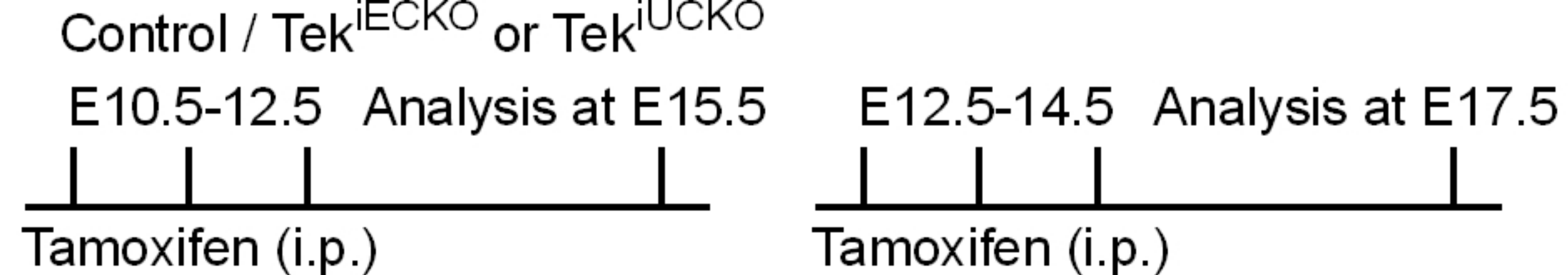
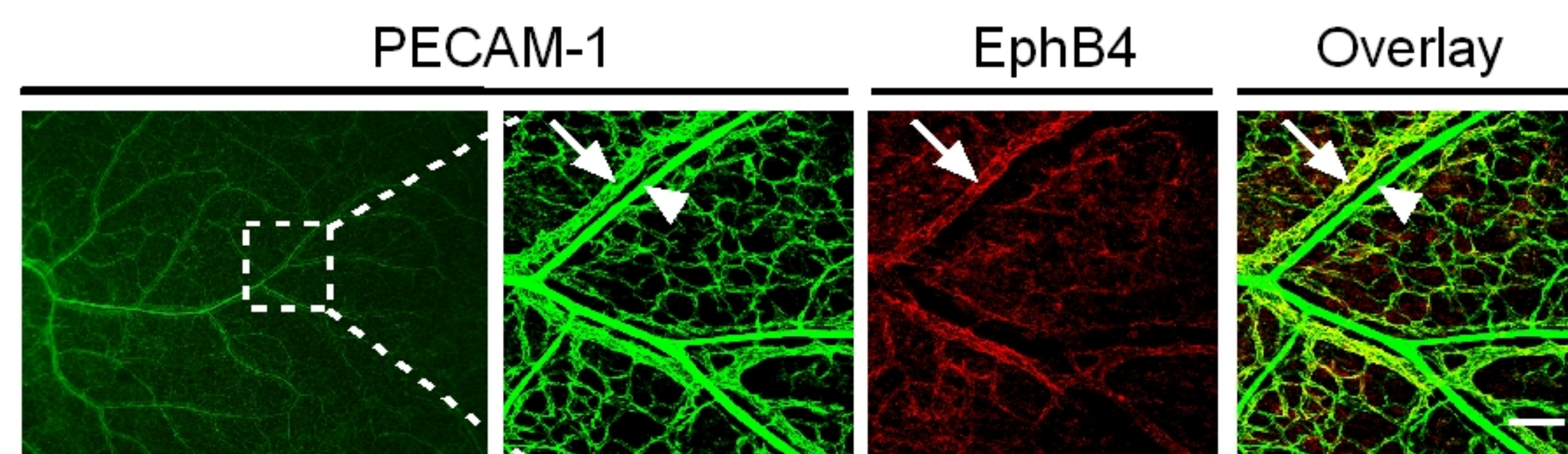
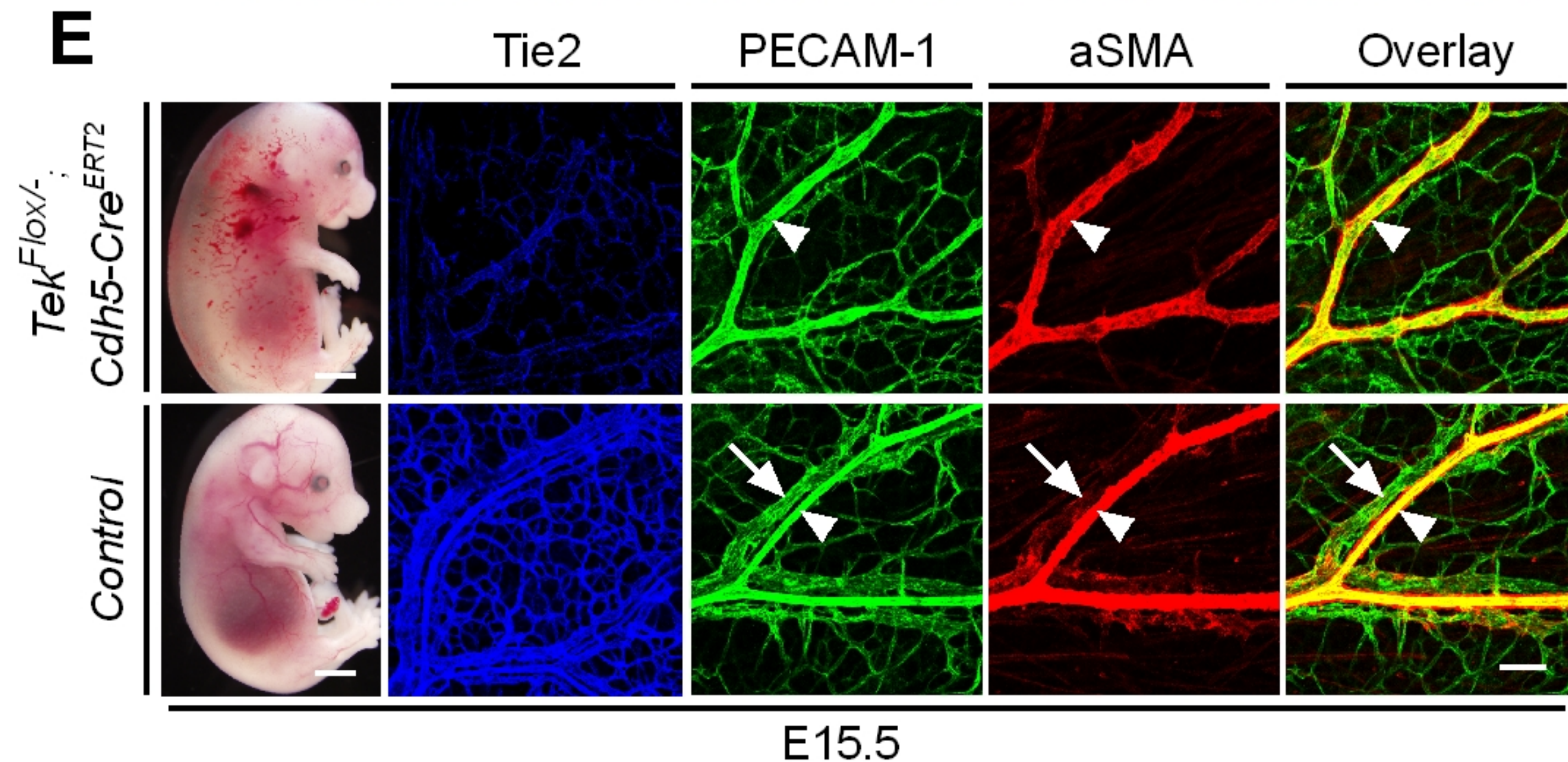
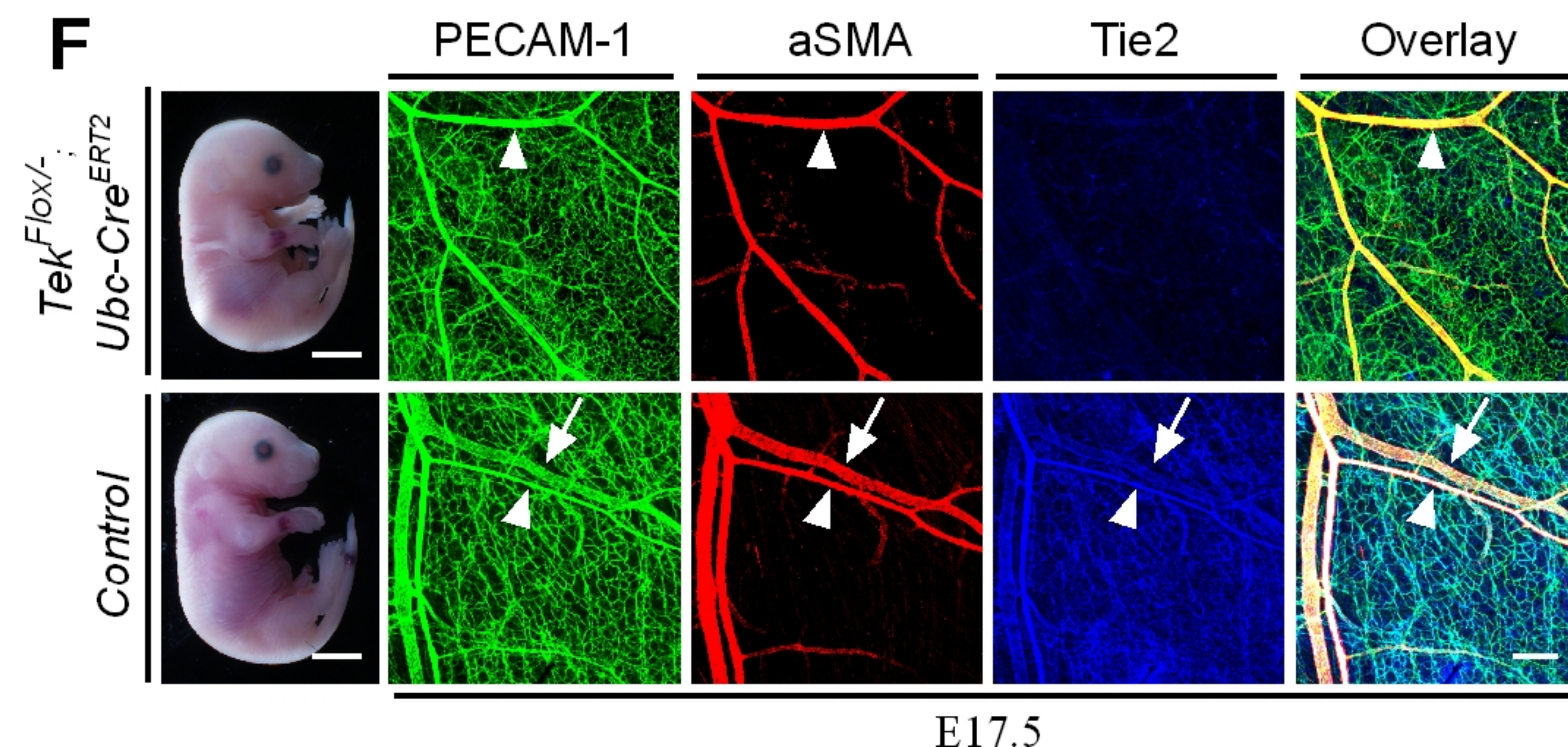
697

698 **Figure 6—figure supplement 1 Analysis of COUP-TFII in the liver. A.** Western blot  
699 analysis of COUP-TFII in liver lysates from *Tek* mutant ( $\text{Tek}^{-f/\text{UCKO}}$ ) and control mice. **B.**  
700 Quantification of COUP-TFII normalized against beta-actin ( $\text{Tek}^{-f/\text{UCKO}}$ :  $0.65 \pm 0.30$ ;  
701 *Control*:  $1.0 \pm 0.19$ , n=9 for each group; P=0.0093).

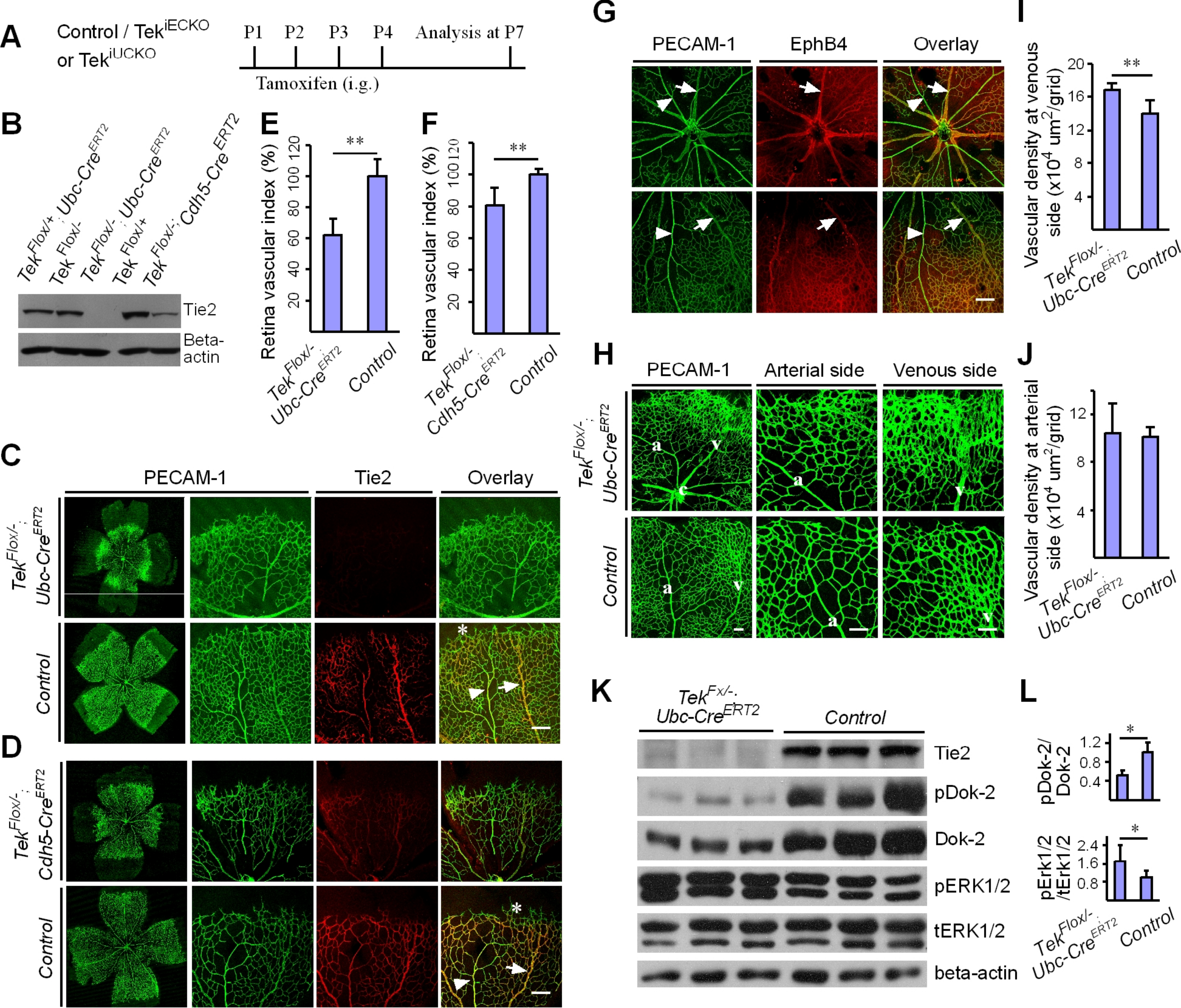
702

703

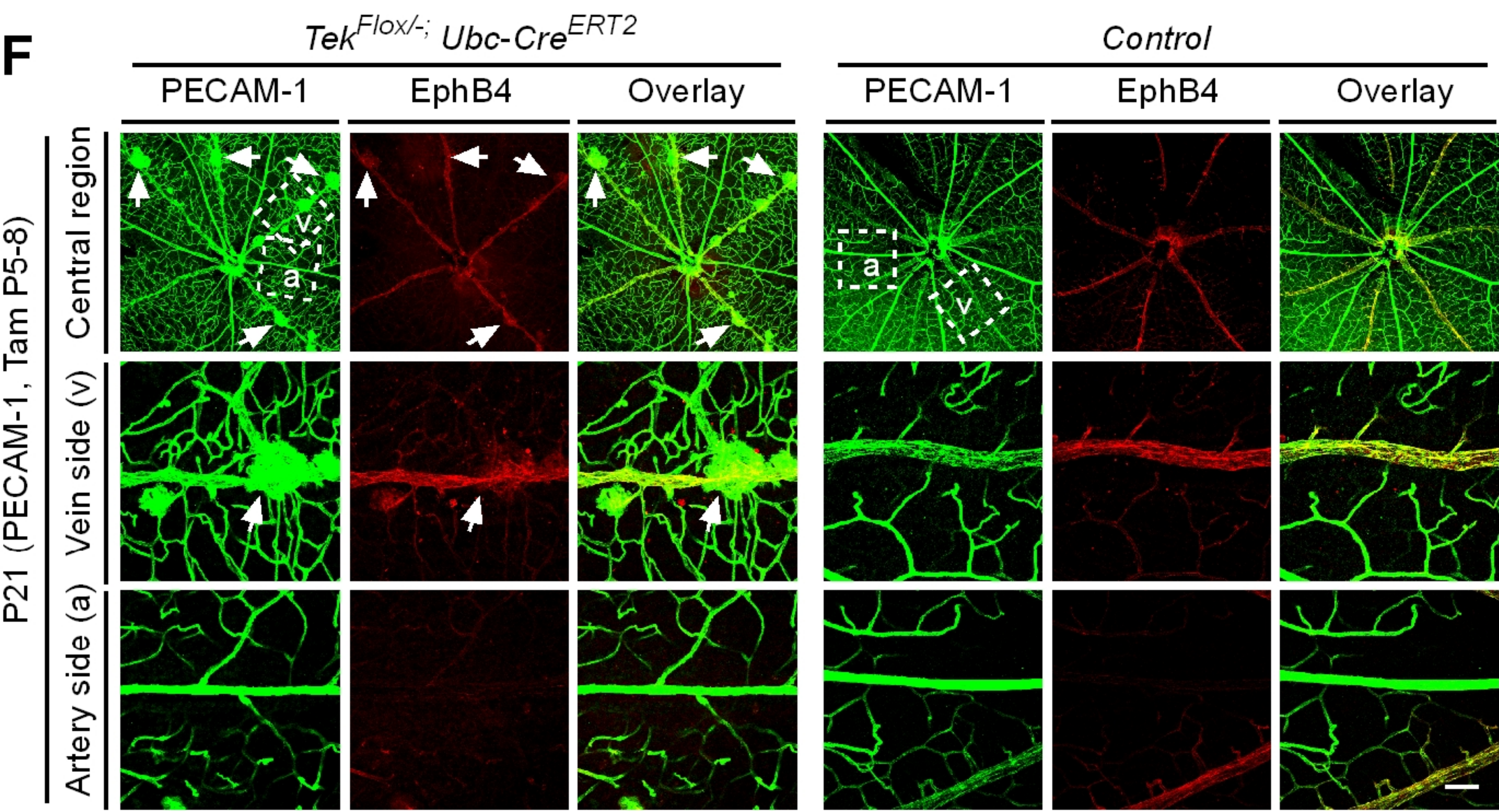
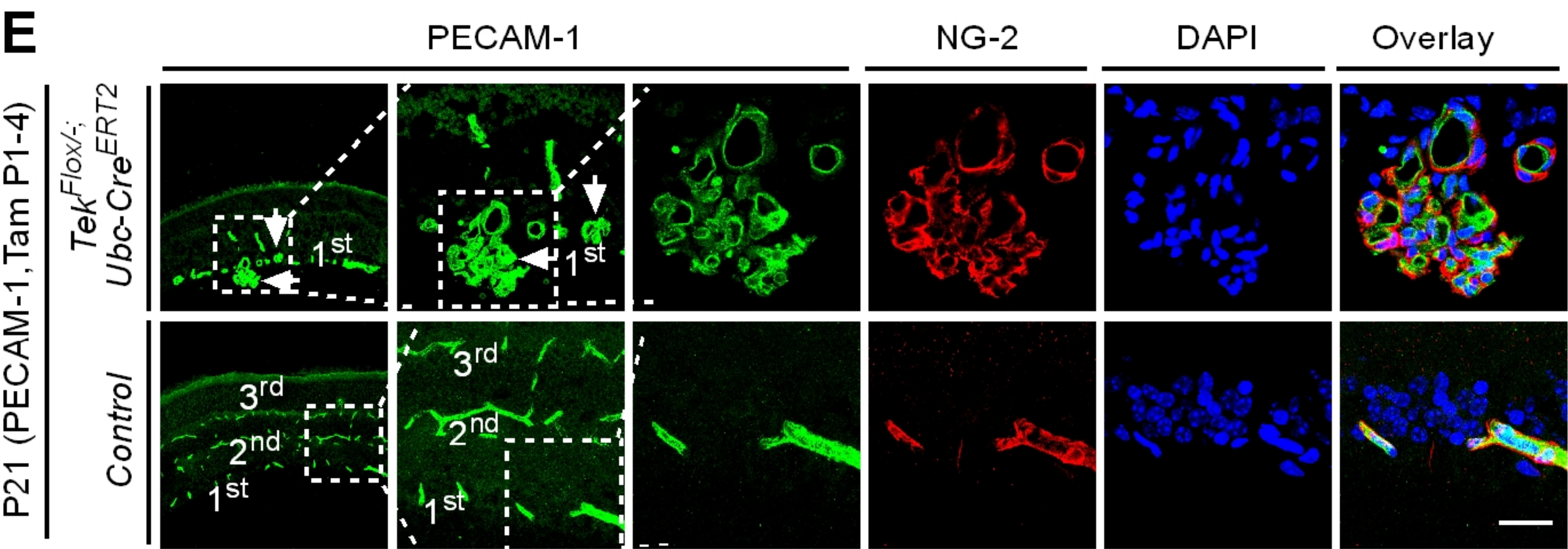
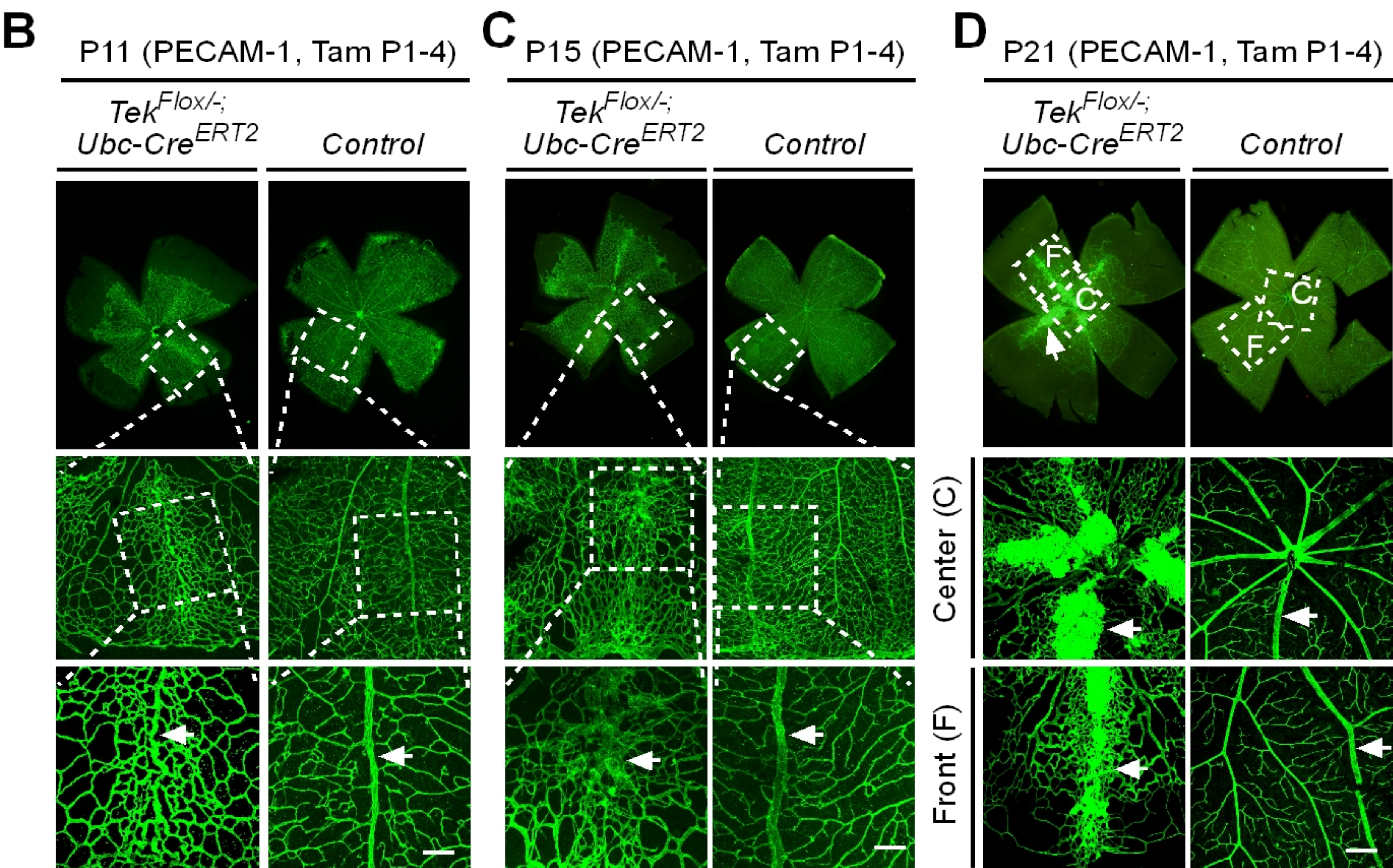
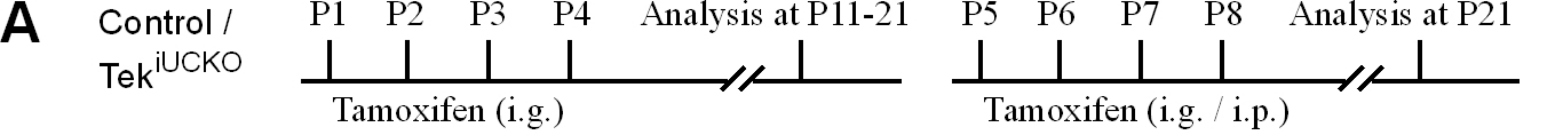


**A****B****C****D****E****F**











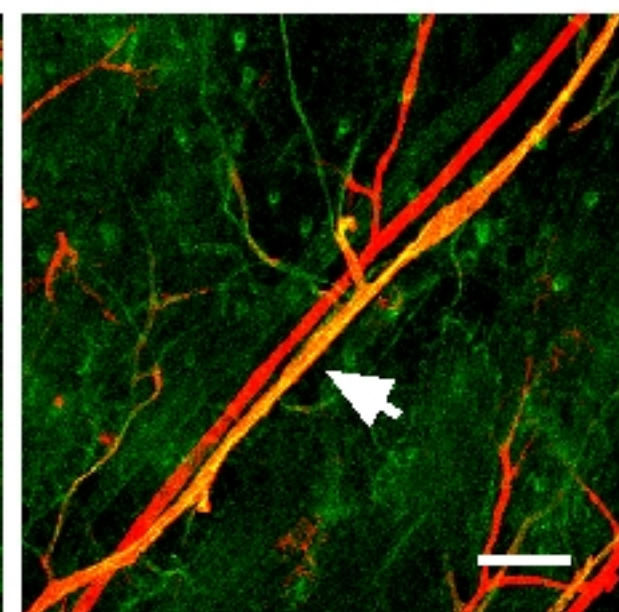
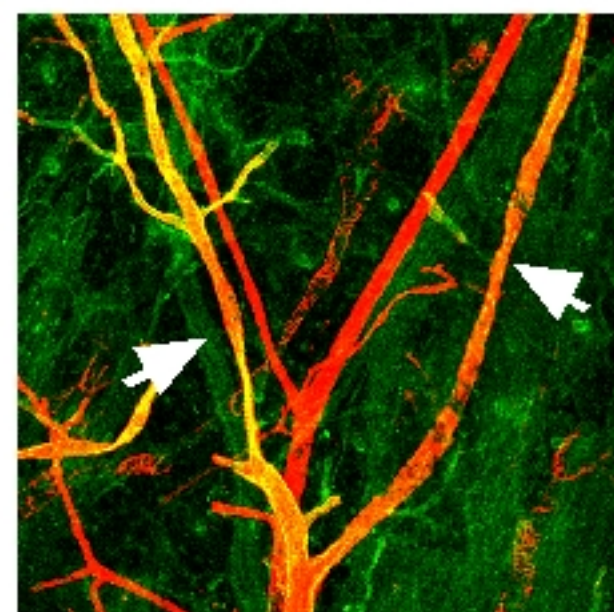
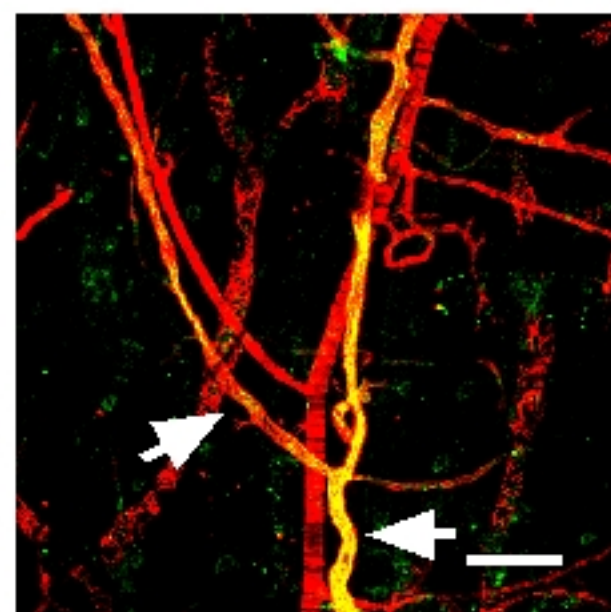
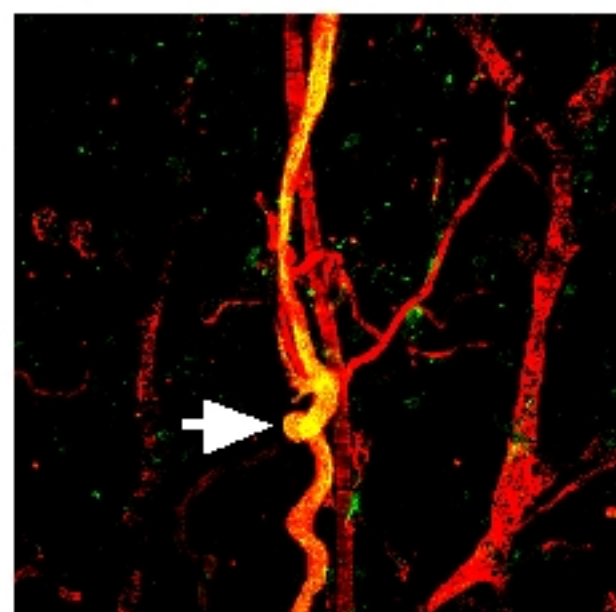
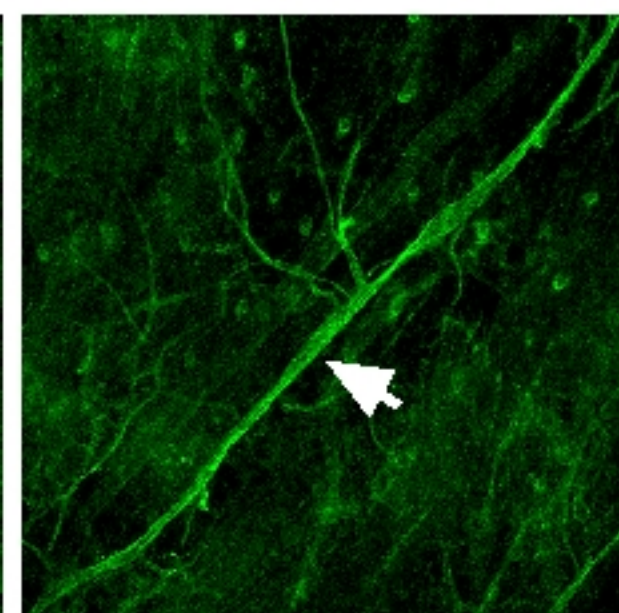
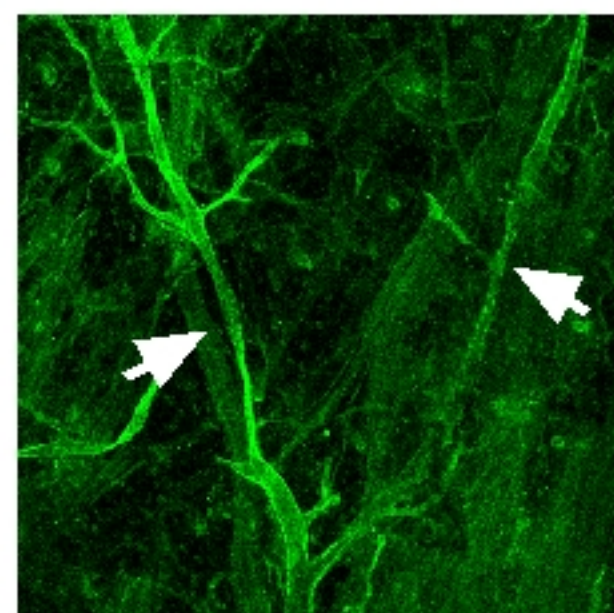
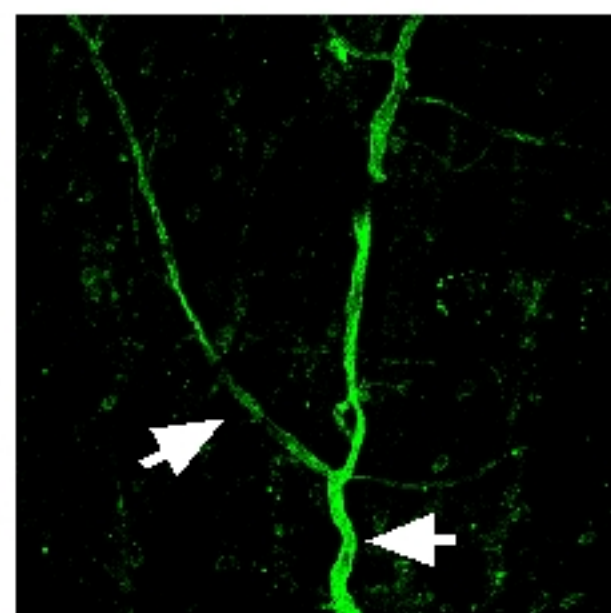
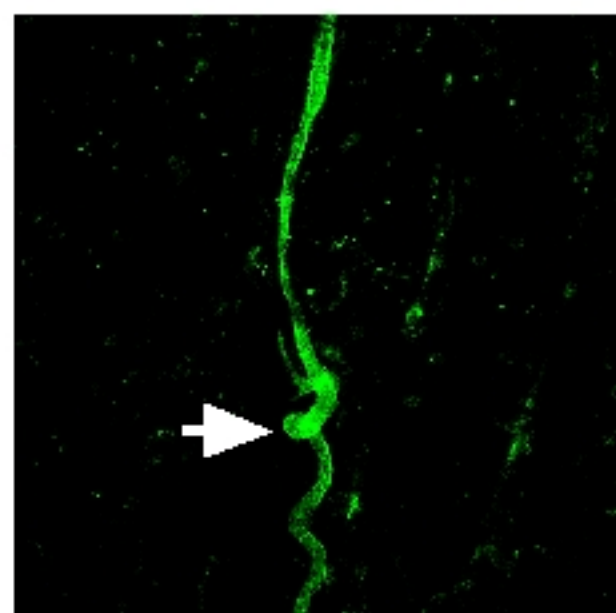
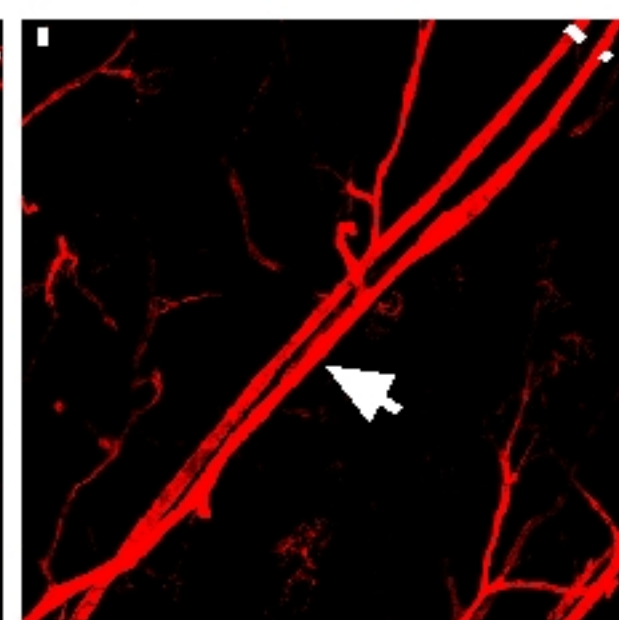
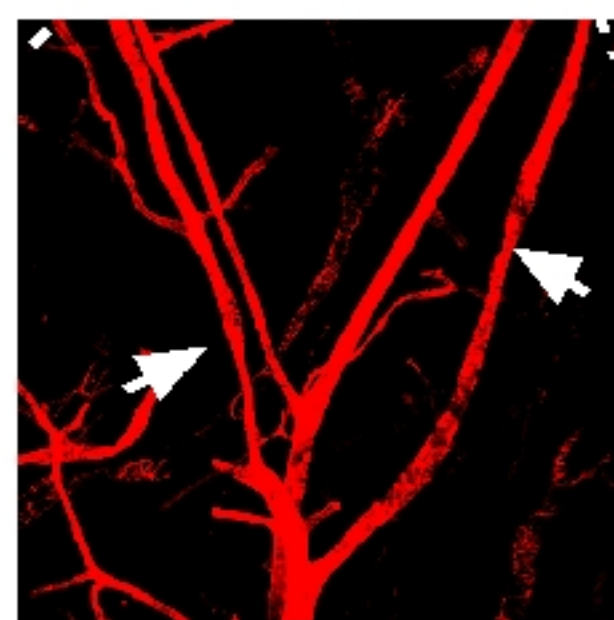
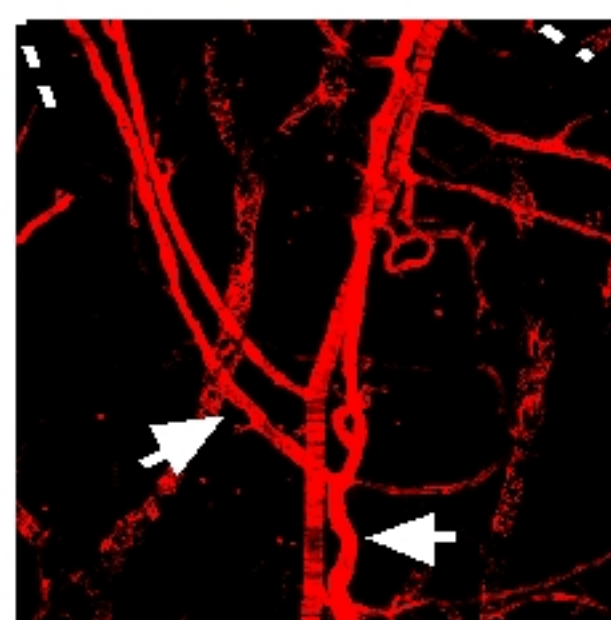
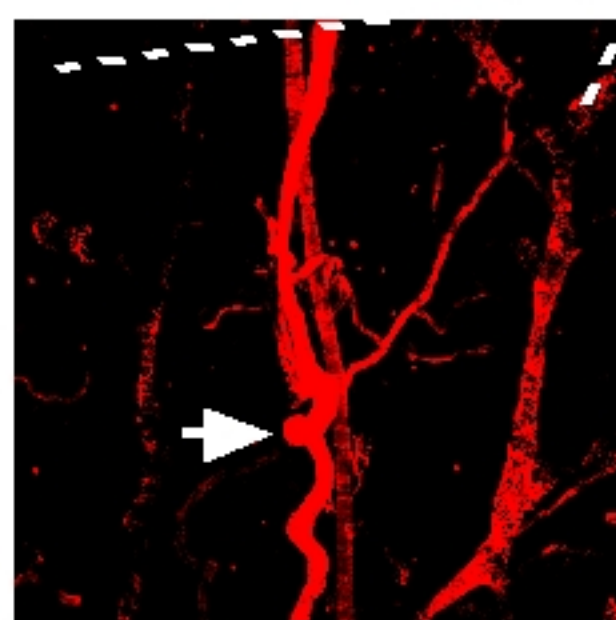
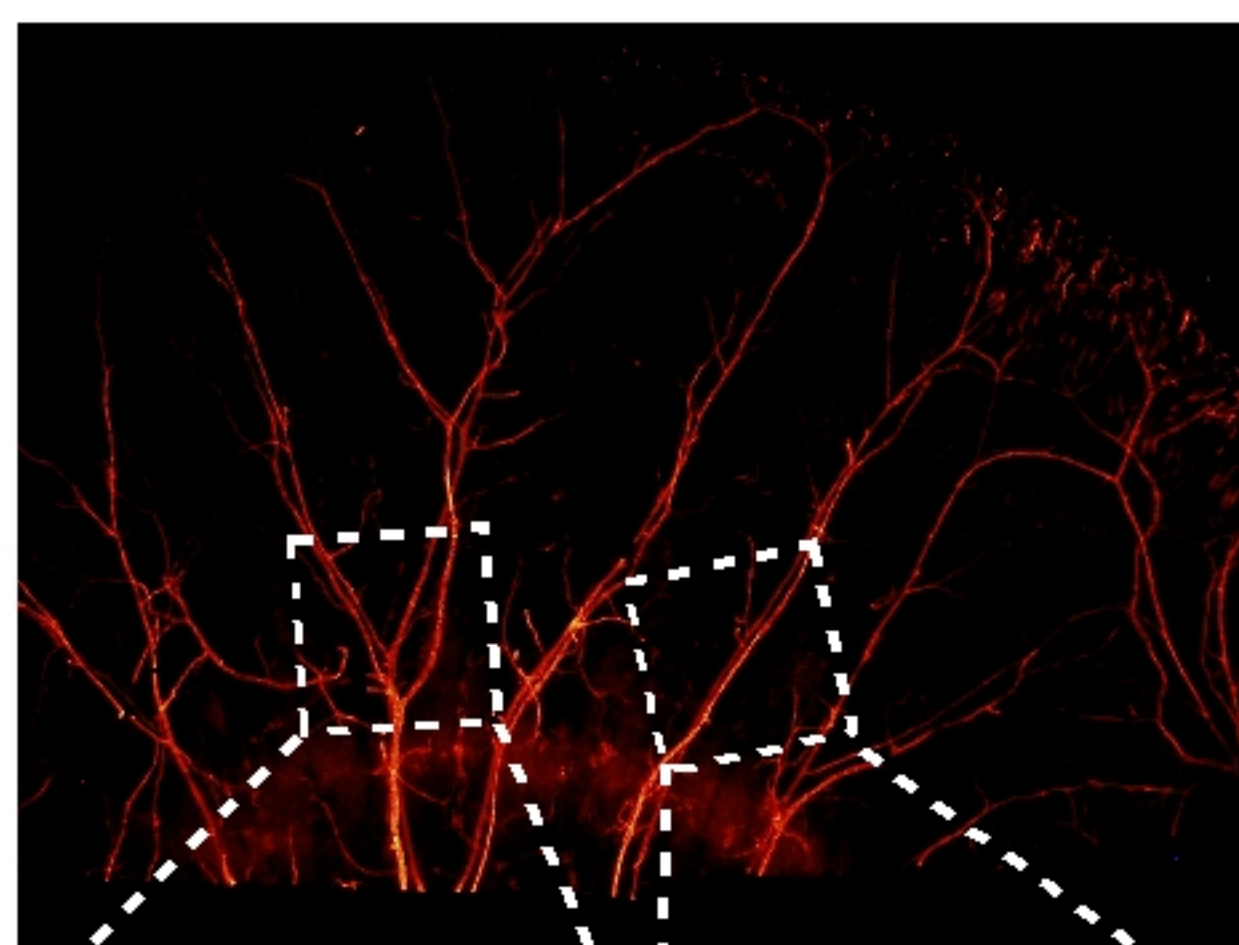
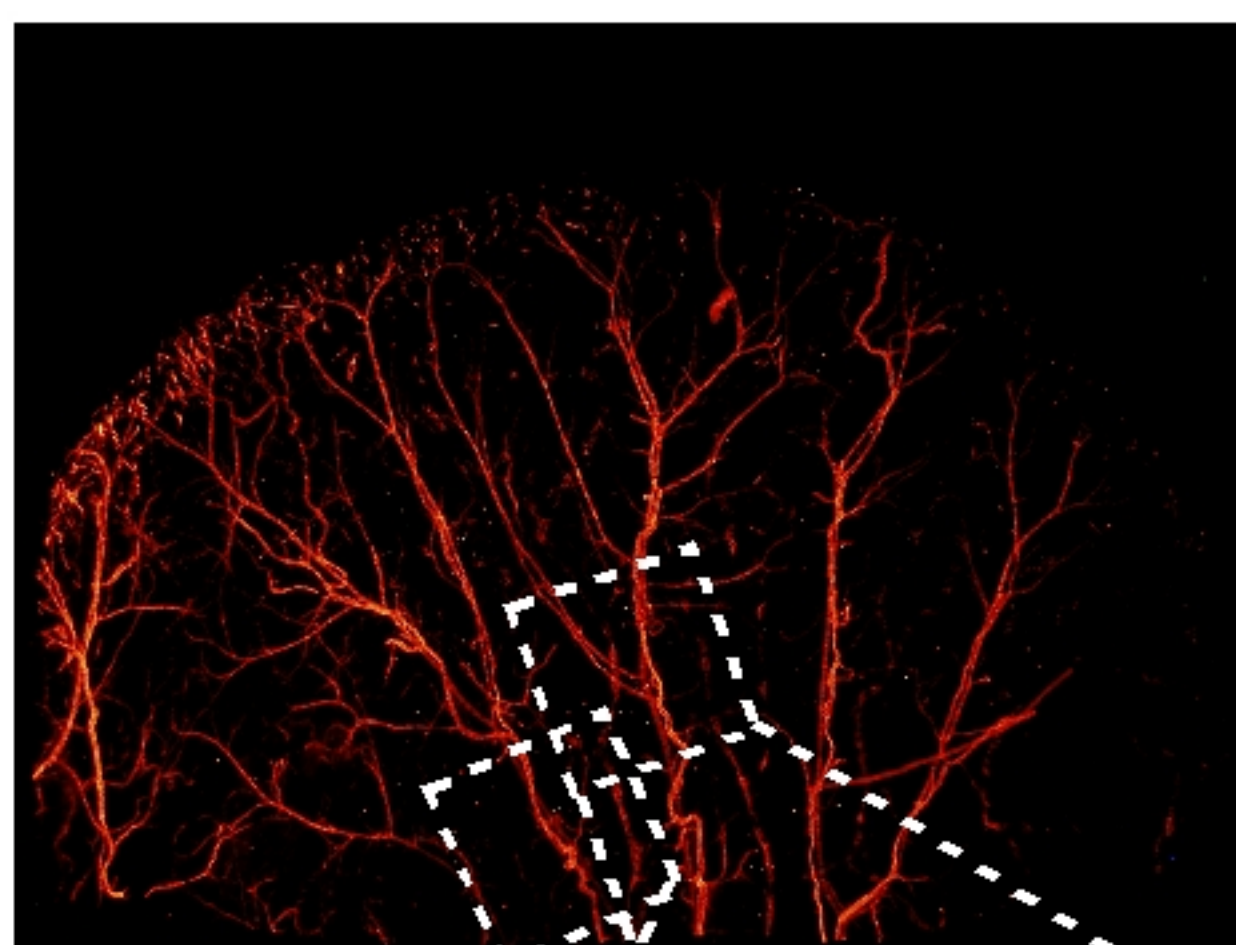
**A***Tek*<sup>Flox/-</sup>; *Ubc-Cre*<sup>ERT2</sup>

Control

aSMA

EphB4

Overlay



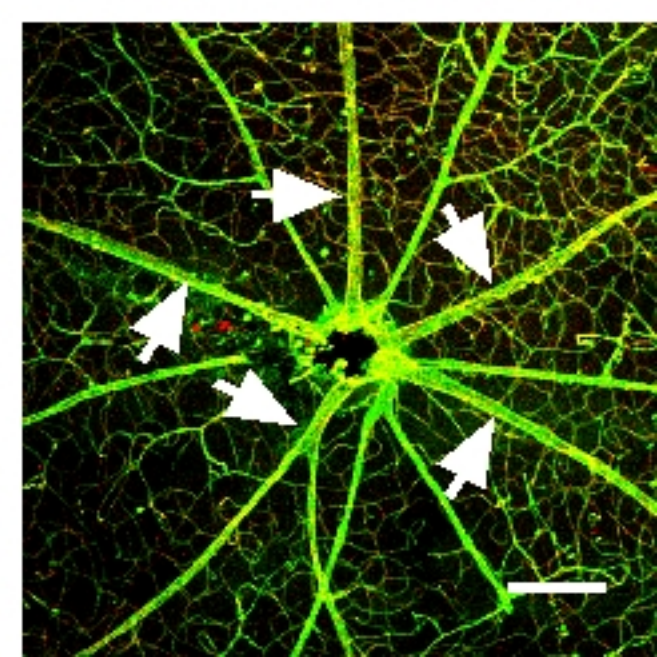
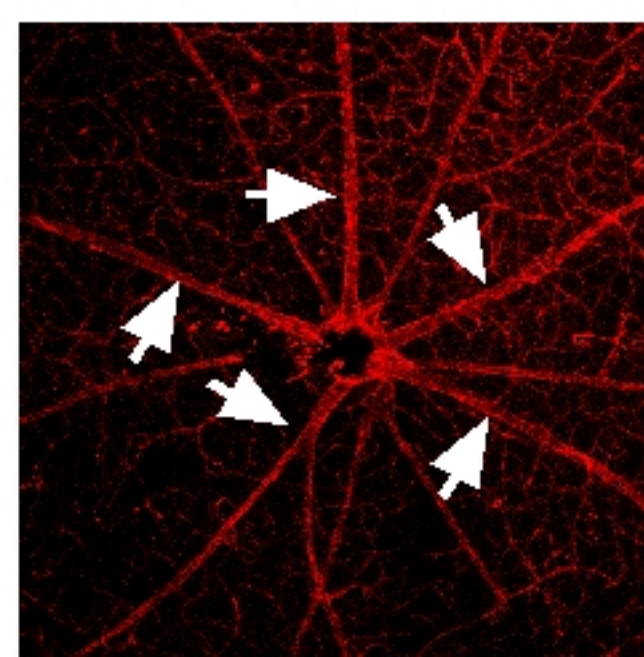
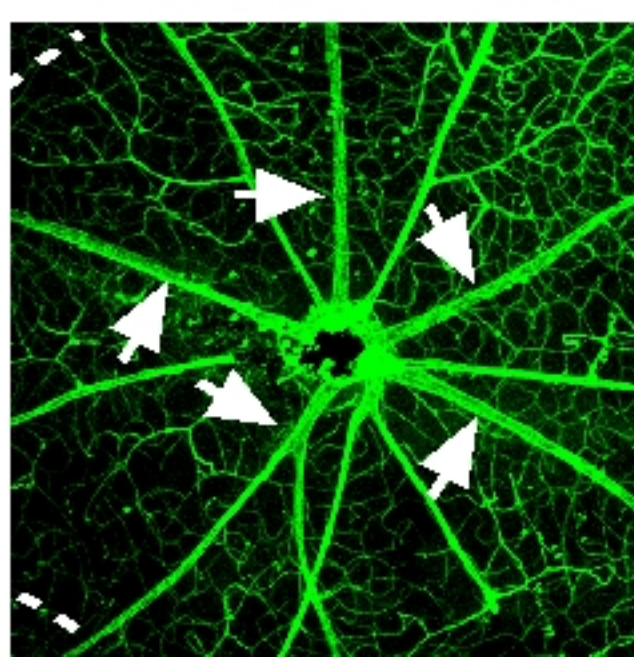
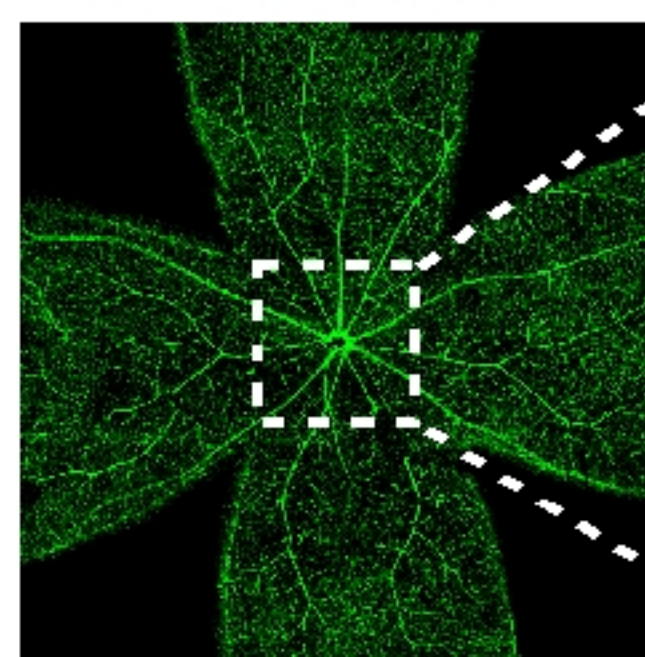
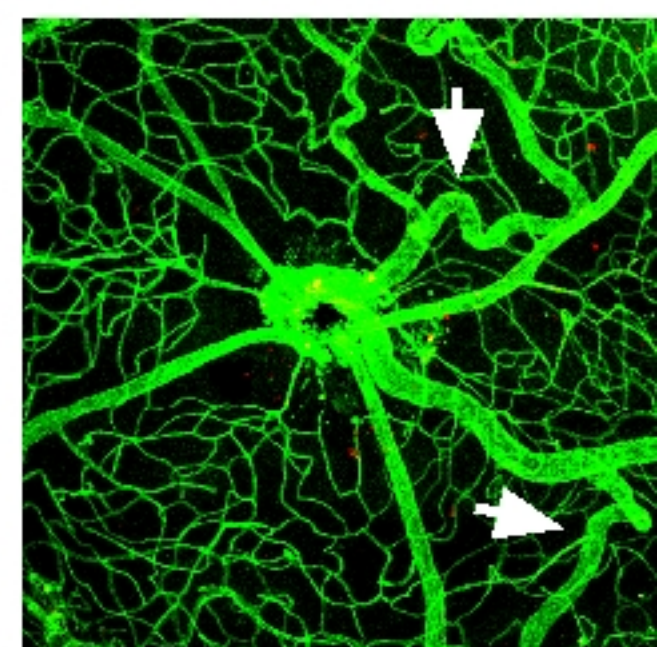
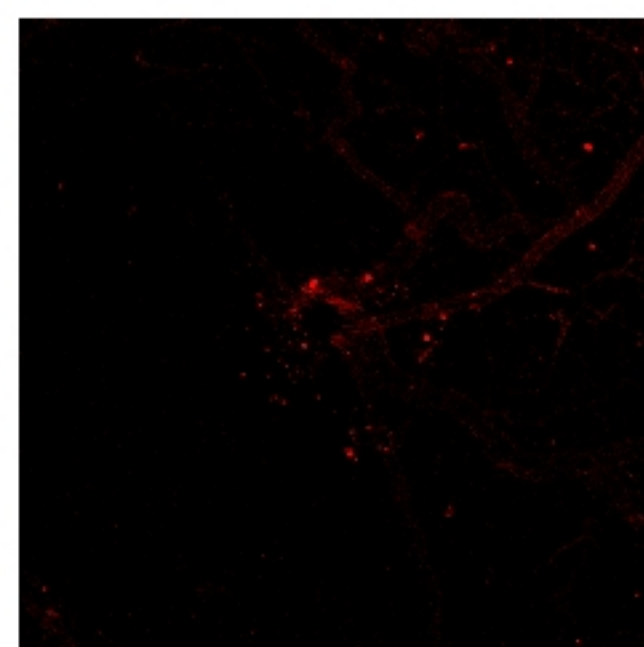
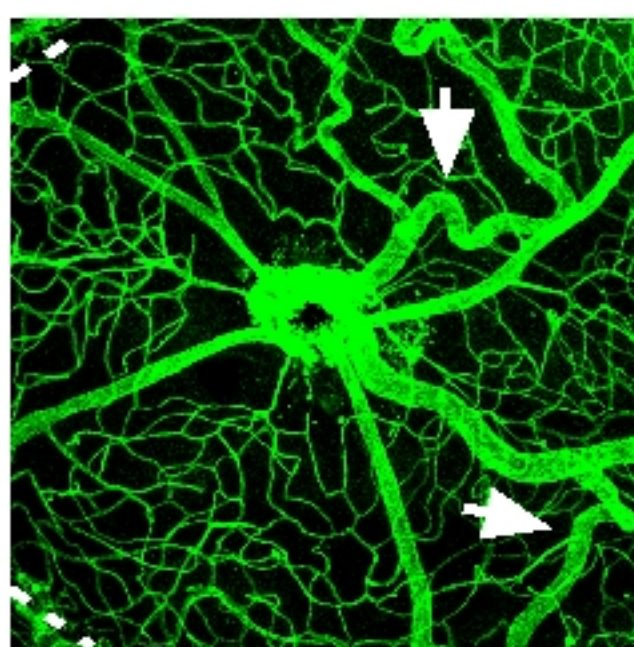
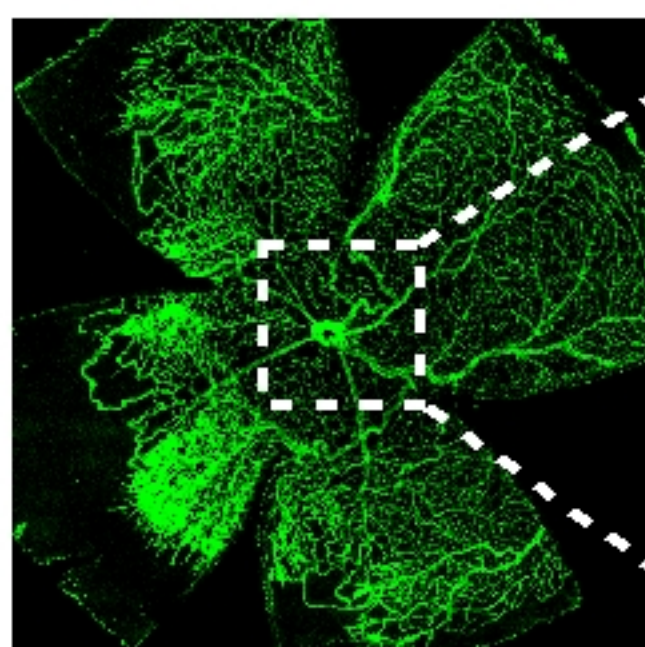
PECAM-1

Tie2

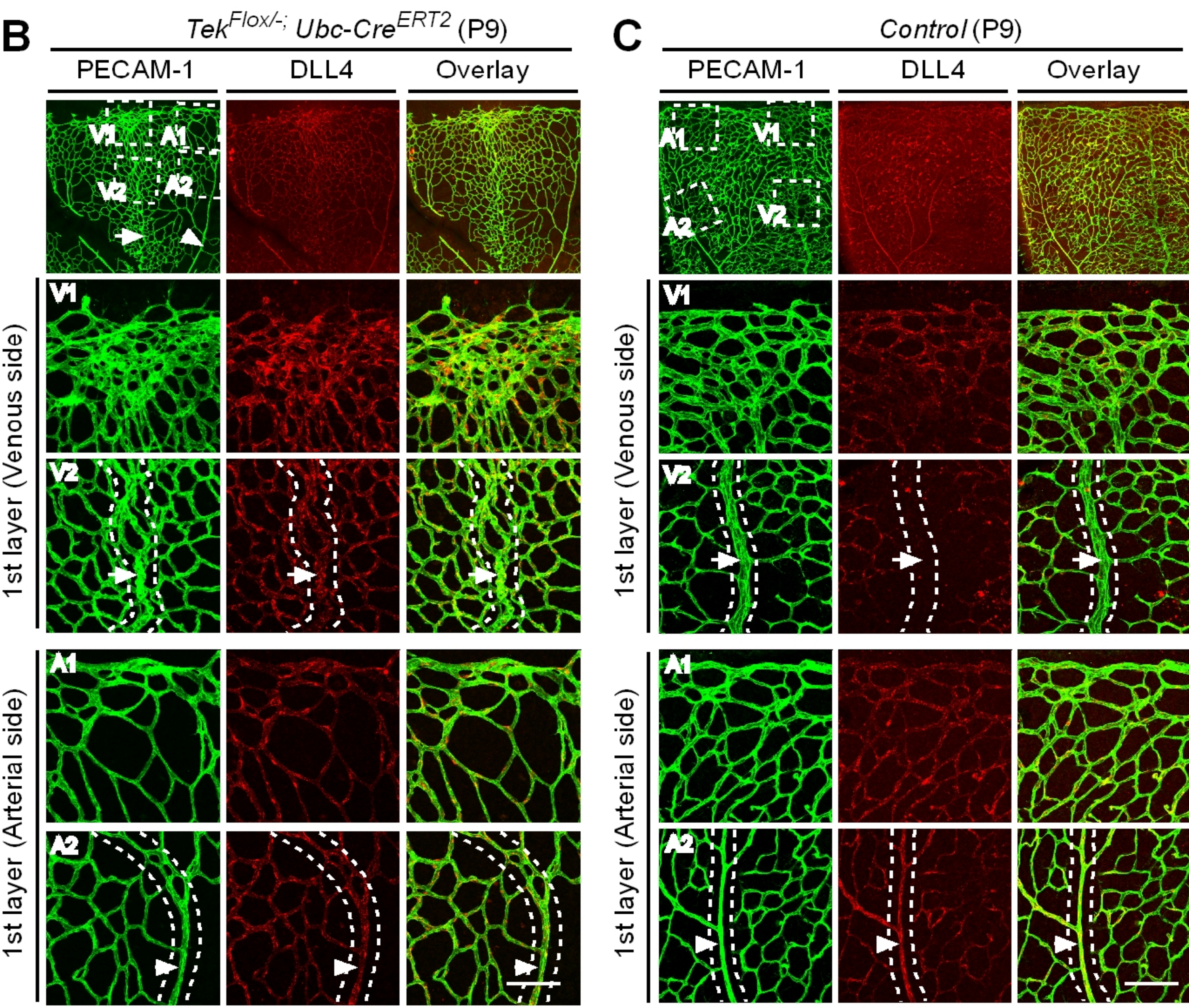
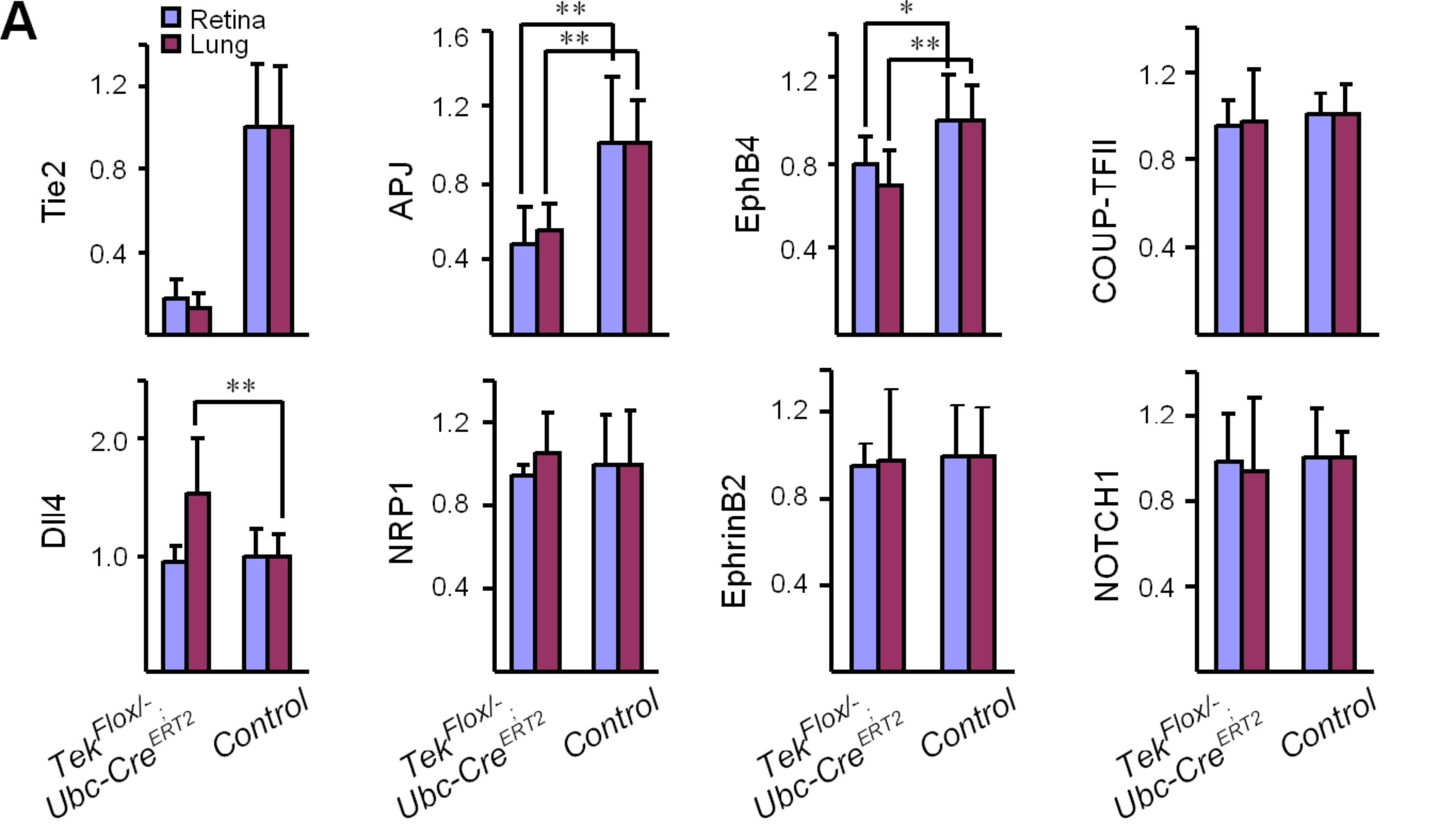
Overlay

**B***Tek*<sup>Flox/-</sup>; *Ubc-Cre*<sup>ERT2</sup>

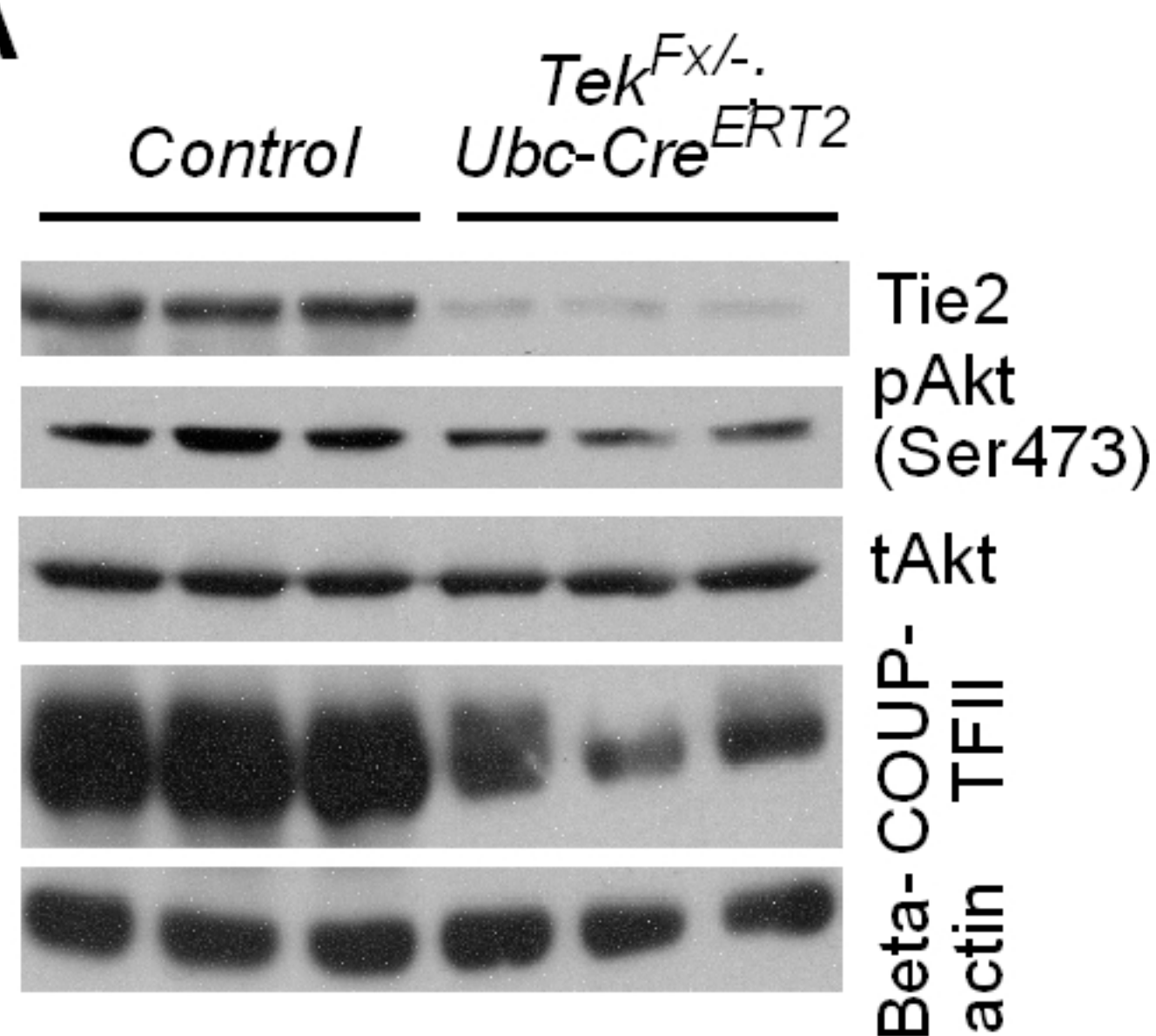
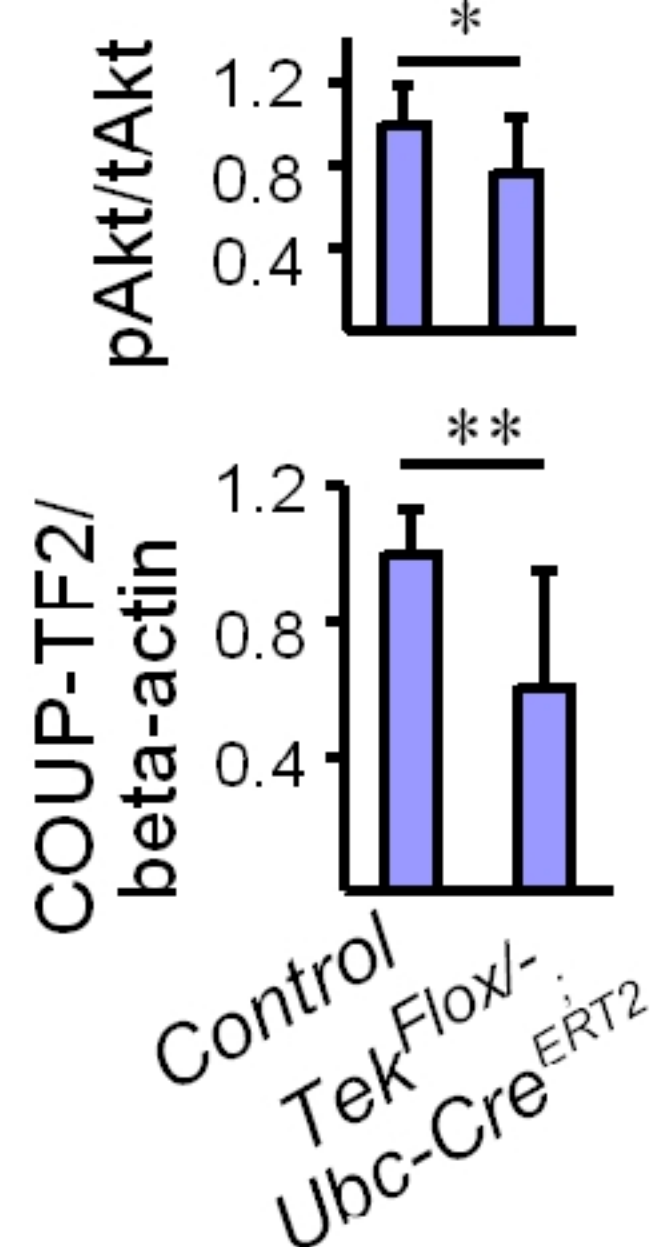
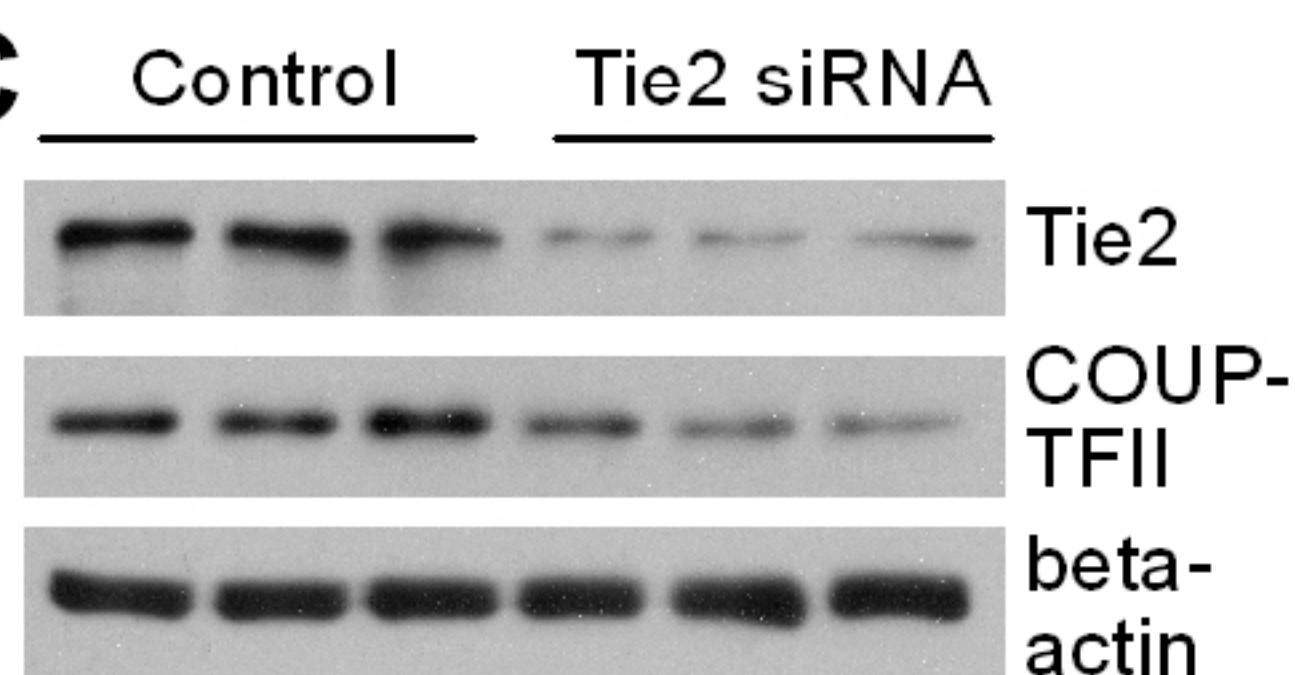
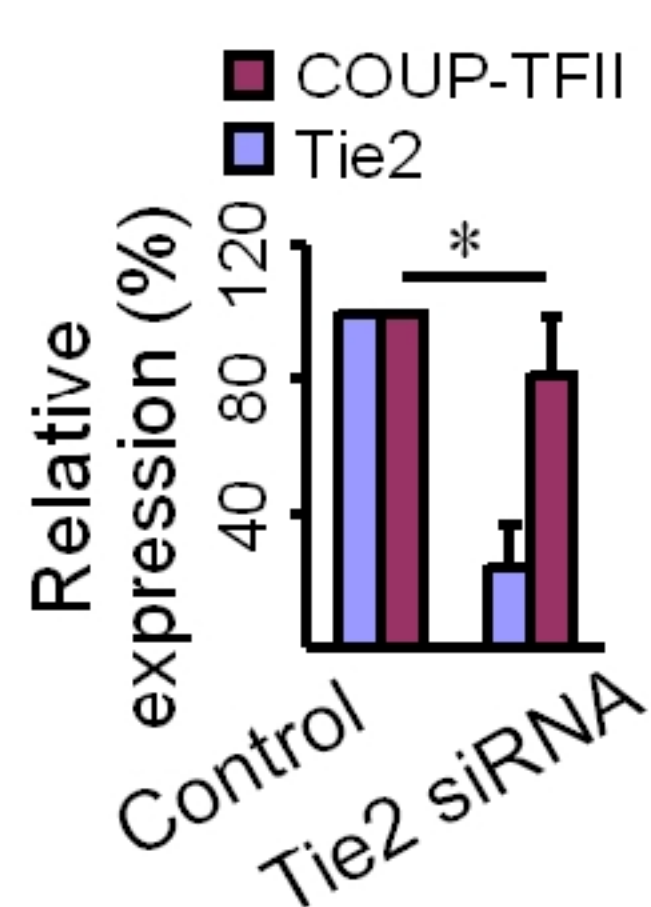
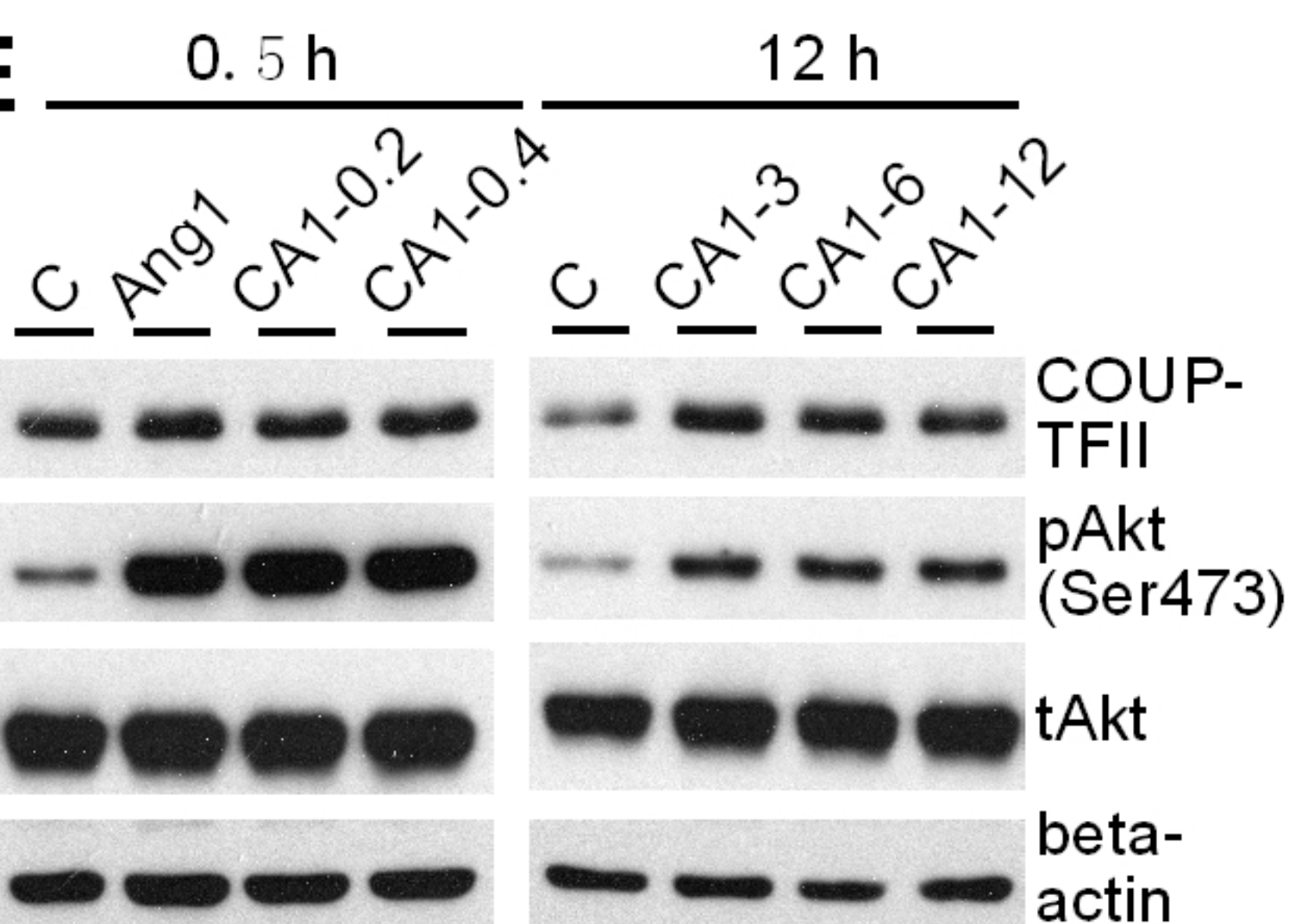
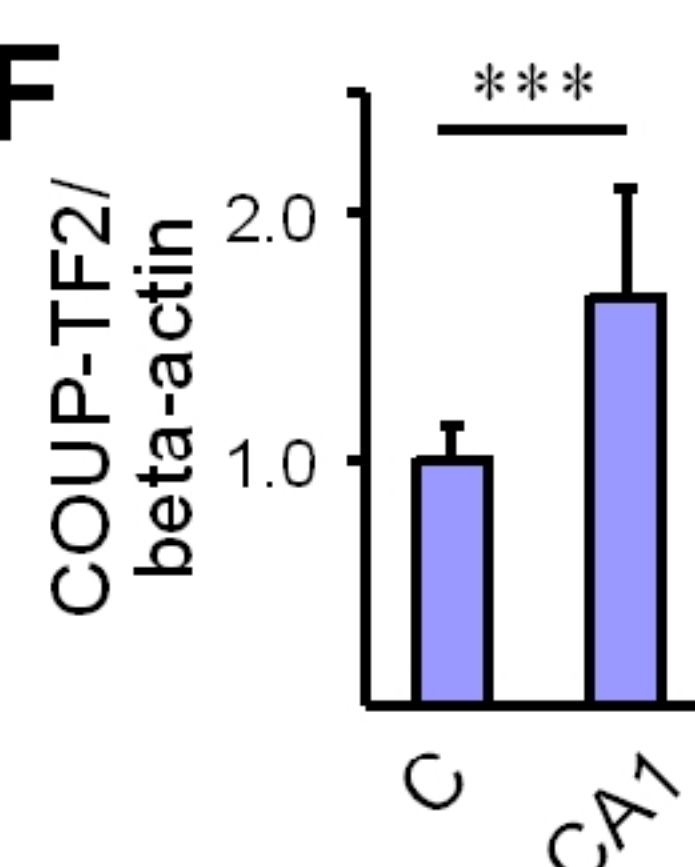
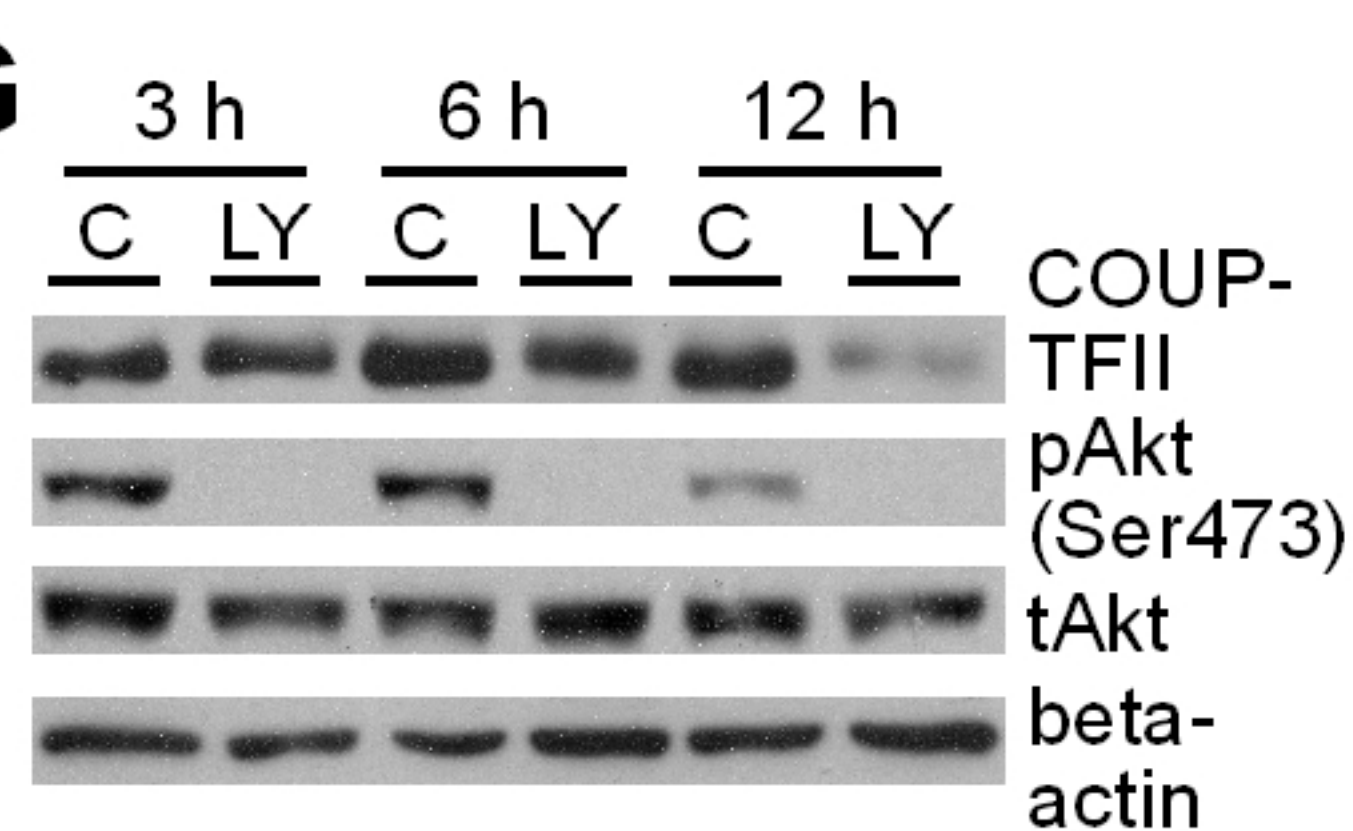
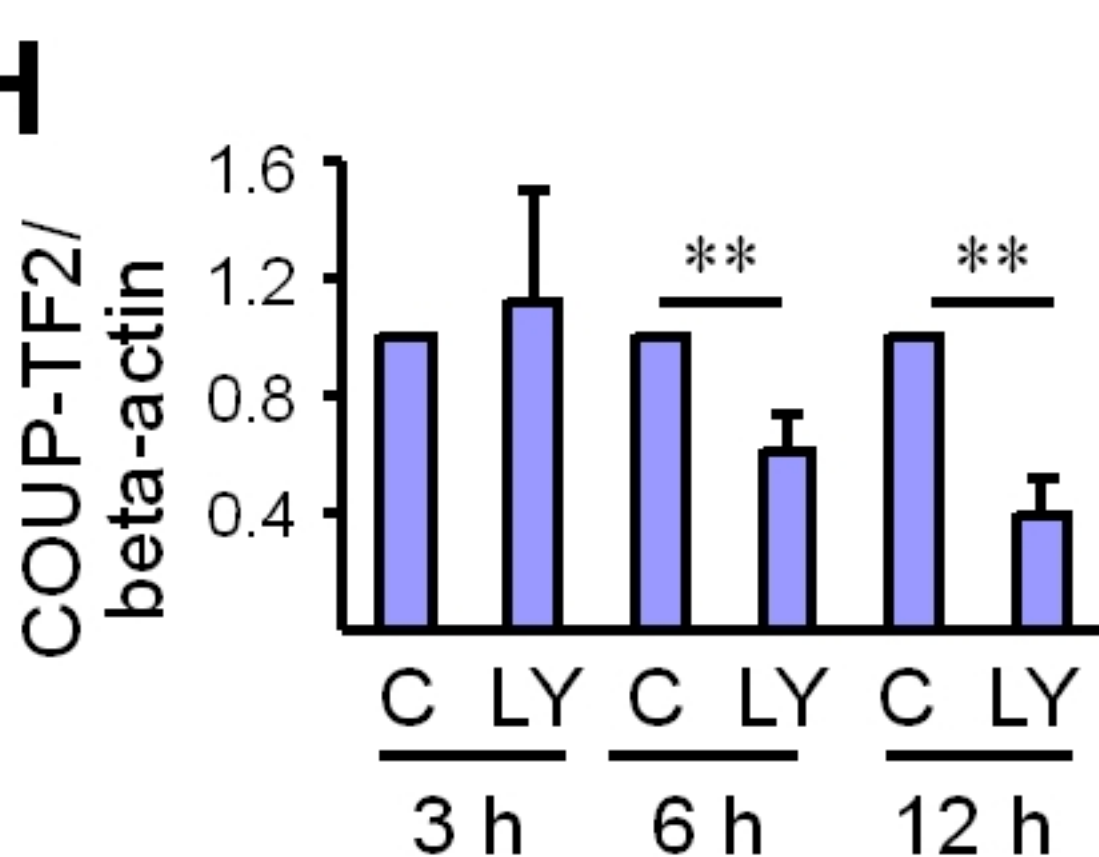
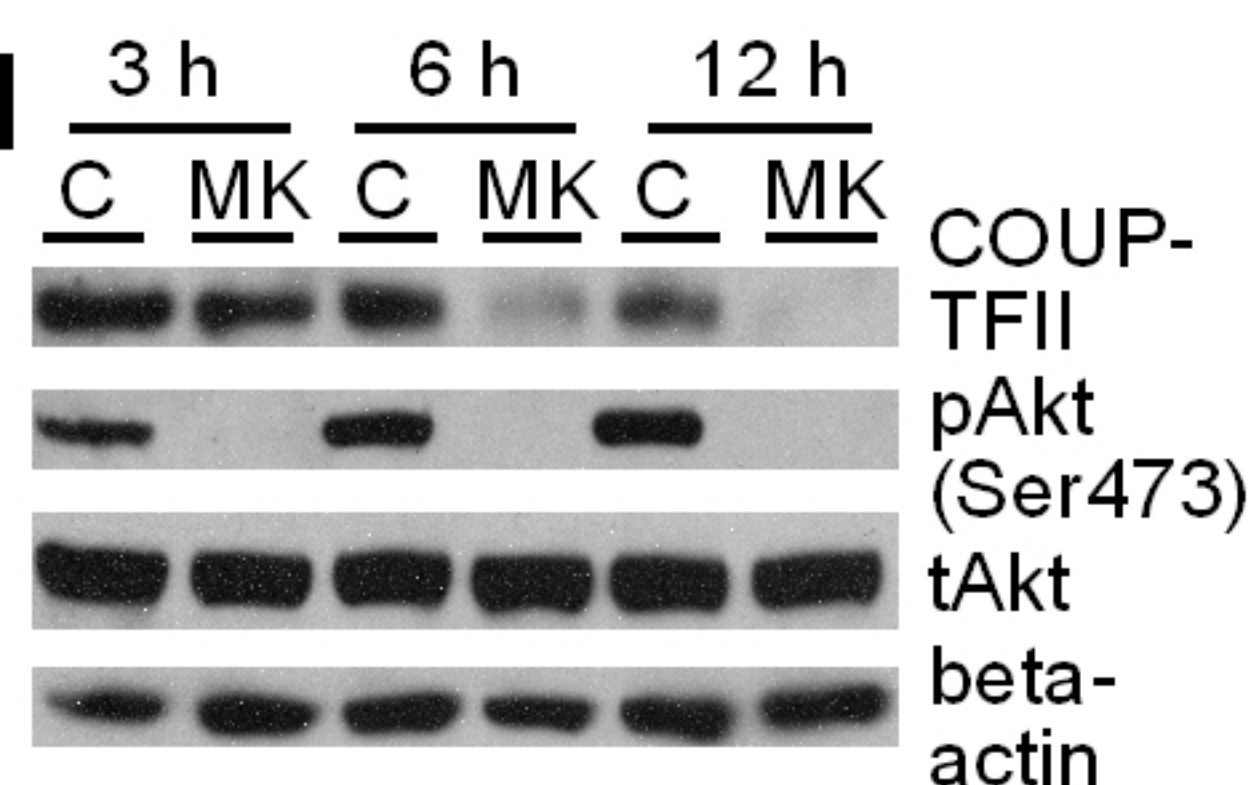
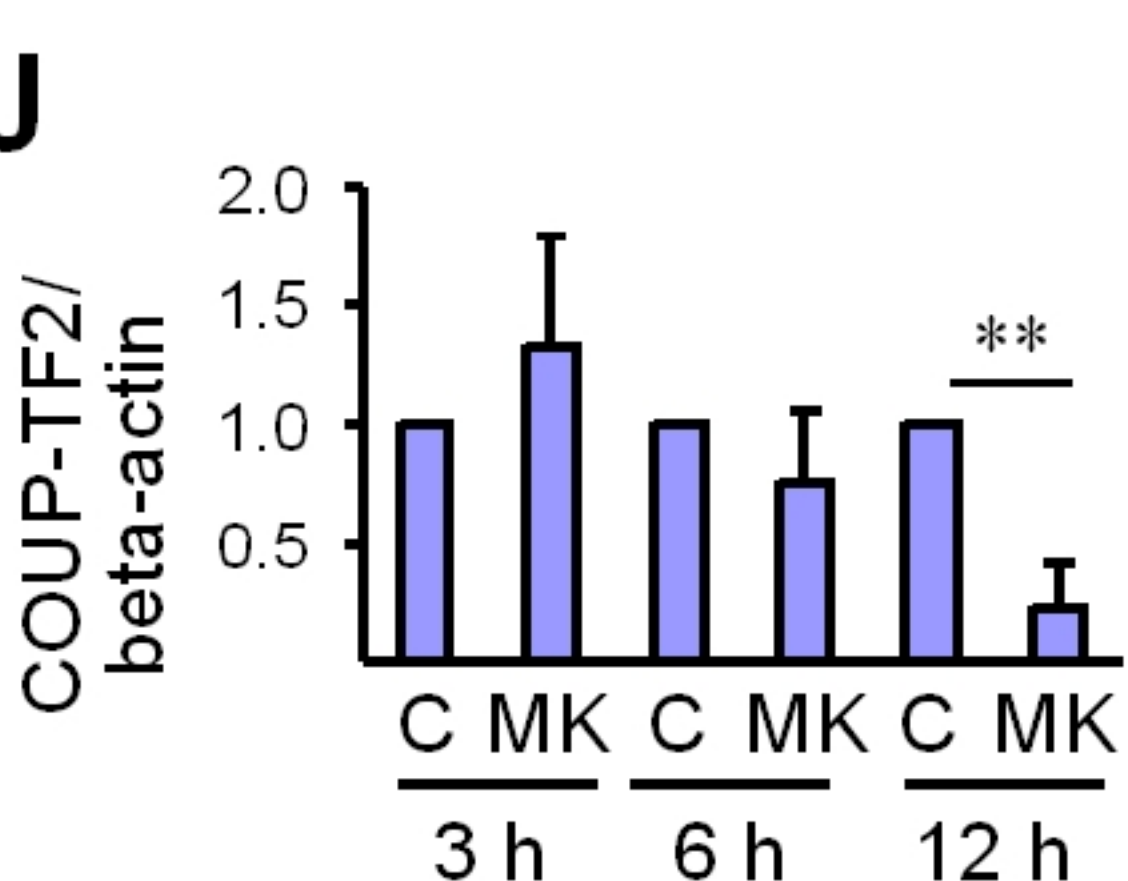
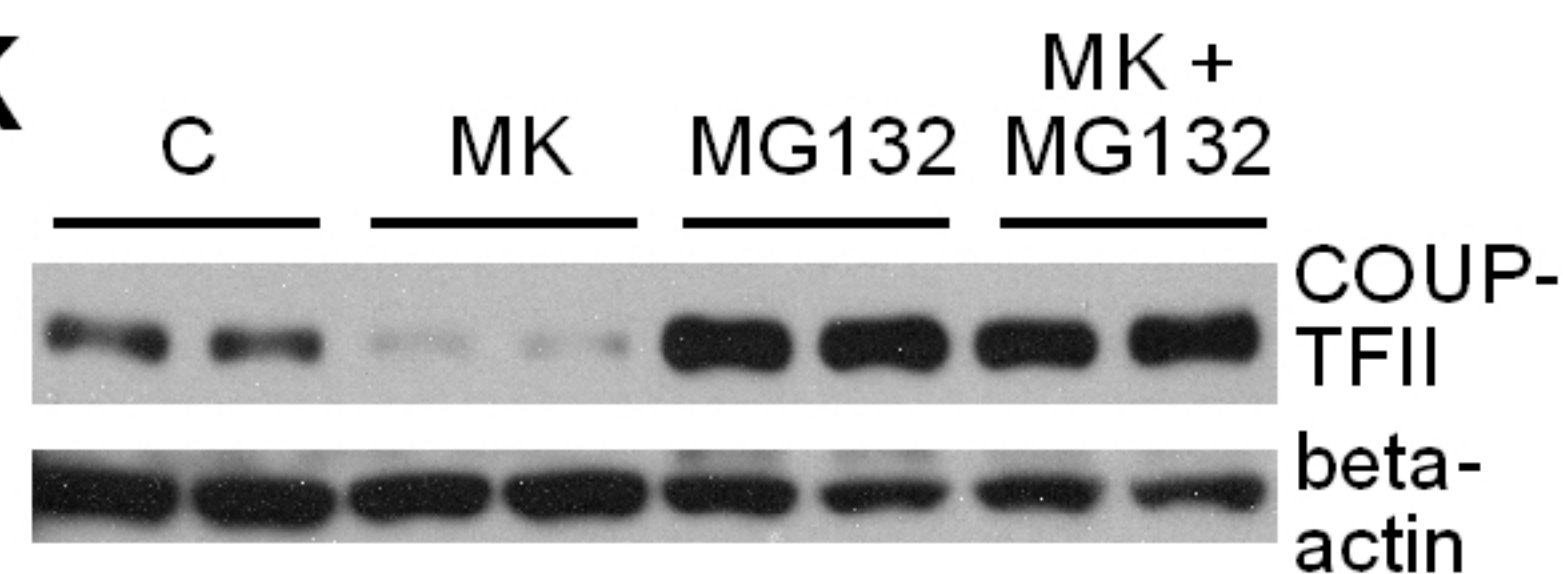
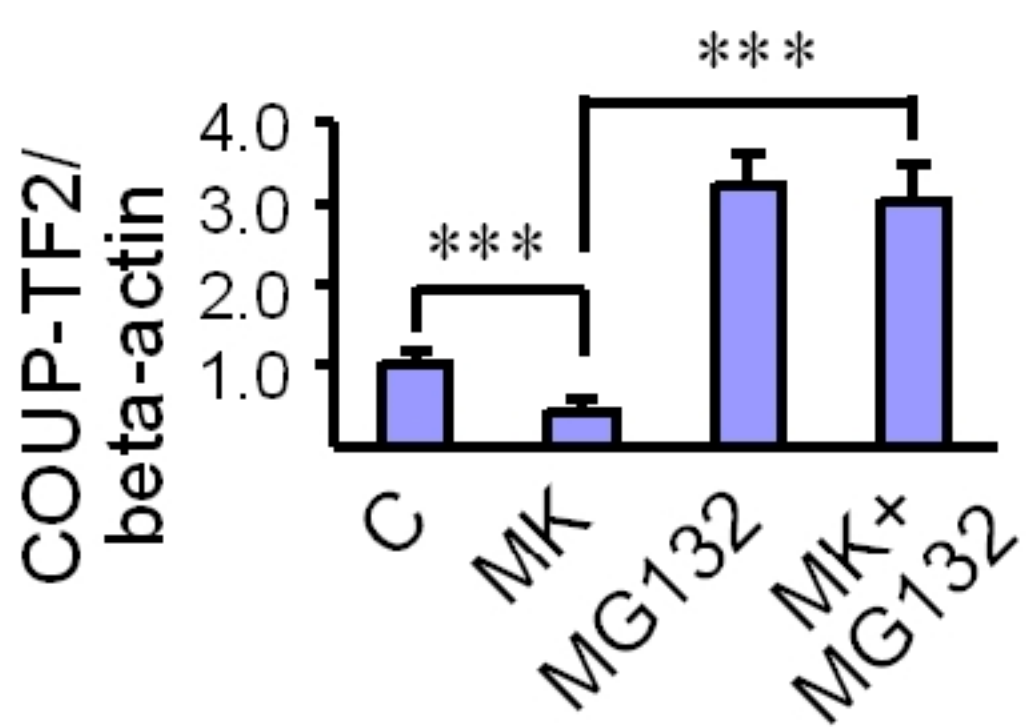
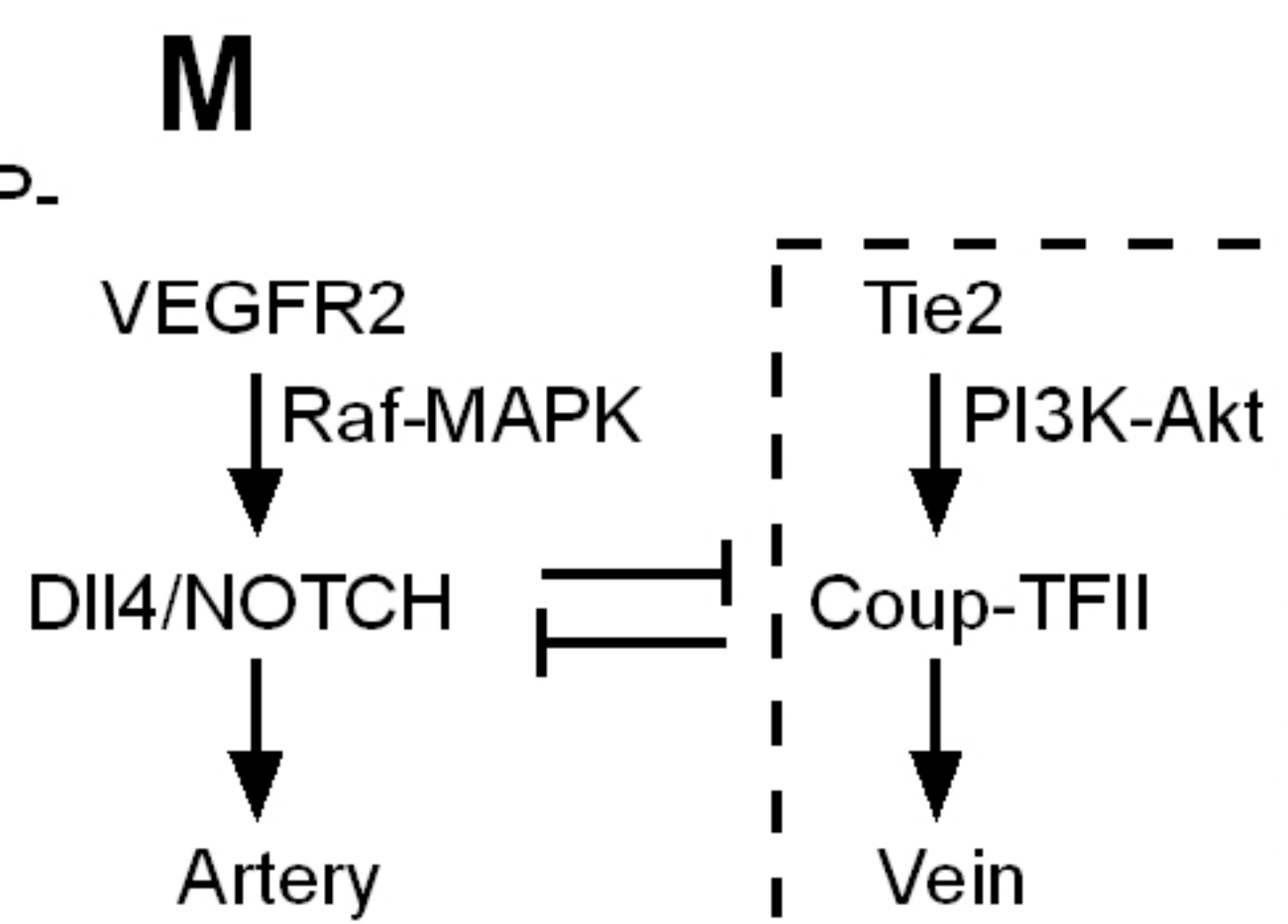
Control



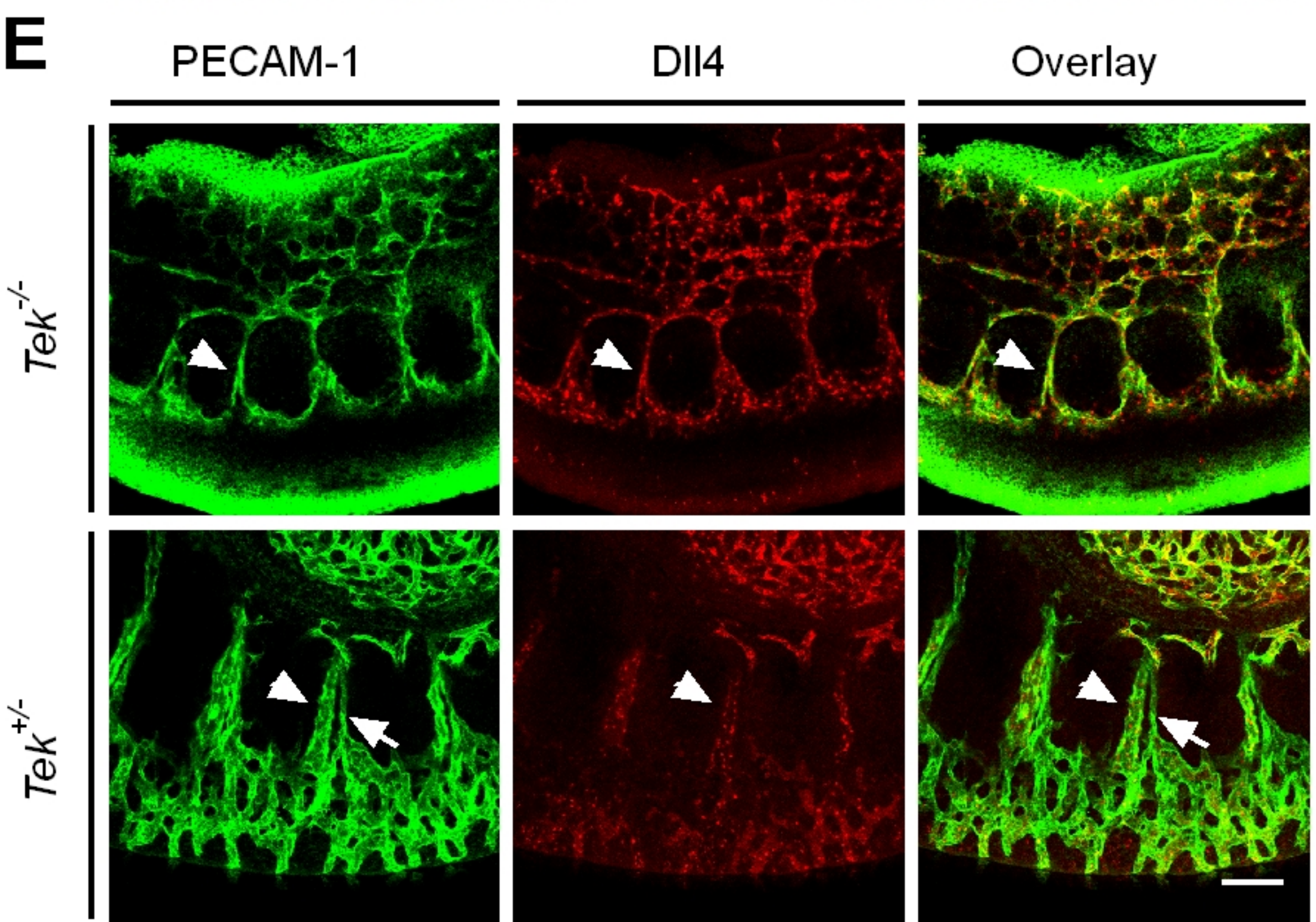
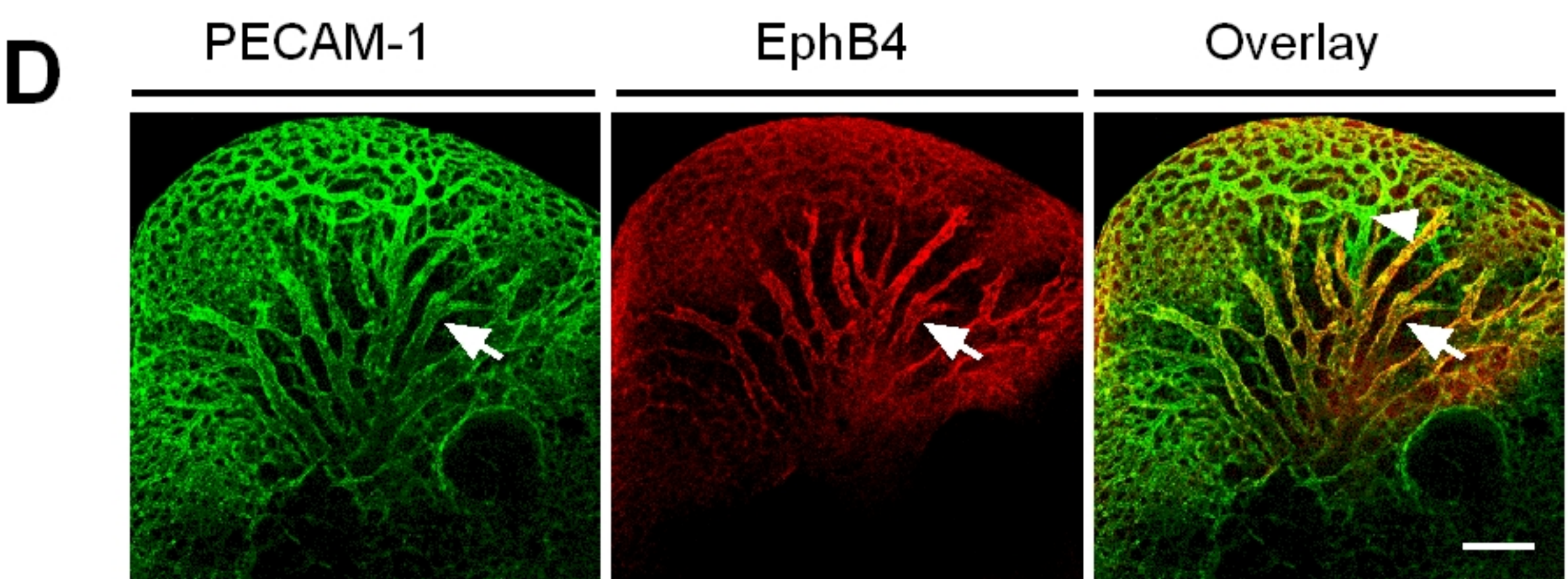
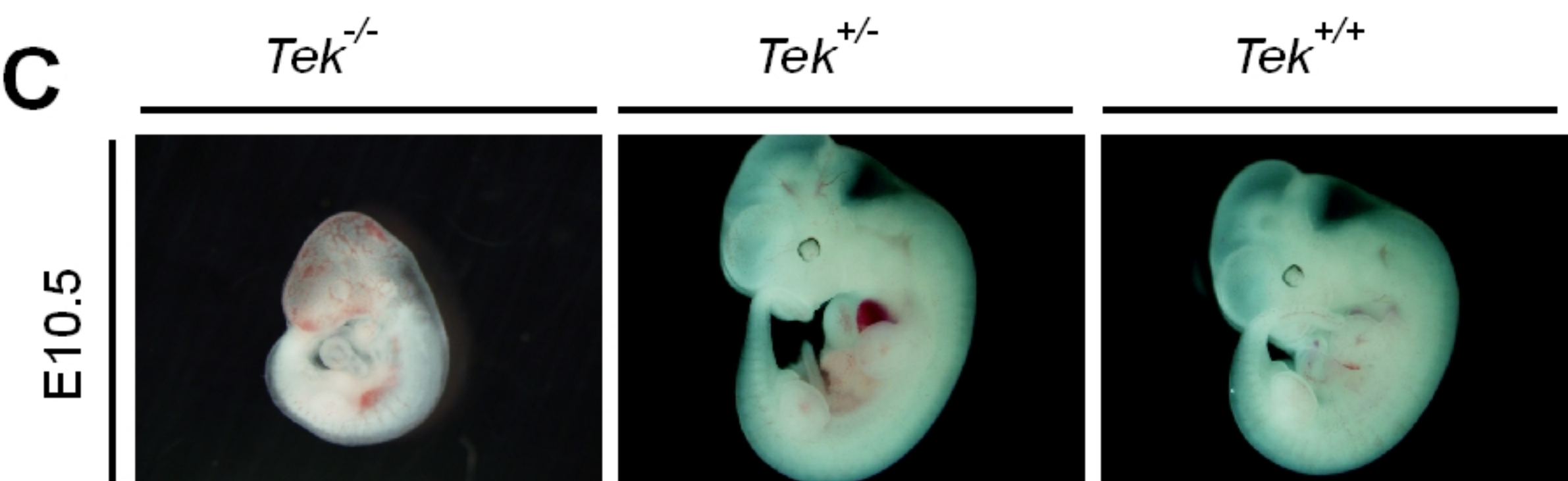
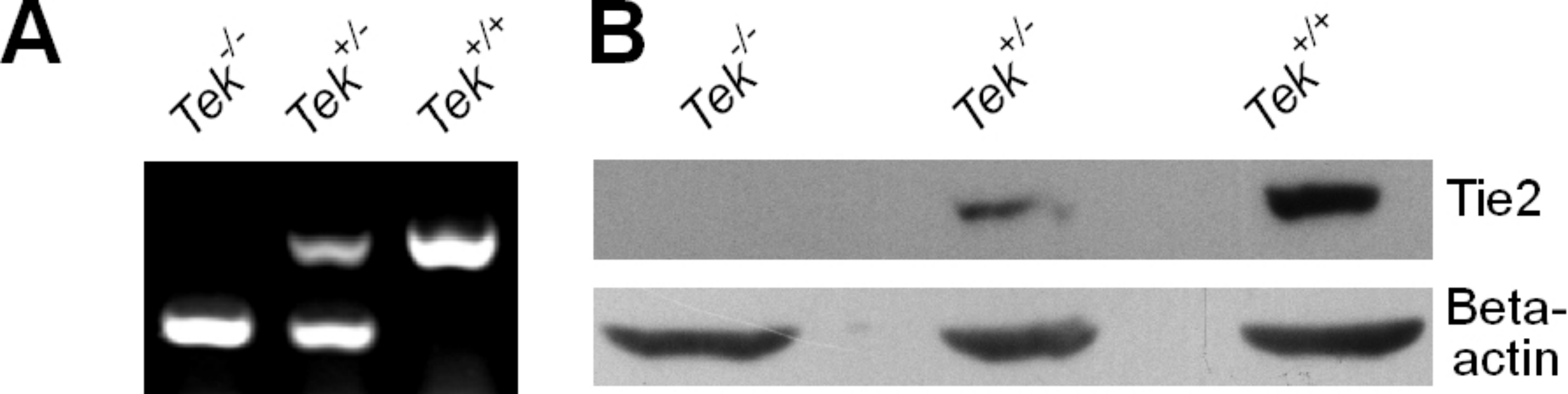






**A****B****C****D****E****F****G****H****I****J****K****L****M**





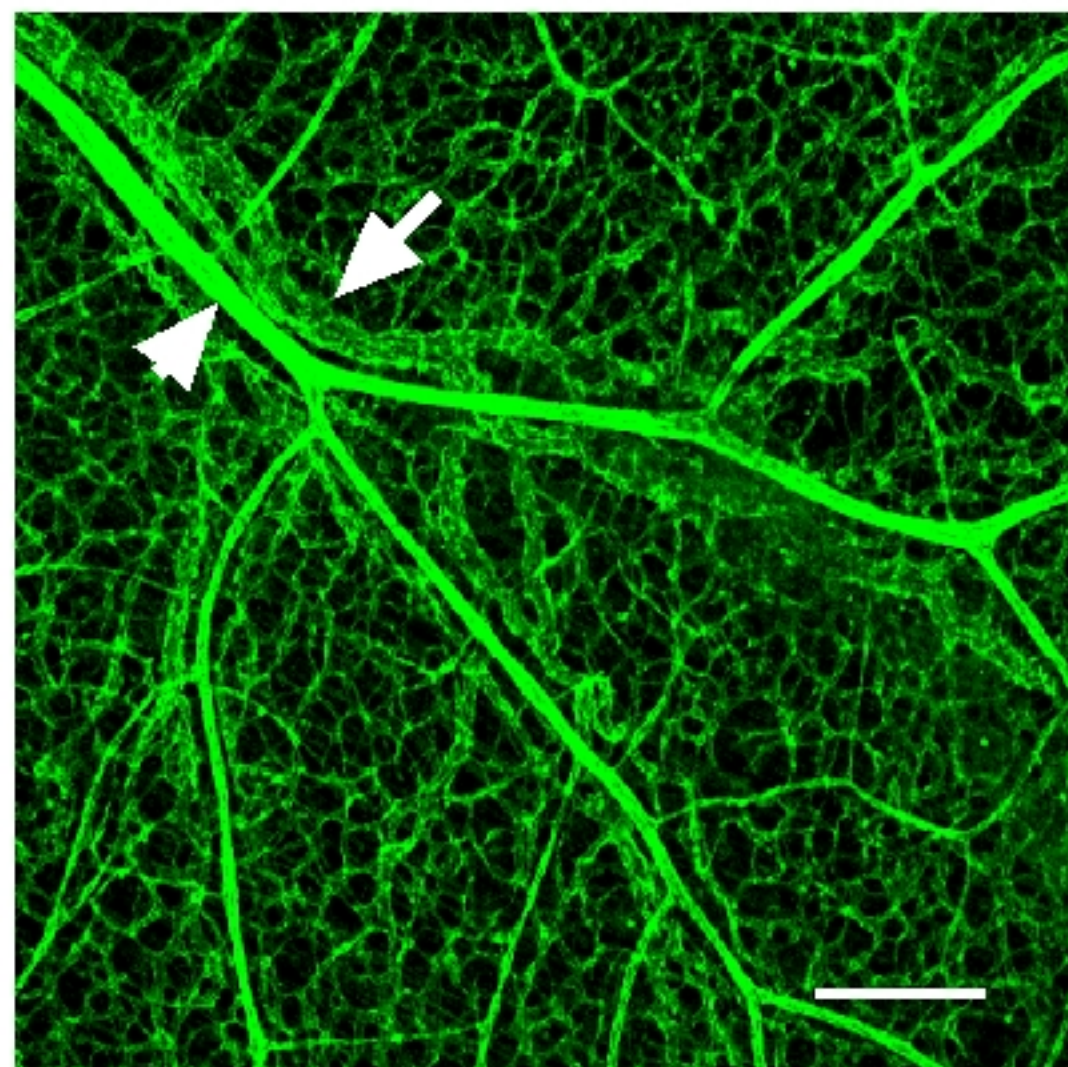
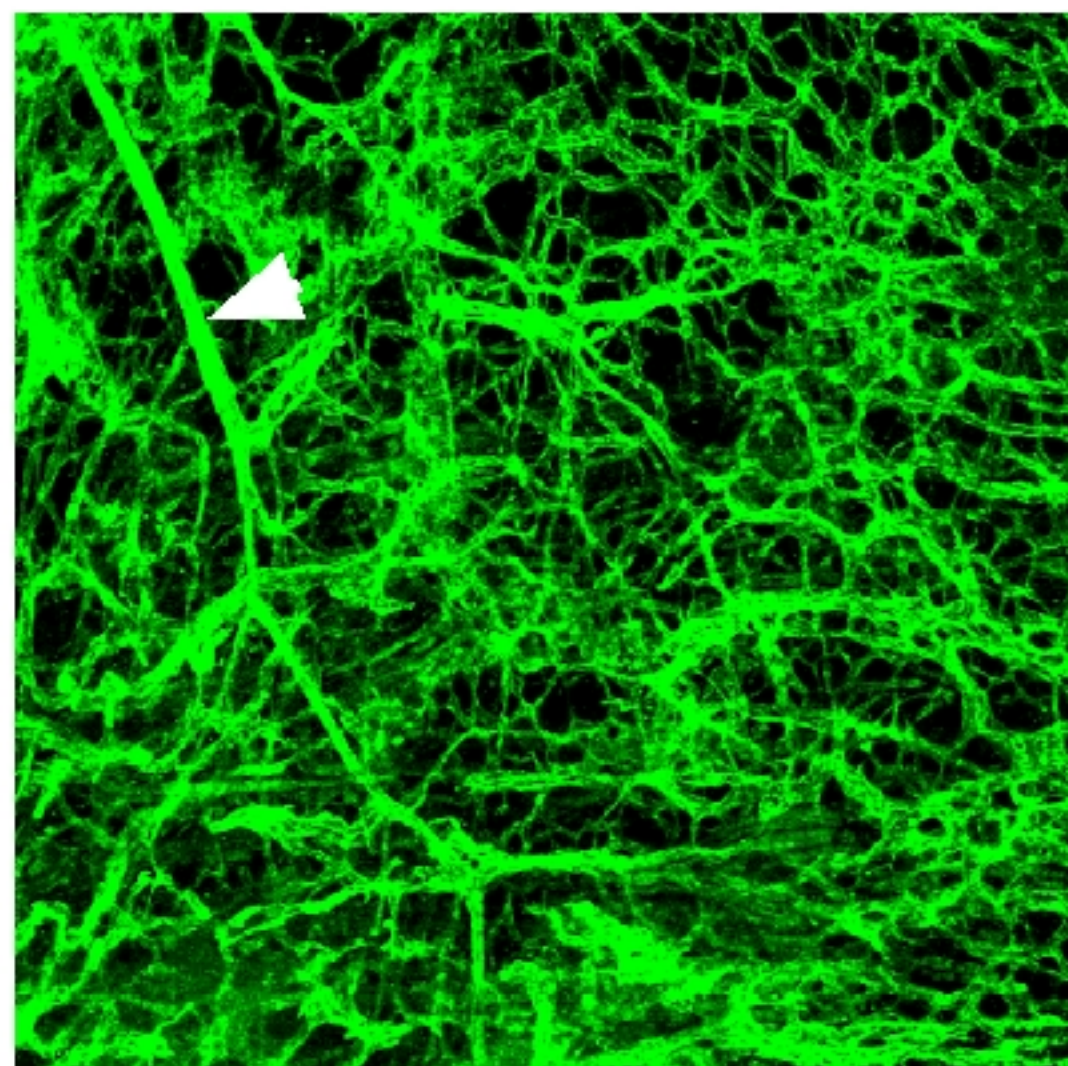


**A***Tek*<sup>Flox/-</sup>;  
*Ubc-Cre*<sup>ERT2</sup>

Control

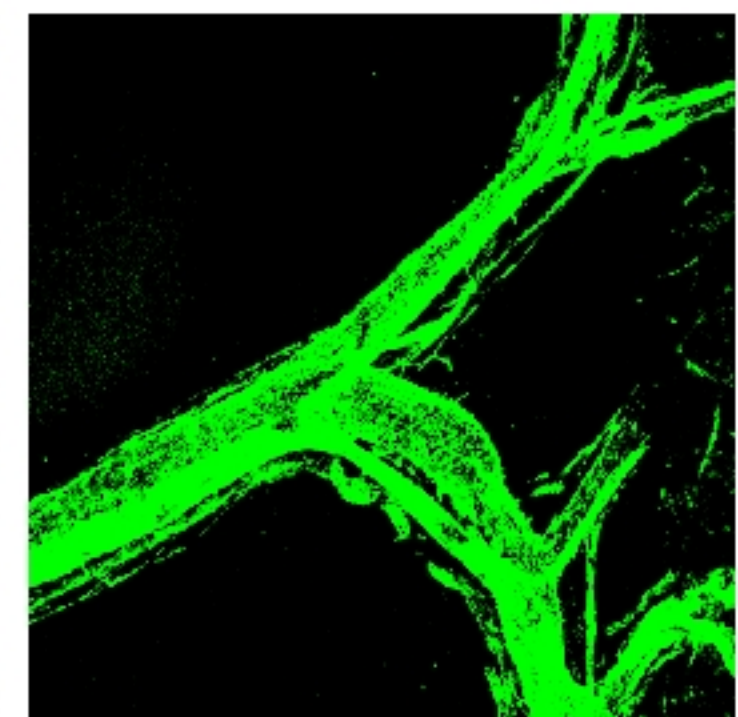
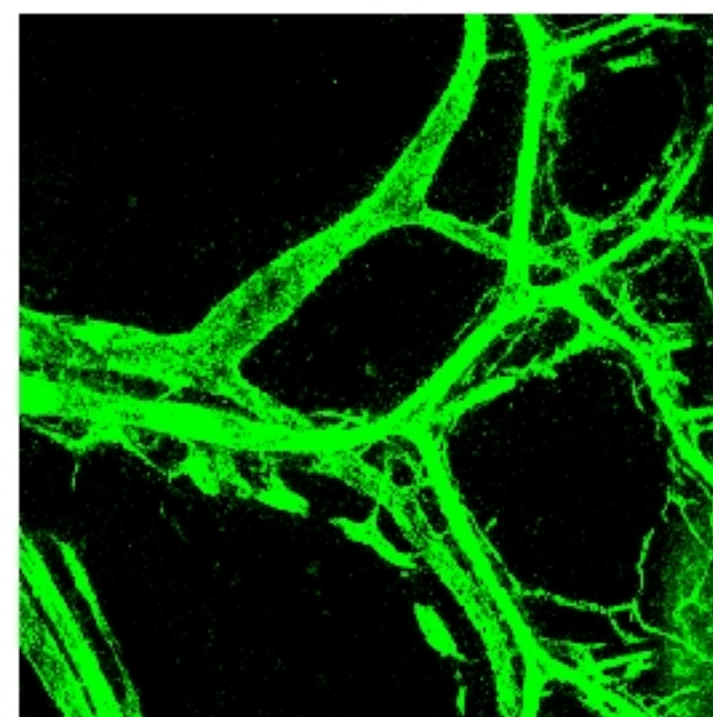


PECAM-1

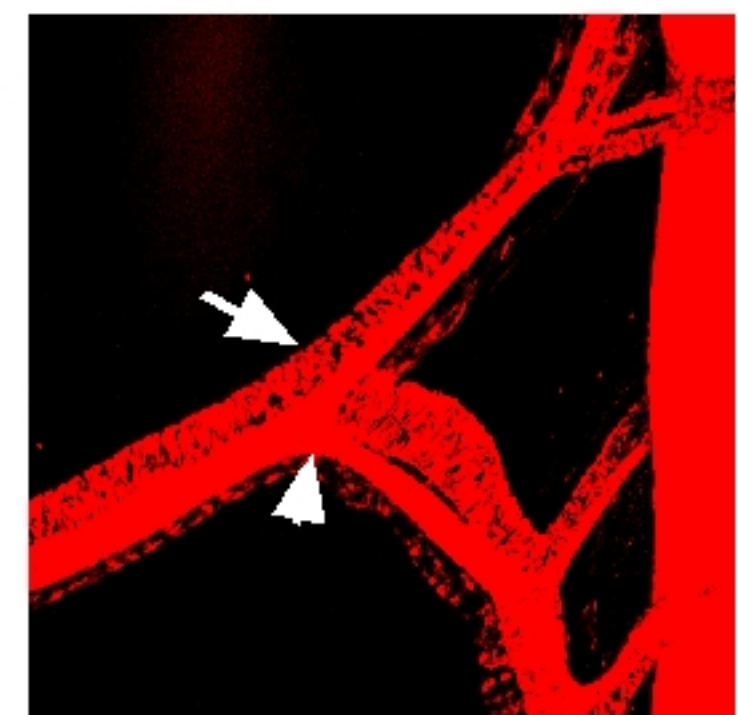
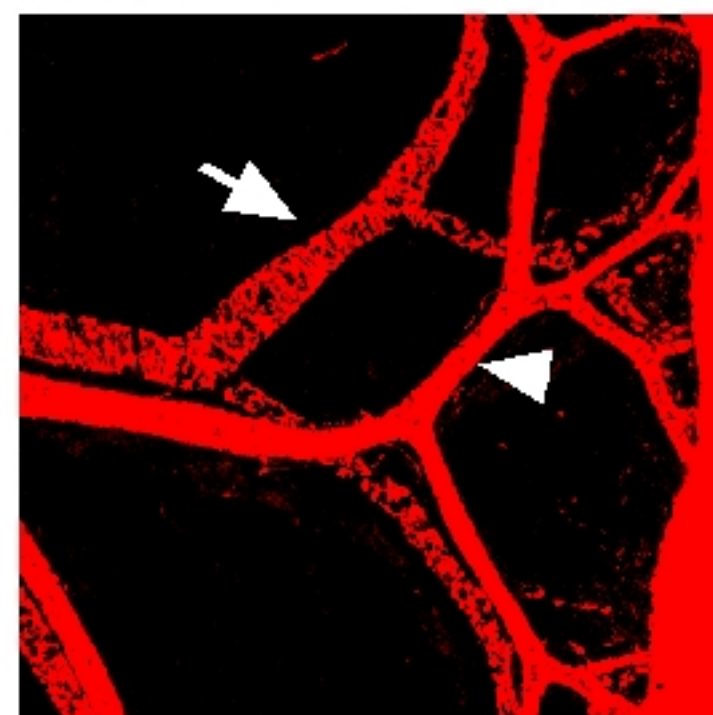
**B***Tek*<sup>Flox/-</sup>;  
*Ubc-Cre*<sup>ERT2</sup>

Control

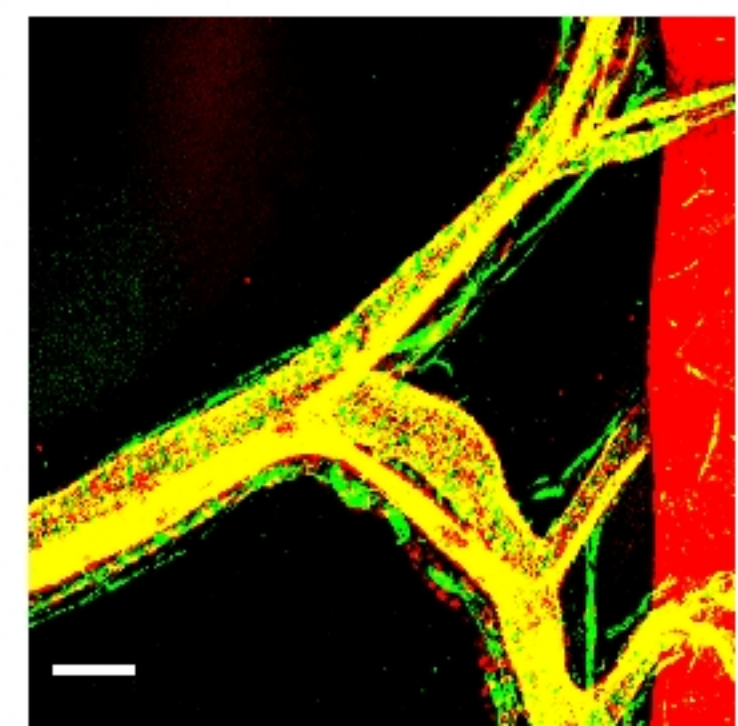
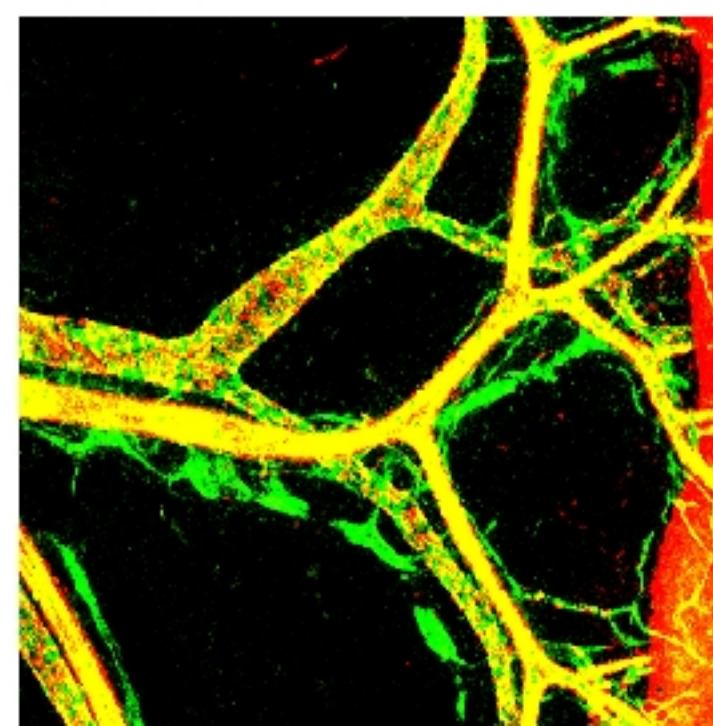
PECAM-1



aSMA

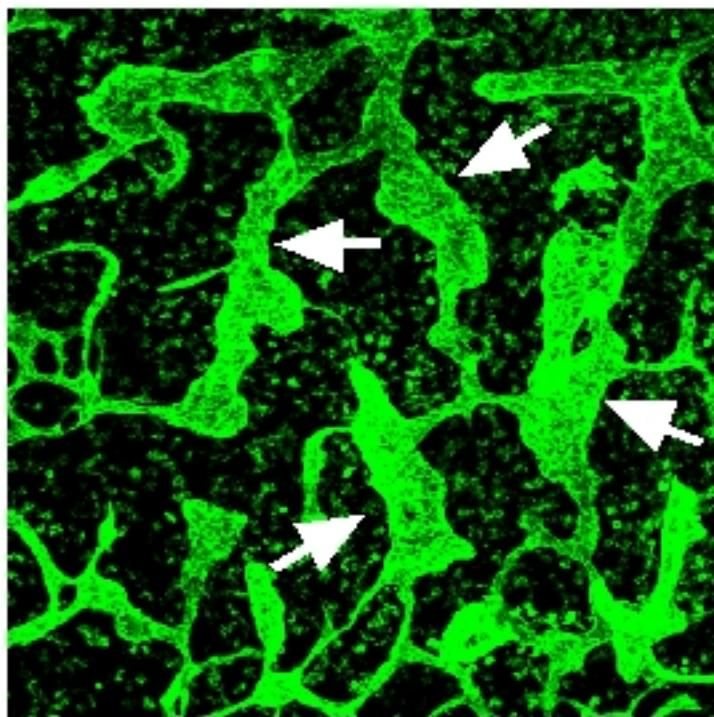
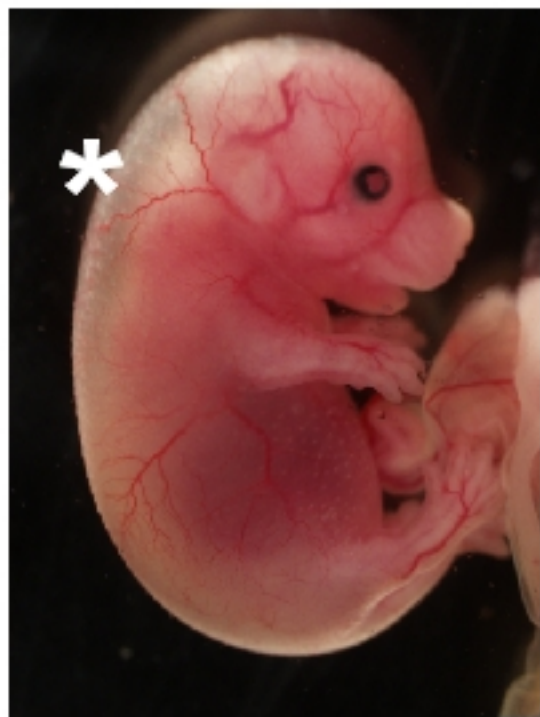


Overlay

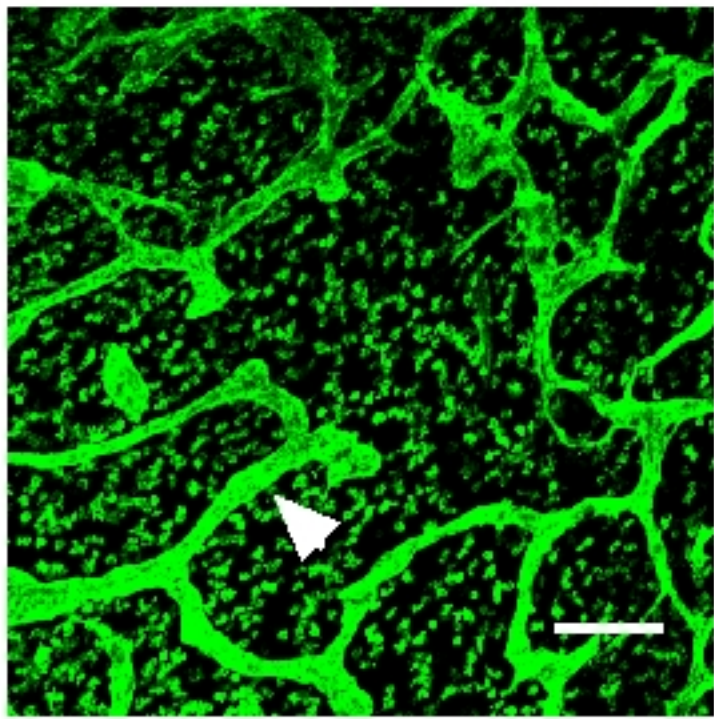




*Flox<sup>-/-</sup>;  
Tek<sup>ERT2</sup>  
Cdh5-Cre*



*Control*



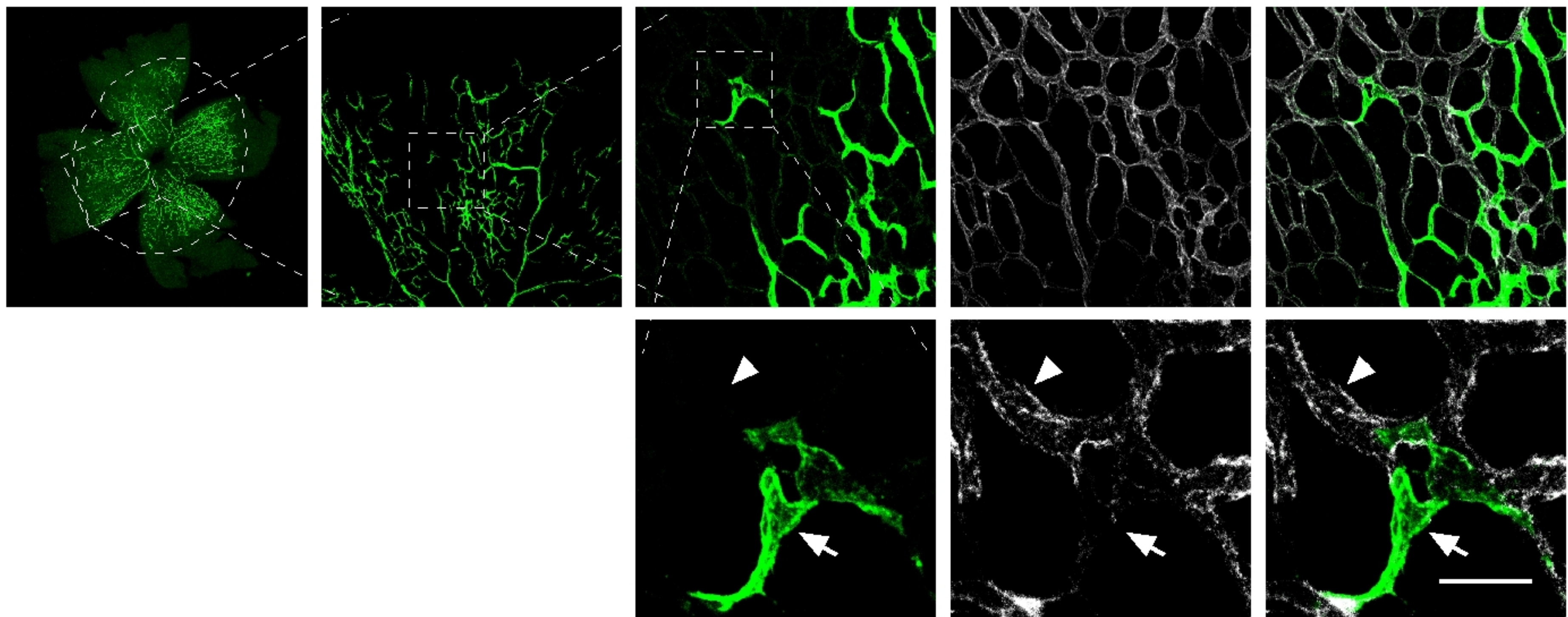
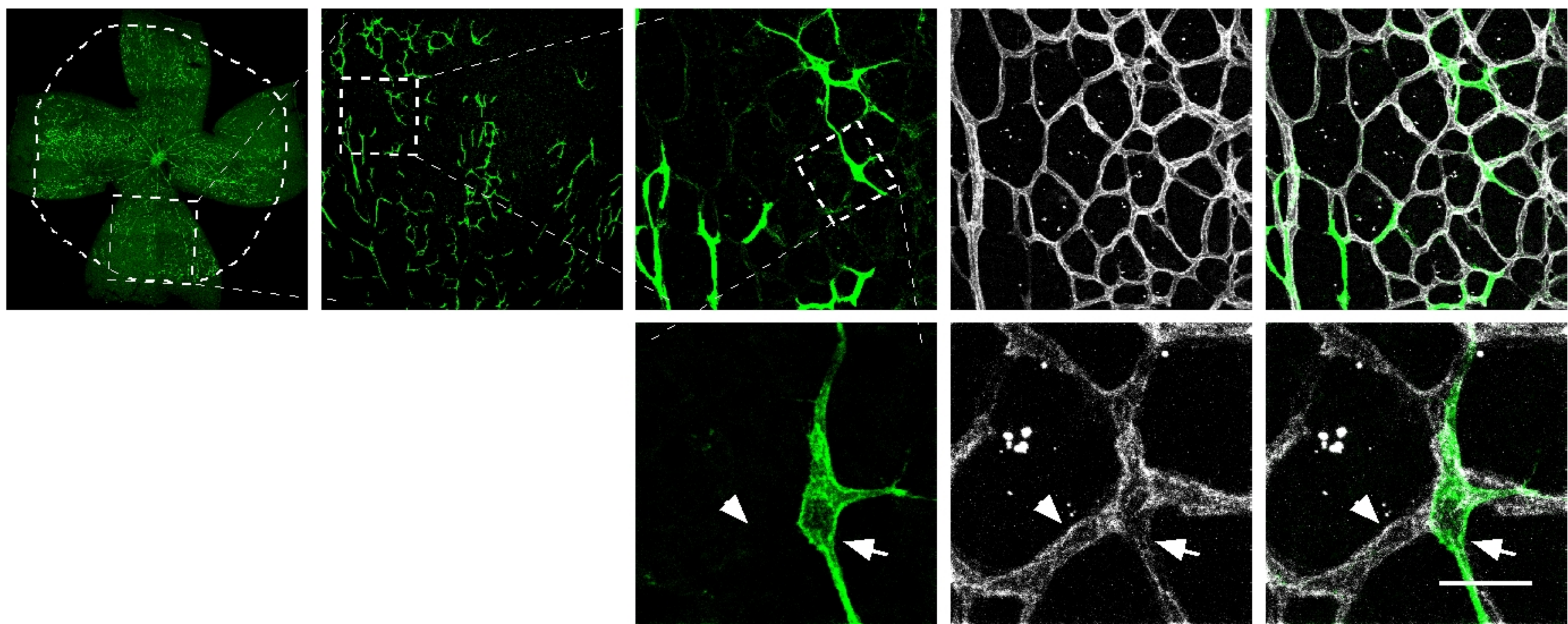


**A***Tek<sup>Flox/-</sup>; mTmG*  
*Cdh5-Cre<sup>ERT2</sup>*

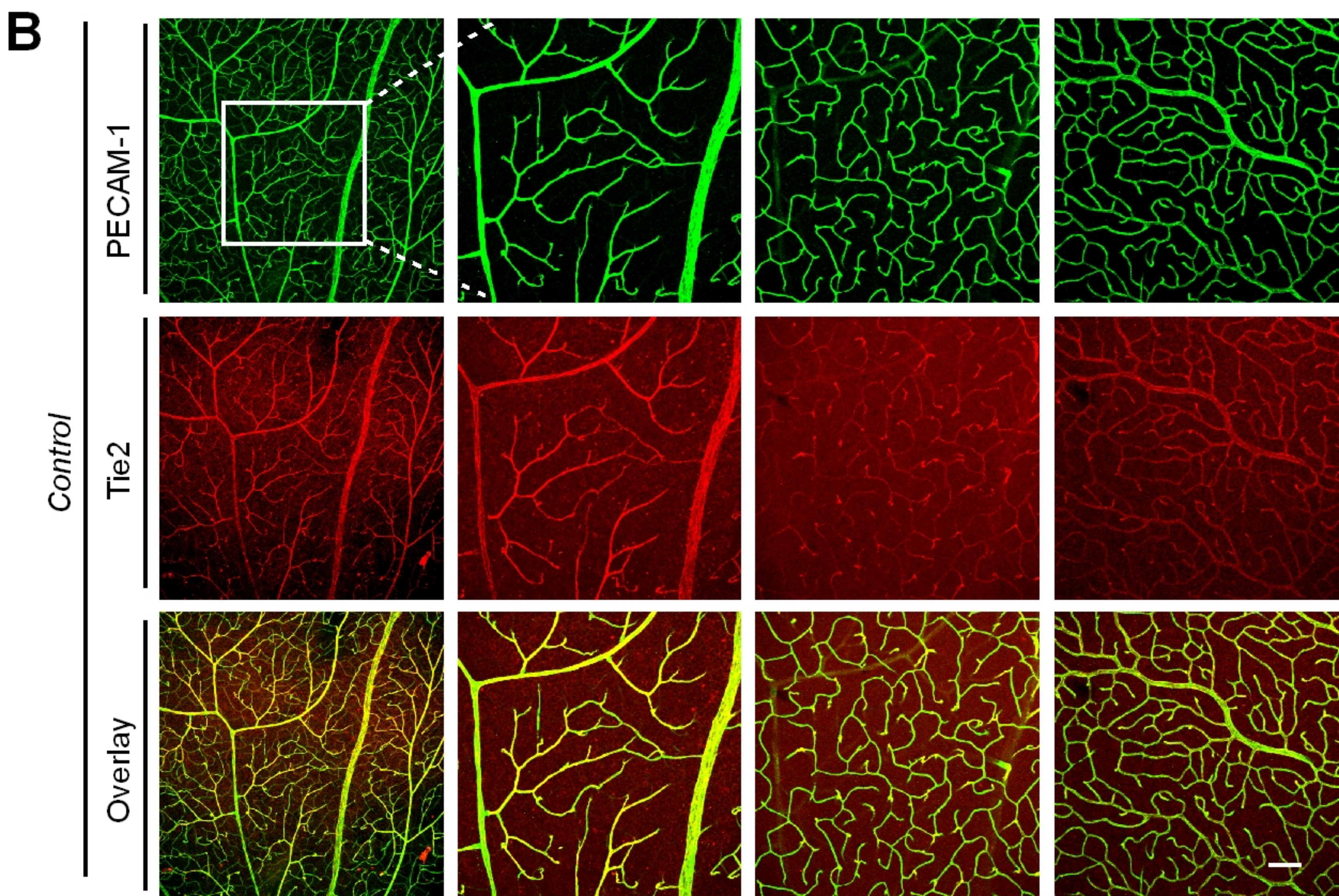
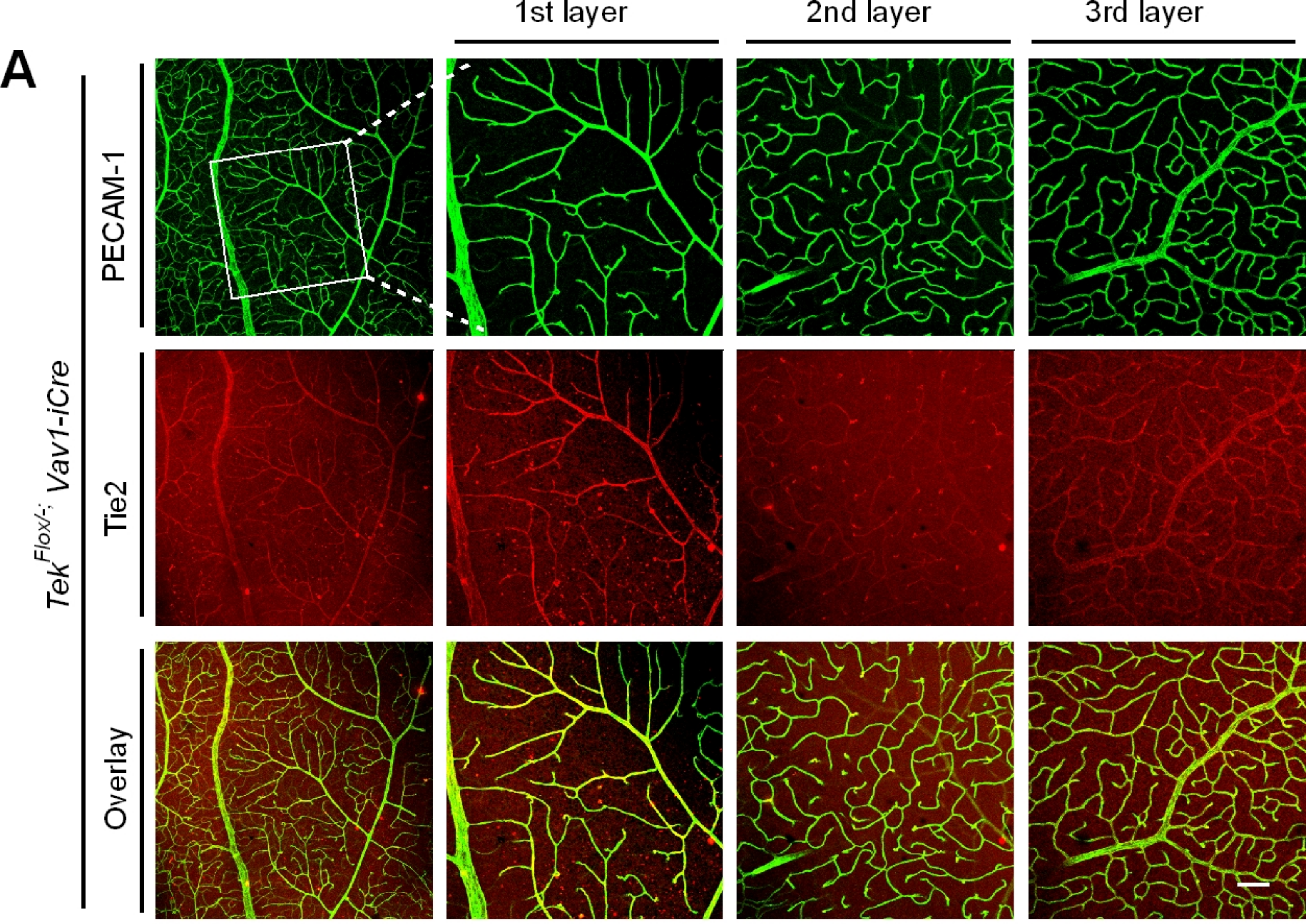
EGFP

Tie2

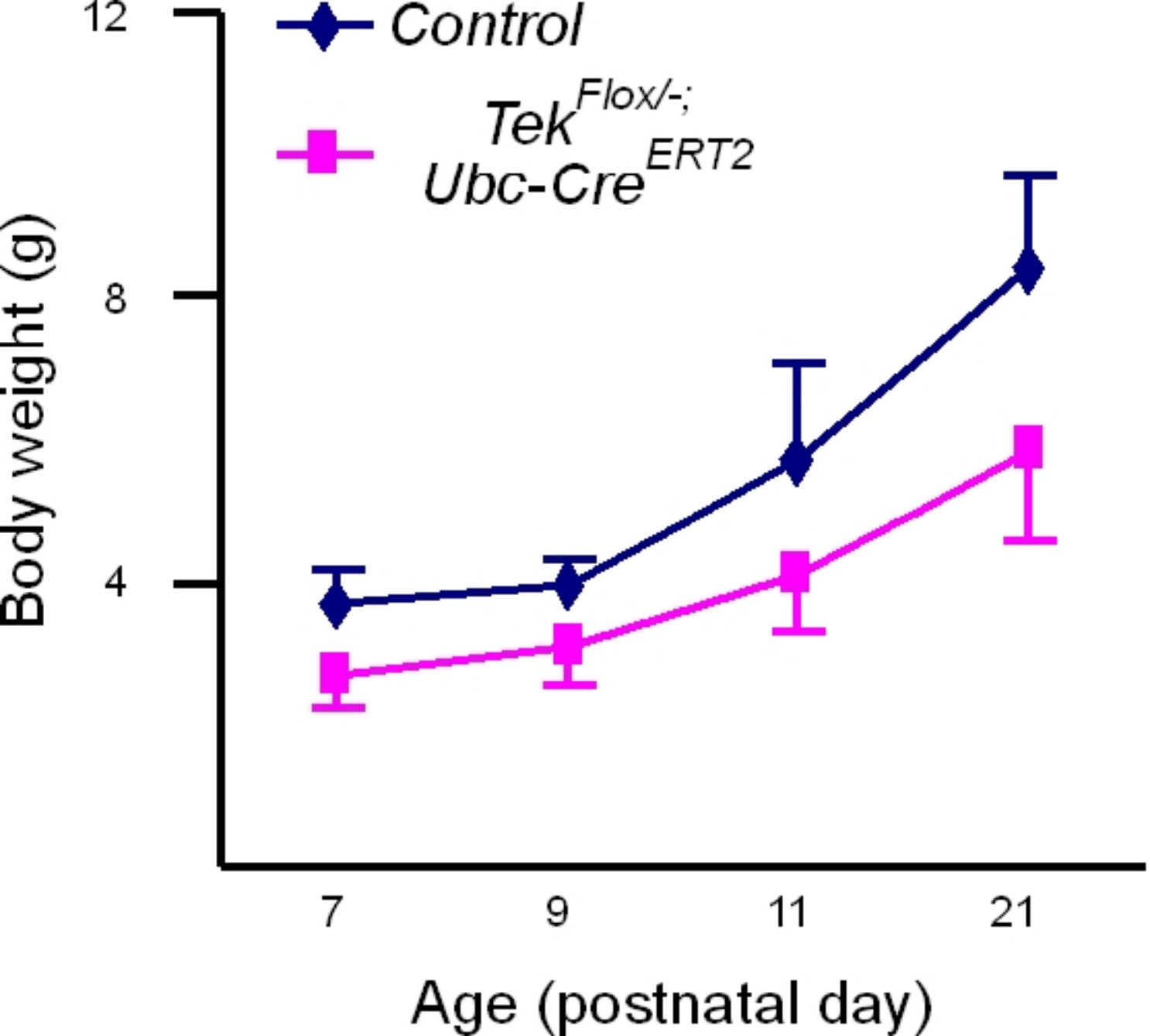
Overlay

**B***Control; mTmG*

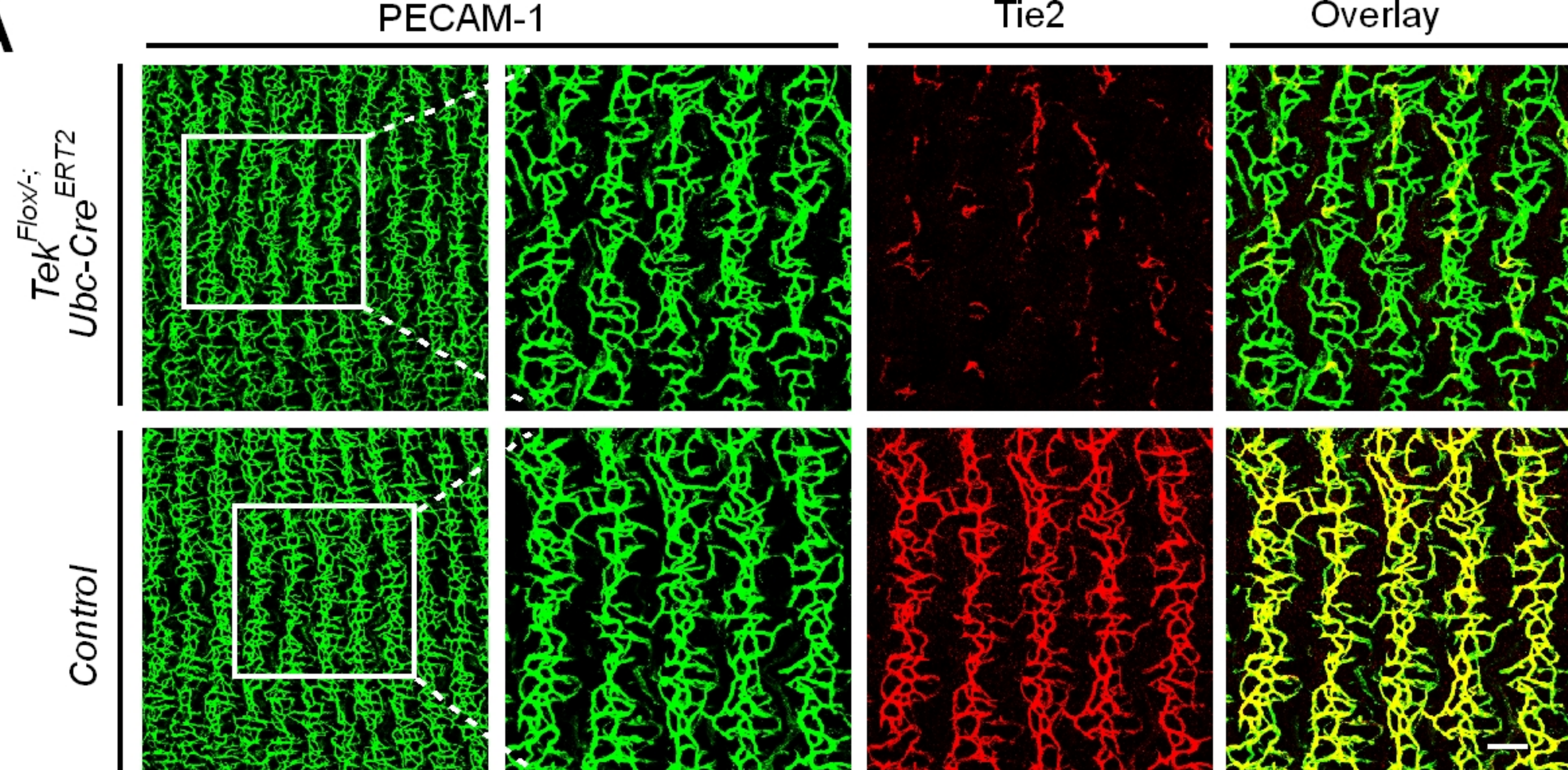










**A****B**